BEZMIALEM VAKIF UNIVERSITY
INSTITUTE OF HEALTH SCIENCES

GENE TARGETING STUDIES OF THE MALARIA PARASITE DNA PHOTOLYASE GENE USING CRISPR-CAS9 GENOME EDITING TECHNOLOGY

MASTER THESIS

İlknur YILMAZ
(185309006)

Biotechnology Department

Biotechnology Master of Science Program

Thesis Advisor: Assoc. Prof. Dr. Binnur TEMEL
Co-Advisor: Prof. Dr. Bedia GEMİCİ PALABIYIK

FEBRUARY 2021

After fulfilling all the necessary conditions determined by the related regulations, Master of Science student İlknur YILMAZ (student ID number: 185309006) successfully presented her thesis titled as "GENE TARGETING STUDIES OF THE MALARIA PARASITE DNA PHOTOLYASE GENE USING CRISPR-CAS9 GENOME EDITING TECHNOLOGY" in front of the jury members.

Thesis Advisor	**:**	**Assoc. Prof. Dr. Binnur TEMEL** Bezmialem Vakif University	.....
Co-Advisor	**:**	**Prof. Dr. Bedia G. PALABIYIK** Istanbul University	.....
Jury Members	**:**	**Assist. Prof. Dr. Ahmed S. I. ALY** Bezmialem Vakif University	.....
		Assist. Prof. Dr. Matteen RAGIQI Bezmialem Vakif University	.....
		Assist. Prof. Dr. Çağatay TARHAN Istanbul University	.....

Date of Submission : 24 February 2021
Date of Defense Exam : 01 February 2021

FOREWORD

First of all, I would like to thank my family, who has always been with me in my support and love, who has always been with me at every moment, good and bad.
My dear advisor, who I consider as the greatest chance of my academic life and whom I have taken as an example with her professional and human values, I would like to thank Assoc. Prof. Dr. Binnur TEMEL for always guiding and encouraging me with her experiences.
My precious teacher, who showed me how I was a real scientist since I met, and who gave me the conclusion of my thesis, which allowed me to learn English at a high level. I present my gratitude to Assist. Prof. Dr. Ahmed Aly. I would like to thank him for thinking that I can complete the project to the end, with great confidence, teaching all information and experiments about malaria, and for giving me full moral support in this process.
In this challenging period when I did my thesis, I would like to thank my co-advisor, Prof. Dr. Bedia PALABIYIK, who opened the doors of Istanbul University's research responsible for Molecular Biology and Genetics Department. I would like to thank Assist. Prof. Dr. Çağatay TARHAN and Yeast Biotechnology Laboratory esteemed team Research Assistant Burcu KARTAL, Research Assistant Merve YILMAZER for supporting me in the laboratory harmonization process.
A dear researcher who always corrects my mistakes in presentation and writing with a critical attitude. I sincerely thank Assist. Prof. Dr. Matteen RAFIQI.
I would like to thank post doctoral scientist who helped me with thesis experiments dear Dr. Mohd KAMIL for his effort and support.
This study was supported by the Scientific Research Projects Commission of Bezmialem Vakif University with project number 6.2019/12.

December 2020

İlknur YILMAZ
(Molecular Biologist)

DECLARATION

I declare that; this thesis study is mine, I do not have any unethical behavior at all stages of the thesis, I have obtained all the information within academic and ethical rules, I have referred to all information and comments that have not been obtained through this thesis study and I have included them in the list of references, I have not violated any patent and copyright during the study and writing of this thesis.

İlknur YILMAZ

CONTENTS

Page

FOREWORD ... **iii**
DECLARATION ... **iv**
CONTENTS ... **v**
ABBREVIATIONS ... **ix**
TABLE LIST ... **xi**
FIGURE LIST ... **xii**
SUMMARY ... **xv**
ÖZET ... **xvi**
1. INTRODUCTION ... **1**
1.1 Hypothesis ... 1
1.2 Purpose of the Thesis ... 1
1.3 Expectations on Hypothesis ... 3
1.3.1 Novelty ... 3
1.3.2 Innovation ... 3
1.3.3 Impact ... 4
2. THEORICAL INFORMATIONS ... **5**
2.1 Malaria Disease ... 5
2.1.1 Physical syndrome of malaria disease ... 6
2.1.2 Diagnosis of malaria disease ... 7
2.1.3 Parasites of malaria disease ... 8
2.1.3.1 Human malaria parasite *P. falciparum* ... 8
2.1.3.2 Human malaria parasite *P. knowlesi* ... 9
2.1.3.3 Human malaria parasite *P. vivax* ... 9
2.1.3.4 Human malaria parasite *P. malariae* ... 9
2.1.3.5 Human malaria parasite *P. ovale* ... 10
2.1.3.6 Rodent malaria parasite *P. berghei* ... 10
2.1.3.7 Rodent malaria parasite *P. yoelii* ... 10
2.1.3.8 Rodent malaria parasite *P. chabaudi* ... 10
2.1.4 Development of malaria parasite ... 11
2.1.5 Current treatments for malaria infections ... 12
2.2 DNA Photolyase Gene ... 13
2.3 CRISPR-Cas9 Gene Editing Technology ... 20
2.4 Photoconvertible Protein (mEos4b) ... 23
3. MATERIAL AND METHOD ... **27**
3.1 Materials ... 27
3.1.1 Working places ... 27
3.1.2 Devices ... 27
3.1.3 Experimental stuffs ... 29
3.1.4 Software ... 30

3.1.5 Chemicals 30
3.1.6 Stocks 32
3.1.6.1 Antibiotic stock 32
3.1.6.2 Competent cell stock 32
3.1.6.3 Frozen malaria parasite stock 33
3.1.7 Solutions 33
3.1.7.1 Mosquito-breeding solution 33
3.1.7.2 Freezing solution 33
3.1.8 Media 33
3.1.8.1 Bacterial media 33
3.1.8.2 Parasite media 34
3.1.8.3 Mosquito dissection medium 34
3.1.9 Buffers 34
3.1.9.1 Buffers for DNA purification and analysis 34
3.1.9.2 Buffers for competent cell preparation 36
3.1.10 Molecular biological reagents 37
3.1.10.1 Enzymes 37
3.1.10.2 Molecular biological kits 37
3.1.10.3 Molecular markers for gel electrophoresis 37
3.1.11 Biochemical and cellular biological reagents 38
3.1.11.1 Pyrimethamine drug solution preparation 38
3.1.11.2 1X Heparin preparation 38
3.1.11.3 Blood sample preparation for Flow Cytometry 38
3.1.11.4 Ketamine/ Xylasine preparation 38
3.1.11.5 Mounting gel preparation 38
3.1.12 Biological materials 38
3.1.12.1 Experimental live organisms and cells 38
3.1.12.2 Experimental animals 39
3.1.12.3 Mosquitoes 39
3.1.12.4 Parasite strains 39
3.1.13 Nucleic acids 39
3.1.13.1 Oligonucleotids 39
3.1.13.2 Transfection vectors 42
3.2 Method 44
3.2.1 Amplification of the DNA sequences by PCR 46
3.2.2 Analysis and purification of the DNA molecules 51
3.2.2.1 Analysis of DNA molecules by agarose gel electrophoresis 51
3.2.3 Purification of the DNA by the PCR purification kit 52
3.2.4 Purification of the DNA by the ethanol precipitation 52
3.2.5 Determination of the DNA concentration 52
3.2.6 Digestion of inserts after PCR purification 53
3.2.6.1 Left arm of PbDNA Photolyase gene insert digestion and purification 54
3.2.6.2 Right-arm of PbDNA Photolyase gene insert digestion and purification 54
3.2.7 Gel Extractions 54
3.2.7.1 Gel extraction and digestion of Pb Photolyase overlap PCR product (iy05) 54
3.2.7.2 Gel extraction and digestion of MKO1 mEos4b gen region (iy03) 55
3.2.8 Digestion and dephosphorylation reactions of plasmids 55

3.2.8.1 Digestion and dephosphotylation of AA20 Vector 55
3.2.8.2 Digestion and dephosphotylation of AA31 Vector 55
3.2.8.3 Digestion and dephosphotylation of IY03 Vector 56
3.2.8.4 Digestion and dephosphotylation of IY04 Vector 56
3.2.8.5 Digestion and dephosphotylation of UKO6 Vector 57
3.2.9 Designing CRISPR-Cas9 vector 57
3.2.10 Ligations 58
3.2.11 Transformation of recombinant plasmid vectors 59
3.2.12 Isolation of the recombinant plasmids 59
3.2.13 Large-scale DNA preparation of recombinant plasmid vectors 60
3.2.14 Transfection of *Plasmodium berghei* parasites 60
3.2.14.1 Transfection culture preparation 60
3.2.14.2 Isolation of the mature schizonts 61
3.2.14.3 Preparation of transfection plasmids 61
3.2.14.4 Electroporation 62
3.2.15 Positive selection of recombinant parasites 62
3.2.16 Long-term storage of blood stage parasites 62
3.2.17 Isolation of parasite genomic DNA from infected blood 63
3.2.18 Parasite cloning 63
3.2.19 Parasite genotyping 64
3.2.20 Phenotypical analysis of the parasites 64
3.2.21 Mosquito breeding 64
3.2.22 Phenotypical analysis of the midgut oocysts 67
3.2.23 Midgut extraction for oocysts observation 67
3.2.24 Isolation and determination of sporozoite numbers 69
3.2.25 Exflagallation assay 69
3.2.26 Determination of salivary gland sporozoite numbers 69
3.2.27 General phenotypical analysis of rats with sporozoites 70
3.2.27.1 Intravenous injection of rats with sporozoites 70
3.2.28 UVB studies 70
3.2.29 Confocal microscopy studies 71
3.2.30 Dark- light studies 71
3.2.31 Parasitemia pecentage calculations 73
4. RESULTS AND DISCUSSION 74
4.1 Gel Results 75
4.1.1 PCR gel results of Photolyase knock-out inserts 75
4.1.2 PCR gel results of Photolyase knock-in inserts 77
4.1.3 Test digestion gel results of smallscale DNA productions 79
4.1.3.1 Test digestion result for knock-out construct 80
4.1.3.2 Test digestion result for knock-in construct 81
4.1.3.3 Test digestion result for sgRNA construct 82
4.1.4 Diagnostic PCR gel result of knock-out parasite genomic DNA 82
4.1.5 Diagnostic PCR gel result of knock-in parasite genomic DNA 83
4.2 Nanodrop Concentration of Vectors and Inserts 84
4.3 Flow Cytometry Results of Transgenic Parasites 85
4.3.1 FACs result for Photolyase knock-out parasites 85
4.3.2 FACs result for Photolyase knock-in parasites 86
4.4 Light Microscopy Results for Knock-Out Parasites 87
4.5 Confocal Fluorescent Microscopy Results 88
4.5.1 Confocal fluorescent microscopy results for knock-out parasites 88

4.5.2 Confocal fluorescent microscopy results for knock-in parasites 89
4.5.3 Confocal fluorescent microscopy results for mEos4b model 90
4.6 Results of Mosquito Studies 92
4.7 Results of Mouse Studies 94
5. CONCLUSION 99
REFERENCES 101
AUTOBIOGRAPHY 111

ABBREVIATIONS

aa : Amino acids
ATP : Adenosine Triphosphate
ACT : Artemisinin combination treatment
BSA : Bovine serum albumin
BALB/c : Albino experimental mouse
bps : Base pairs
C : Celsius degree
C terminal : Carboxyl terminal
CRISPR : Clustered Regularly Interspaced Short Palindromic Repeats
CPDs : Cyclobutane pyrimidin dimers
CPF : Cryptochrome/Photolyase protein family
CRY : Cryptochrome
CrRNA : CRISPR-RNA
DMEM : Dulbecco's modified eagle medium
DNA : Deoxyribonucleotide acid
dNTP : Deoxyribonucleoside triphosphate
ddwater : Double distilled water
ddH_2O : Double distilled water
dCas9 : Dead Cas9
DNA : Deoxyribonucleic acid
E. coli : *Escherichia coli*
F : Forward, in the sense direction of a gene
FAD : Flavin adenine dinucleotid
gRNA : Guide ribonucleic acid
g : Gram
GFP : Green Flourescence Protein
hDHFR : Human dihydrofolate reductase
h : Hour
HDR : Homology DNA repair
In vitro : *in vitrum(glass),* in a test tube
In vivo : *in vivus(living),* in a living organism
ITNs : Pesticide treated nets
IRs : Insecticide residual spraying
IPTp : Intermittent preventive treatment
kDa : Kilodalton
kb : Kilo base pairs
kg : Kilogram
kb : Kilobase
KO : Knock-out
KN : Knock-in
l : Liter
JOVE : Journal of Visual Experiments

LB Medium : Luria-Broth medium
LS : Liver-stage
LLINs : Long-term pesticide impregnated nets
m : Meter
M : Molar
mg : Miligram
min : Minute
ml : Milliliter
mM : Milimolar
mEos4b : Fusion protein
MTHF : Methyltetrahydrofolate
NHEJ : Non-homologous end joining
NER : Nucleotide excision repair
N terminal : Amino terminal
nm : Nanometer
OD : Optimal density
P. : Plasmodium
PAM : Protospacer contigous motif
pH : Potentia hyrogenii
PbWT : *Plasmodium berghei* wild type
PbPhoto(-) : *Plasmodium berghei* Photolyase deletion
PbPhoto(+) : *Plasmodium berghei* Photolyase insertion
P.berghei *: Plasmodium berghei*
P.yoelii *: Plasmodium yoelii*
P.falciparum *: Plasmodium falciparum*
P.vivax *: Plasmodium vivax*
PBS : Phosphate buffered saline
PtFP : Phototransformable Fluorescence Protein
PcFP : Photoconvertible Fluorescence Protein
PaFP : Photoactivable Fluorescence Protein
PCR : Polymerase chain reaction
R : Reverse, in the anti-sense direction of a gene
RBC : Red blood cell
RNA : Ribonucleic acid
RDT : Rapid diagnostic test
rpm : Revolutions per minute
RPMI : Rosewell Park Memorial Institute
sec : Second
sgRNA : Single guide ribonucleic acid
Taq : Thermus aquaticus
TB : Terrific broth
TracrRNA : Non-coding trans-activating crRNA
U : Unit, biochemical unit for enzymatic activity
UVB : Ultraviolet B light
V : Volt
WT : Wild type
wtGFP : Wild type Green Fluorescence Protein
µl : Microliter
µg : Microgram
µM : Micromolar

TABLE LIST

Page

Table 3.1 : %1 Agarose gel reagents..... 35
Table 3.2 : % 0.9 Agarose Gel Reagents 35
Table 3.3 : Transgenic vector names created by Ilknur Yilmaz (IY). 43
Table 4.1 : Results for digested inserts 84
Table 4.2 : Results for digested vectors. 84
Table 4.3 : Results for maxipreps. 85
Table 4.4 : Results for linearized precipitated DNA. 85
Table 4.5 : FACs sort statistics for Pb (-) IV injection. 86
Table 4.6 : Animal normal light- dark, UVB light study parasitemia (%) results. .... (Red- Green: WT, Blue- Black: KO). 95

FIGURE LIST

Page

Figure 2.1 : The map shows areas where *Plasmodium falciparum* is endemic ..... around the world..... 5
Figure 2.2 : The image shows a thin (left) and thick (right) smear in Malaria ..... positive patient..... 8
Figure 2.3 : Malaria parasite life cycle 12
Figure 2.4 : DNA Photolyase gene discovery by Prof. Dr. Aziz SANCAR..... 14
Figure 2.5 : Characterization and over production of DNA photolyase enzyme in .. *E.coli*..... 15
Figure 2.6 : Homologous region of Photolyase and Cryptochrome gene..... 17
Figure 2.7 : DNA Photolyase enzyme 3D..... 19
Figure 2.8 : CRISPR-Cas9 protein 3-step working mechanism. 21
Figure 2.9 : mEos4b a phototransformable fluorescent protein..... 25
Figure 3.1 : AA20 Plasmid used for knock-out, knock-in vector..... 43
Figure 3.2 : Study plan..... 44
Figure 3.3 : Knock-out study construct..... 45
Figure 3.4 : Knock-in tagging study construct..... 46
Figure 3.5 : Red enzyme PCR program. 47
Figure 3.6 : Q5 PCR program. 49
Figure 3.7 : Overlap PCR for Pb DNA Photolyase gene. 50
Figure 3.8 : An example for nanodrop result of DNA concentration. 53
Figure 3.9 : Designed Cas9 expression vector for Photolyase knock-out. 58
Figure 3.10 : *E.coli c*olony image for AA31 transgenic stbl3 cells. 59
Figure 3.11 : Pupa collection. 65
Figure 3.12 : Mosquito cage with eggs into dish. 66
Figure 3.13 : Larva and pupa of *Anopheles stephensi* mosquitoes. 67
Figure 3.14 : Mosquito infection..... 68
Figure 3.15 : The plan of UVB application study after parasite transfection. 71
Figure 3.16 : Animal study **A.** Two Wistar rat has been used as donor for *P.berghei* parasite development for trasfection parasite culture. **B.** Three Balb/c mice has been used for each Knock-out, Knock-in strain for parasite .. genotyping via drug sellection. **C.** Three Balb/c mice used for each .... transgenic strain under three light applications. 72
Figure 4.1 : PCR gel result of *Plasmodium berghei* DNA Photolyase 5' UTR (left arm). 75
Figure 4.2 : PCR gel result of *Plasmodium berghei* DNA Photolyase 3' UTR (right arm)..... 76
Figure 4.3 : PCR gel result of mEos4b gene integration into the knock-out vector. A) Scheme for expected mEos4b integration. B) Gel result for 5' Test (5'Forward primer with mEos4b R primer), 3' Test (mEos4b F primer with 3' R primer) and PbPhoto open reading frame..... 76
Figure 4.4 : The scheme of overlap PCR for *Plasmodium berghei* DNA Photolyase gene amplification. 77

Figure 4.5 : Q5 PCR result of 1-2 insert and 3-4 insert. L: DNA Ladder, A: Q5 ..... PCR products of 1-2 insert at 68 ^{o}C extension, B: Q5 PCR products of 1-2 insert at 64 ^{o}C extension, C: Red enzyme PCR product of 3-4 ..... insert as control, D: Q5 PCR products of 3-4 insert at 64 ^{o}C extension, E: Q5 PCR products of 3-4 insert at 68 ^{o}C extension..... 78
Figure 4.6 : Q5 Overlap PCR result of *Plasmodium berghei* DNA Photolyase ..... gene..... 79
Figure 4.7 : Test digestion gel result of IY03 minipreps.The minipreps were cut ... with HindIII-Kpn1 restriction enzymes..... 79
Figure 4.8 : Test digestion gel result of IY04 minipreps. The minipreps were cut .. with Sac2-BamH1 restriction enzymes. L: DNA Ladder, M: Miniprep 80
Figure 4.9 : Test digestion gel result of PbPhoto(-) construct. L: DNA Ladder 1) .. Sac2-Bamh1 digestion of IY10 vector, 2) HindIII-Kpn1 digestion of .. IY10 vector, 3) Sac2-Kpn1 digestion of IY10 knock-out vector. 81
Figure 4.10 : Test digestion gel result of PbPhoto (+) a) miniprep (small scale DNA production) and b) maxiprep (large scale DNA production) of IY05 ... vector. L: DNA Ladder..... 81
Figure 4.11 : Test digestion results of IY26 (gRNA+ Cas9) minipreps. L: DNA ..... Ladder, M: Miniprep (small scale DNA product of one colony). 82
Figure 4.12 : Targeted deletion of the DNA Photolyase gene into *P. berghei* ..... parasite with CRISPR-Cas9 technology. Gel result of diagnostic PCR. (Pink dot shows knock-out parasite genomes, grey dot showes Pb WT genome)..... 83
Figure 4.13 : Targeted insertion of the DNA Photolyase gene into *P. berghei* ..... parasite with CRISPR-Cas9 technology. Gel result of diagnostic PCR. (Pink dot shows knock-out and knock-in parasite genomes, grey dot .. showes Pb WT genome)..... 84
Figure 4.14 : Flow cytometry result for PbPhoto(-) parasites..... 85
Figure 4.15 : Flow cytometry result for PbPhoto(+) parasites..... 87
Figure 4.16 : Giemsa stained PbWT (Plasmodium berghei wild-type) throphozoite . form of parasite enfected blood cells thin smear result under light ..... microscopy. 88
Figure 4.17 : Giemsa stained PbPhoto(-) throphozoite form of parasite enfected ..... blood cells thin smear result under light microscopy. 88
Figure 4.18 : Confocal fluorescent result P. berghei DNA Photolyase knock-out ..... parasites. a) 40X, DAPI, b) 40X, GF, c) 40X, Bried-field, d) 40X, RF. 89
Figure 4.19 : *P. berghei* DNA Photolyase knock-in-tagging parasites..... 90
Figure 4.20 : PbPhoto(-) parasites a) before and b) after one minute of blue light .... application. 91
Figure 4.21 : PbPhoto(-) parasites before blue light application. Blood cells ..... captured with brield-field, DAPI, green and red fluorescence. 91
Figure 4.22 : PbPhoto(-) parasites after 30 seconds of blue light application blood .. cells captured with brield field, green and red green and red ..... fluorescence. 92
Figure 4.23 : Pb Photolyase (-) sporozoites exctracted from a *Anopheles stephensi* .. mosquito salivary gland..... 93
Figure 4.24 : Pb Photolyase (-) oocysts in midgut of a *Anopheles stephensi* ..... mosquito. 93

Figure 4.25 : Parasitemia percentage of PbWT vs. PbPhoto(-) light condition..... 97
Figure 4.26 : Parasitemia percentage of PbWT vs. PbPhoto(-) dark condition..... 98

GENE TARGETING STUDIES OF THE MALARIA PARASITE DNA PHOTOLYASE GENE USING CRISPR-CAS9 GENOME EDITING TECHNOLOGY

SUMMARY

Ultraviolet (UV) light damages DNA by converting two adjacent thymine bases into pyrimidine dimers. In all organisms, except mammals, this damage is repaired by the photolyase enzyme [1, 2]. Prof. Dr. Aziz SANCAR has won the Nobel Prize for the characterization of the role of a homolog of the photolyase enzyme in higher eukaryotes in the control of the circadian rhythm. Surprisingly, no research has been conducted on the photolyase gene of the malaria parasite or of any other parasitic protozoa. Recently, it was confirmed that a genetically- regulated circadian rhythm tightly controls the development and growth of malaria parasites according to external light stimuli [3]. However, the genetic factors that control this system have not yet been discovered.

In order to investigate the role of the malaria parasite DNA Photolyase enzyme in the mechanism of the circadian rhythm regulation of the malaria parasite, in addition to its putative function as a DNA repair enzyme, we utilized a novel CRISPR-Cas9 system with enhanced-specificity Cas9 function, to limit the genome off-target endonuclease activity, to investigate the function of DNA Photolyase by targeted gene knock-out deletion and knock-in tagging.

The DNA photolyase knock-out parasites failed to grow normally compared to wildtype (WT) parasites, with even more severe growth attenuation when perturbations of ambient light conditions were applied.

Thus, we are initially confirming the role of malaria parasite DNA photolyase in the regulation of the responses to the light/ dark cycle, and an additional function in DNA repair due to UV light exposure. Therefore a more in-depth investigation is needed to detail the molecular function of the DNA Photolyase in the malaria parasite and in other pathogenic microorganisms.

Keywords: Malaria, *Plasmodium berghei*, DNA Photolyase, UVB DNA Damage, Circadian Rhythm, CRISPR-Cas9

CRISPR-CAS9 GENOM DÜZENLEME TEKNOLOJİSİ KULLANILARAK MALARYA PARAZİTİ DNA FOTOLİYAZ GENİ İÇİN GEN HEDEFLEME ÇALIŞMALARI

ÖZET

Ultraviyole (UV) ışık, iki timin bazını pirimidin dimerlerine dönüştürerek DNA'ya zarar verir. Memeliler dışındaki tüm organizmalarda bu hasar fotoliyaz enzimi tarafından onarılır [1, 2]. Prof. Dr. Aziz SANCAR, sirkadiyen ritmin kontrolünde yüksek ökaryotlarda fotoliyaz enziminin homologunun fonksiyon karakterizasyonu ile Nobel Ödülü'nü kazanmıştır. Şaşırtıcı bir şekilde, sıtma parazitinin veya herhangi bir başka parazitik protozoanın fotoliyaz geni üzerinde hiçbir araştırma yapılmamıştır. Yakın zamanda, genetik olarak düzenlenmiş bir sirkadiyen ritmin sıtma parazitlerinin gelişimini ve büyümesini dış ışık uyaranlarına göre sıkı bir şekilde kontrol ettiği doğrulanmıştır [3]. Ancak bu sistemi kontrol eden genetik faktörler henüz keşfedilmemiştir.

DNA onarım enzimi olarak varsayılan işlevine ek olarak kemirgen sıtma paraziti DNA Fotoliyaz enziminin parazit sirkadiyen ritim düzenlenleme mekanizmasındaki rolünü araştırmak için, genomda hedef dışı endonukleaz aktivitesini sınırlandırma ve DNA Fotoliyaz geninin fonksiyonunu araştırma amacıyla gen delesyonu ve insersiyonu, etikletlenmesi için gelişmiş özgüllük özelliğine sahip yeni bir CRISPR-Cas9 sistemi kullanılmıştır.

DNA Fotoliyaz nakavt parazitleri, doğal tip (WT) parazitlere kıyasla normal olarak kan-evre aşamasında parazit çoğalmasında başarısız olmuştur, ortam ışığı koşullarının bozulmaları uygulandığında parazit çoğalmasında daha şiddetli azalma olmuştur.

Böylece, başlangıçta sıtma parazit DNA fotoliyaz geninin, ışık / karanlık döngüsüne verilen yanıtların düzenlenmesindeki rolünü ve UV ışığına maruz kalma nedeniyle DNA onarımında ek bir işlevi doğruluyoruz. Bu nedenle, sıtma parazitindeki ve diğer patojenik mikroorganizmalardaki DNA Fotoliyaz geninin moleküler işlevini ayrıntılandırmak için daha derinlemesine bir araştırma yapılmasına ihtiyaç duyulmaktadır.

Anahtar Kelimeler: Malarya, *Plasmodium berghei*, DNA Fotoliyaz, UVB DNA Hasarı, Sirkadiyen Ritim, CRISPR-Cas9

1. INTRODUCTION

1.1 Hypothesis

DNA Photolyase plays a very important role in DNA repair mechanisms. In this thesis, the importance of the photolyase gene for the development and life of the malaria parasite emphasized by providing deletion and insertion of the malaria parasite DNA Photolyase gene, which has not been investigated before. The deletion of this gene in the rodent malaria parasites and creating mutations by UVB light can find different knowledge about parasite life cycles or unknown genes. Also, in this thesis, by integrating phototransformable fluorescent proteins in the Plasmodium parasite we are having a novel powerful fluorescent biological model system.

The hypothesis is in the absence of the DNA Photolyase gene, malaria parasites accumulate massive number of mutations in their DNA while inside their mammalian or mosquito host.

1.2 Purpose of the Thesis

In this effort, we aimed to generate a CRISPR-Cas9-based vector specific for targeting genes in rodent malaria parasites.

Specific aims of our study;

We aim to utilize CRISPR-Cas9 technology to genetically characterize the DNA photolyase enzyme (that Prof. Dr. Aziz SANCAR has first characterized in higher eukaryotes) in the rodent malaria parasite species *P.berghei* by performing,

Gene knock-out, to study the loss of function phenotype of the malaria parasites under exposure of normal and UV light [4].

Gene knock-in-tagging, to study the subcellular localization of the photolyase and as a control for the knock-out to determine the chromosomal locus accessibility if the gene cannot be deleted.

To date, no research has been performed for the DNA Photolyase gene in malaria parasites or pathogens. The main objective of our study is to determine the function of deletion and insertion of the DNA Photolyase gene by using *Plasmodium berghei* rodent (mouse model) malaria parasite using CRISPR-Cas9 technology, to detect unknown genes of the parasite by detecting DNA mutations by using UV light and to determine the significance of the parasite. We generated transgenic malaria parasite species by parasite transfection of knock-out, knock-in, which we created for detailed function research of the gene. We applied the UVB light to the transgenic species and monitored the effect of the parasite genome change and the struggle of the parasite in the mosquito-stage and mouse blood-stage. Photolyase gene deletion (knock-out) to examine phenotype change with the loss of function of malaria parasites exposed to normal and UVB light.

We made DNA Photolyase gene insertion and labeling as a control of the knock-out plasmid to examine the subcellular localization of Photolyase to determine the availability of the chromosomal locus if the gene is not detected. For the gene insertion study, we labeled the malaria parasite vector, the bright green to red photoconvertible mEOS4b fluorescent proteins.

After the deletion of this gene, we applied the UVB light to cause a pause or weakening in the life cycle of the rodent malaria parasite. This will give us the chance to design an ideal vaccine for malaria disease. At the same time, we can say that the absence of this gene in humans will only affect the parasite, not the normal cells of the infected people. By applying UV light, mutations in the parasite DNA will allow us to discover the function of an unknown gene. Photo-convertible fluorescent proteins are widely used for plastid dynamics, monitoring peroxisomes, protein dynamics in cilia, mitochondrial dynamics, and autophagy activity sensors. Thus, in this project, we have a new and powerful fluorescent biological model system by integrating photo-convertible fluorescent proteins into the knock-out vector. We examined the development of the parasite in the *Anopheles stephensi*, mosquito abdomen or in the salivary glands, the infected BALB/c mouse blood, and any problems that occur there can be visibly observed through the photoconvertible protein. Parasitic cytocidal (light green, light pink glow), cytotoxic (red glow, parasite death), or green glow (normal) will determine the direction of our research by making the case. In the future, we will investigate the function of photolyase transgenic parasite strains exposed to UV (480

nm) light exposure in the salivary gland and BALB-c liver-blood stages in the Anopheles mosquito midgut lumen, using UV light in transgenic rodent malaria parasites we designed [5].

1.3 Expectations on Hypothesis

1.3.1 Novelty

DNA Photolyase, an important repair protein in damaged DNA repair, is still a question mark for malaria parasites. Although recent research has shown that the presence of circadian rhythm in malaria parasites and their phenotypic genes play a role in activation times, little is known about the name and functional and biological roles of this gene. Therefore, in this thesis, we aim to genetically characterize the DNA Photolyase protein in the regulation of malaria parasite DNA dimers. As far as we know, this is the first of its kind to focus on systematically functioning characterizing as a role in the life cycle of an important pathogen with DNA damage. Therefore, innovation for this project can be summarized as follows:

1- This is the first study for the genetic characterization of the plasmodium DNA Photolyase gene in any mouse malaria model.

2- This is the first study to control the role of gene deletion at different stages of the malaria parasite life cycle.

3- The first study to suggest that the parasite vector be labeled with photoconvertible markers.

4- It is the first study of its kind to discover unknown genes in malaria parasites by applying UV light.

1.3.2 Innovation

The experimental procedures include the use of innovative state of the art technologies to achieve the specific aims of this project. These innovative approaches include;

1- The use of novel enhanced-specificity Cas9, that nearly abolishes off-target double strand breaks, in transfection experiments of the malaria parasite.

2- Using CRISPR-Cas9 gene editing technology to label the parasite DNA Photolyase gene without using a positive drug selection marker.

3- The use of the most advanced fluorescent protein marker, mEos4b.

1.3.3 Impact

The knowledge accrued from this novel and innovative project will have multiple positive future outcomes like:

1- The study will help in the identification of key proteins required in different life cycle stages of the malaria parasites.

2- The outcome of the study may help in designing novel targeted therapies for the effective treatment of malaria and other diseases caused by eukaryotic pathogens, which can be explored in many collaborating laboratories mainly inside but also outside of Turkey.

3- The findings of the study are expected to be published in high impact journals.

If we lack the gene repair mechanism we target, we will prevent parasite reproduction and weaken the parasite. Thus, vaccine and drug candidates that can be tried on the mouse in the first place can be created.

Feasibility of the thesis study

The experimental models, facilities and trained personnel that are required for the success of these experiments have been fully established in the lab of Dr. Aly (Advisor of the study and PI of the lab) at the Beykoz Institute of Life Sciences and Biotechnology. We have published a video article in JOVE, which features our current experiments with the mouse and mosquito models [6].

2. THEORICAL INFORMATIONS

2.1 Malaria Disease

Malaria is a contagious and deadly disease spread by female Anopheles mosquitoes [6]. Half of the almost 3.3 billion people population in Sub-Saharan Africa are at risk of malaria due to lifestyle conditions [7]. The mild climate (over 19-20°C) and long wet seasons in Africa create areas of standing water ideal for mosquitoes to breed [8]. The bad habitats of people in these areas (houses without doors and windows open) increase the likelihood of mosquitoes coming into contact with humans [9]. Some homes are close to forests that provide ideal habitats for mosquito species [10].

Figure 2.1 shows that the highest malaria levels are between the Tropic of Cancer and Tropic of Capricorn. People traveling from Europe and Asia to malaria-endemic regions have a 70 % or more risk of developing the disease [11]. People visiting these areas, such as vacationers and migrant workers, are vulnerable to infections as they are not immune to disease [12]. Most malaria deaths occur in children under the age of five [13]. Pregnant women are more vulnerable to malaria, as they have low natural immunity. The effect of the disease may have negative consequences in the unborn babies of pregnant women exposed to malaria.

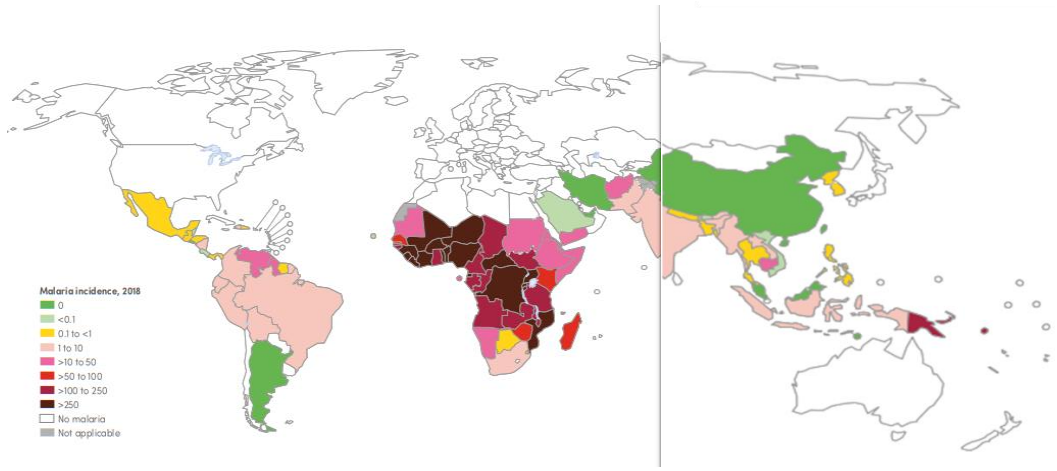

Figure 2.1 : The map shows areas where *Plasmodium falciparum* is endemic around the world [14].

Premature birth or miscarriage may occur in pregnant women with the effect of illness. Placental infections cause low infant mortality. 11 million pregnant women were infected with malaria in 2018 [14]. Even though mosquito nets treated with insecticides are considered an alternative method of protecting pregnant women, preventive malaria medications are not tested by 40 % of patients and are not handled by a trained healthcare professional [15]. Anti-malaria drugs kill the malaria parasite at a certain rate, but these drugs do not sufficiently prevent the patient from being re-infected [16]. The use of malaria medications in the early stages of the disease shortens the duration of infection and prevents potentially fatal complications [17]. Unfortunately, an effective drug against the disease or a vaccine for immunization has not yet been developed. Malaria is a fatal disease in developing countries, particularly in damp and hot areas of the world, affecting women and children [18]. Malaria causes illness in 290 million people and approximately 435,000 people die annually [19]. Since there is no effective treatment for the disease, there is an urgent need for a vaccine that provides sterile protection against pathogenic blood forms of malaria parasites. To be used as a vaccine, microorganisms must be killed or completely weakened. One of the strategies of attenuation is the inactivation of critical pathogenic metabolic pathways [20]. However, the function of many genes belonging to malaria parasites has not been discovered. Therefore, DNA fractures and pyrimidine dimers that we create by using UV radiation may cause loss of function of a gene that we do not know the name of and may cause the development of parasite can be blocked or it may cause attenuated parasites. The proliferation of parasite clones resistant to antimalarial drugs limits the classes of chemicals that can be further developed to combat drug resistance. Therefore, there is a great need for studies to identify novel classes of inhibitors in the metabolic functions of parasites and to identify new classes of inhibitors that can target these metabolic functions in a specific and selective way and prevent the development of parasites at different stages of the life cycle [21].

2.1.1 Physical syndrome of malaria disease

Symptoms of severe malaria include loss of consciousness, prostration (inability to sit without assistance), multiple convulsions, cerebral malaria coma, abnormal bleeding, jaundice, severe anemia, renal failure, hypoglycemia, hyperparasitemia, hyperpyrexia, respiratory distress, and circulatory collapse [22]. Studies show that malaria patients generally have complaints of fever, headache, nausea, vomiting, and muscle pain [23].

Fever, night sweats, chills and weakness are seen in children within a week. Weight loss is seen under their age. There is a slight increase in heart and respiratory rates, and enlarged lymph nodes on both sides of the neck [24]. In a 40-year-old adult, with chills, and fever, malaria starts, jaundice and severe substernal chest pain may occurs six hours later [25].

2.1.2 Diagnosis of malaria disease

Today, malaria infections are diagnosed by microscopy and rapid diagnostic tests (RDT). In Africa, microscopy diagnostic methods can only be used in laboratories with electrical and trained medical personnel. In microscopic diagnosis, a thin smear of a drop of blood is used to determine the presence of malaria parasites in a patient suspected of malaria infection [26]. The second diagnostic method is RDT tests. RDTs are rapid tests using a drop of blood from the fingertip to determine whether it is evaluative malaria. The tests are sensitive to antigens (proteins produced by the parasite) that bind with a dye to create a colored stripe that indicates the presence of parasites in the blood. The time required for the result of an RDT test is 15 minutes [27].

A thin smear is created by spreading the blood cells in a drop on the slide in a single row. After the cells are fixed with methanol and stained with Giemsa, the parasite appears as a purple-blue ring in the red blood cell in malaria-positive people. The purple part indicates the nucleus of the parasite and the blue ring indicates the cytoplasmic membrane. In a thick smear, the blood cells in a drop on the slide are exploded and the parasite is exposed. However, as the vacuolar cavity of the parasite is damaged, only the parasite nuclei appear as purple spots after Giemsa staining. (see Figure 2.2) [28].

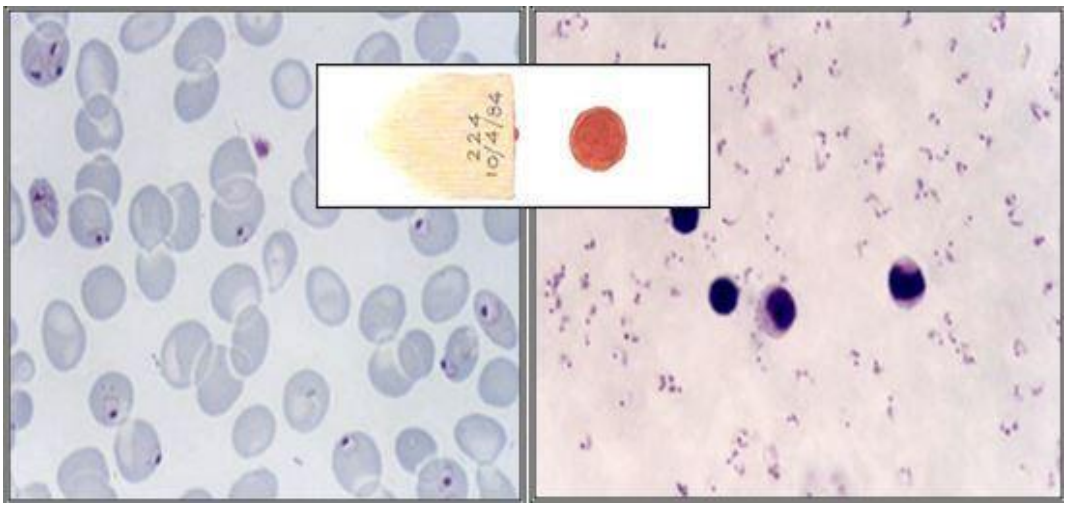

Figure 2.2 : The image shows a thin (left) and thick (right) smear in Malaria positive patient.

2.1.3 Parasites of malaria disease

Malaria is caused by a unicellular eukaryotic protist. The parasite belongs to a genus known as the Plasmodium. Five Plasmodium species infect humans: *Plasmodium vivax, Plasmodium ovale walkeri, Plasmodium ovale curtisi, Plasmodium malariae and Plasmodium knowlesi* [29]. *Plasmodium falciparum* causes serious complications and, if left untreated, has fatal consequences. It is responsible for most deaths due to malaria. *Plasmodium vivax* is located in Turkey's Southeastern Anatolia Region [30].

2.1.3.1 Human malaria parasite *P. falciparum*

Plasmodium falciparum belongs to the phylum Apicomplexan and is characterized by the presence of apicoplasts [31]. The *P. falciparum* (Pf) malaria parasite reinstates the surface of the infected red blood cell with a feature called cytoadherans ("adhesive cell"), creating a sticky phenotype that removes the parasite from circulation during almost half of its asexual life cycle [32]. In the human host, male and female gametocytes are produced in blood-stage *Plasmodium falciparum* parasite development. Gametocytogenesis in this parasite requires a relatively long time (8-12 days) than other human malaria parasite species. It is found in the peripheral blood where gametocytes take an additional 3 days to become infectious to mosquitoes [33]. *P. falciparum* can express allelic variants of hundreds of different versions of erythrocyte surface antigens [34].

2.1.3.2 Human malaria parasite *P. knowlesi*

P. knowlesi (Pk) malaria parasite is found in Southeast Asian countries Malaysia/Indonesia Borneo. The disease occurs when exposed to mosquitoes that feed on long-tailed or pig-tailed macaques [32]. Some of its features are the same as those of *P. falciparum.* These; morphological features are delicate ring forms, two ring forms per cell, and double chromatin spots. Parasitized red blood cells are not enlarged. A common problem is the misidentification of *P. knowlesi* as *P. malariae*, especially as both parasites produce band form trophozoites [35].

2.1.3.3 Human malaria parasite *P. vivax*

Plasmodium vivax is the most common causative agent of malaria worldwide. Infections are rarely fatal but have significant health and economic impacts on populations affected by the disease. The *P. vivax* episode is due to hypnozoite stages in the liver that have been immobilized from previous infections [36]. *Plasmodium vivax* parasites are divided into two in terms of the length of their life cycles and differ primarily in the symptoms of the disease. Elimination of the *Plasmodium vivax* parasite is thought to occur at least two years after the elimination of the plasmodium parasite [37]. *P. vivax* differs from other human malaria parasites in that it infects reticulocytes (newly formed blood cells). Reticulocytes are present in the circulation at a rate of 1-2 %. Since *Plasmodium vivax* parasite could not be cultured in vitro, the mechanism of early blood-stage infection could not be elucidated [38].

2.1.3.4 Human malaria parasite *P. malariae*

P. malariae can be found in tropical and subtropical regions. Due to its phenotypically similar characteristics to *Plasmodium falciparum,* it is difficult to determine the species correctly in sub-Saharan Africa unless molecular techniques such as polymerase chain reaction (PCR) are used for diagnosis. *P. malariae* infection may relapse late years later. However, the absence of hypnozoites in liver cells after infection eliminates the possibility of the parasite being re-infected [39]. *P. malariae* and *P. ovale spp.* are less common and there are limited studies on them. The development of molecular methods on parasite detection has enabled the parasite species to be identified correctly [40].

2.1.3.5 Human malaria parasite *P. ovale*

P. ovale spp, a species of malaria parasite, is rarely found in Africa and some islands of the Western Pacific. This species is morphologically similar to *P. vivax.* As a result of molecular genotyping by PCR, *P. ovale spp.* is divided into two different subspecies: *P. ovale curtis* (Poc) and *P. ovale wallikeri* (Pow). Poc and Pow parasites are morphologically similar but genetically different from each other [40]. The possibility of severe disease or death in patients infected with *P. ovale* parasite is rare [41].

2.1.3.6 Rodent malaria parasite *P. berghei*

P. berghei malaria-causing parasite in rodents isolated from bush mice in central of Africa. Four malaria parasite species *Plasmodium chabaudi, Plasmodium vinckei and Plasmodium yoelii* with *P. berghei* have been identified in African rodents [42]. *P.berghei,* a mouse model of the malaria parasite, is used in all studies on malaria, due to the immune system and organ similarities of human and murine rodents. Generally, *P. berghei* ANKA infection in CBA or C57BL/6 mice is the most widely used malaria model. *Plasmodium berghei* ANKA is the species with the highest ability to sequester within the microcirculation, which is the cause of severe malaria. *P. berghei* infections may cause cerebral complications in experimental mice. It is similar to *Plasmodium falciparum* because of these symptoms [43]. *P. berghei* has been shown to infect *Anopheles stephensi* mosquitoes under laboratory conditions [44]. The *P. berghei* genome is a strain suitable for genetic manipulation [45].

2.1.3.7 Rodent malaria parasite *P. yoelii*

Plasmodium yoelii has been used to infect experimental mice in the laboratory as a model of human malaria because the immune response of the rodent malaria parasite is similar to that of the human immune response [46]. The sporozoites of the rodent parasite *Plasmodium yoelii* transform into oocyst form approximately 10 to 12 days after fertilization [47]. The most suitable animal for investigating *Plasmodium yoelii* infection is BALB/c type mice [48].

2.1.3.8 Rodent malaria parasite *P. chabaudi*

P. chabaudi rodent malaria parasite discovered by infecting bush mouse, since the scrub mouse is not suitable for the laboratory environment, the *P. chabaudi chabaudi*

(AS) clone is studied in vitro in experimental mice [49]. *P. chabaudi chabaudi* resembles human malaria due to pathologies such as anemia, hypoglycemia, changes in body temperature, weight loss, and death in experimental mice [50]. In *P. chabaudi* (AS) BALB/c or C57Bl/6 test mice infection, the course of the disease lasts for at least three months. In this respect, it resembles *P. falciparum* infection (infection lasts up to 1 year) [51]. Another feature of *P. chabaudi* similar to *P. falciparum* infects normocytes [52].

2.1.4 Development of malaria parasite

Malaria infection in humans begins with an infected female Anopheles mosquito biting the human dermis [53]. During the bite, the human malaria parasite from the mosquito salivary glands enters the human bloodstream in sporozoite form (sickle single-cell form) [54]. Sporozoites reach the liver and infect liver cells, hepatocytes. This stage is called the Liver Stage (LS) [55]. The liver stage (LS) parasite is separated from the hepatocyte infected by a selective parasitofor vacuolar membrane (PVM) originating from the host hepatocyte plasma membrane. The growing LS parasite draws nutrients from the host hepatocyte and also prevents its apoptosis. Each infected hepatocyte can produce tens of thousands of merozoites, which then break off from the liver and start the pathogenic blood stage of the infection [19]. Figure 2.3. shows life cycle of malaria parasite. The plasmodium parasite performs part of its life cycle in the human host and the other part in the mosquito vector. There are essentially five basic stages in the life cycle. Anopheles mosquito infects Plasmodium parasite (long, thin, a form of sporozoite that can move between cells and inside) by biting the human. The sporozoites reach the liver through the portal vein blood circulation and occupy it to multiply. In the liver, it turns into thousands of new parasites known as merozoites. Merozoites invade red blood cells and begin to multiply in the blood cell. (Each merozoite enters a red blood cell and after it enters, it divides asexually to form up to 20 new merozoites). Merozoites invade neighboring red blood cells by detonating blood cells. This whole process takes about 48 hours. Some parasites do not form merozoites but turn into a sexual phase of the life cycle called gametocyte. These are taken by a mosquito when they feed on an infected person. After entering the mosquito intestines, gametocytes turn into mature gametes (eggs and sperm) that melt and turn into an ookinete. The ookinete passes through the lining of the mosquito gut wall, where it forms an oocyst, in which tens of thousands of sporozoites are formed. They

burst from the oocyst and go to the salivary gland of mosquitoes, where the cycles restart [56].

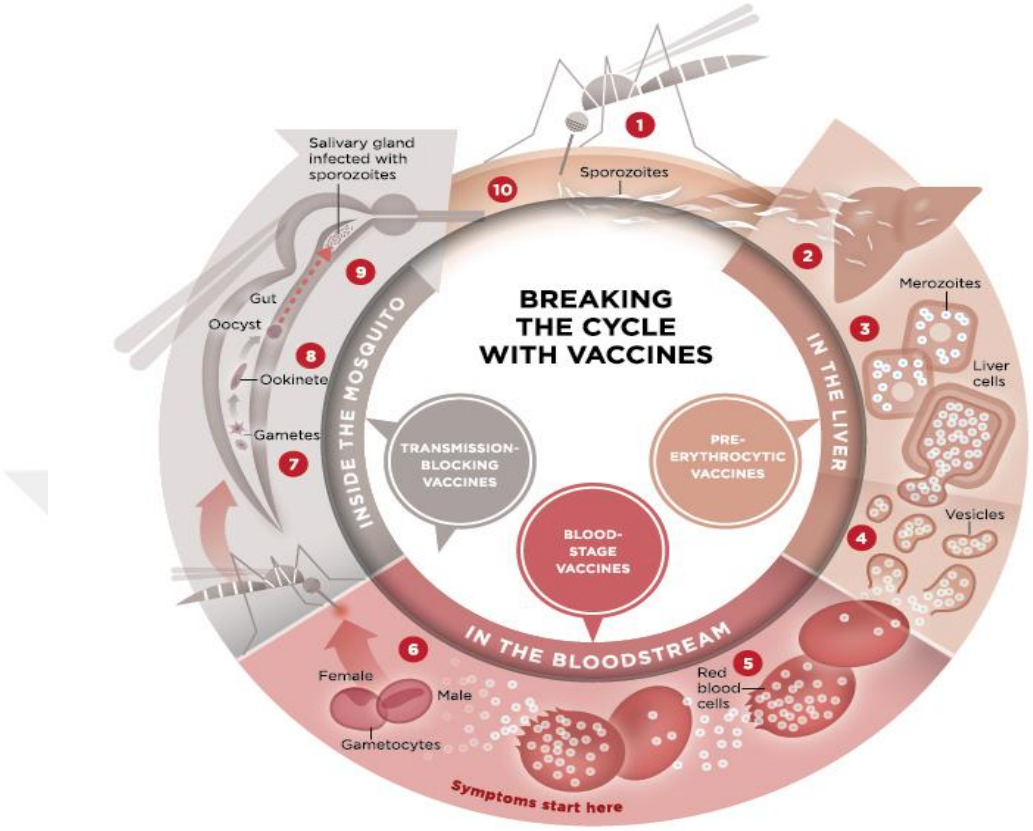

Figure 2.3 : Malaria parasite life cycle [57].

2.1.5 Current treatments for malaria infections

The first defense mechanism developed against malaria infection is that individuals wear mosquito nets inside or provide personal protection against mosquito bites by using insect repellents. Pesticide treated nets (ITNs) and long-term pesticide impregnated nets (LLINs) form a physical and chemical barrier against mosquitoes. LLINs are the preferred form of pesticide-treated networks for public health and are recommended by the World Health Organization for 3-5 years of effectiveness [58]. Another developed way to prevent malaria transmission is residual spraying with insecticides (IRS). Depending on the insecticide and surface type, this method can be effective for 3 to 6 months [59]. Another method that can be used against malaria is the use of DTT. DTT can be effective for 9 to 12 months. However, long-lasting insecticide-impregnated nets (LLINs), pesticide-treated nets (ITNs), indoor spraying, mosquito repellents, and preventive drug treatments do not provide long-term and

effective solutions. Travelers use drugs such as chemoprophylaxis that block the blood-stage stage of the malaria parasite. However, since these drugs cannot prevent the parasite from entering the body, the parasites that settle in the liver cannot prevent the recurrence of the infection in the future [60]. Intermittent Preventive Treatment (IPTp) is applied during pregnancy in order to reduce possible complications such as severe anemia and placental infections due to malaria infection that can threaten the life of the mother and child [61]. WHO recommends combination treatments (ACT) of artemisinin to treat *Plasmodium falciparum* infections. Medicines such as chloroquine and primaquine are recommended for *Plasmodium vivax* malaria [62]. Anti-malarial drugs kill the parasite but do not prevent the patient from reinfecting. Early and effective treatment of malaria with anti-malaria drugs can shorten the duration of the infection. Uncontrolled use of single-drug treatments such as chloroquine in the past has led to the parasite developing drug resistance. Malaria parasites have developed resistance to today's malaria drugs [63]. Discovered in the 1990s, Artemisinin is used in combination with other drugs to prevent *Plasmodium falciparum* infections. Artemisinin is recommended by the World Health Organization as the first-line treatment for malaria [64].

2.2 DNA Photolyase Gene

In his doctoral studies, Prof. Dr. Aziz Sancar acquiesced the bacterium to produce Photolyase enzyme extraordinary, separately from the genome by cloning the gene sequence into the expression vector to obtain the Photolyase gene function, which repairs UV damaged pyrimidine dimers in bacterial DNA. Professor Dr. Aziz Sancar demonstrated the existence of the enzymatic DNA repair mechanism of the DNA Photolyase gene in bacteria. Hence he explained the photo-activation mechanism [65].

Figure 2.4 shows Prof. Dr. Aziz Sancar and his supervisor Dr. Rupert. In the upper right corner of the figure, photo-activation in *E. coli* is indicated. Below the figure, the general model for DNA Photolyase based on Dr. Rupert's pioneering work is shown. UV induces the construction of a cyclobutane thymine dimer (T <T), binds to the pyrimidine dimer, absorbs the blue light photon, and its dimer converts into two tenets.

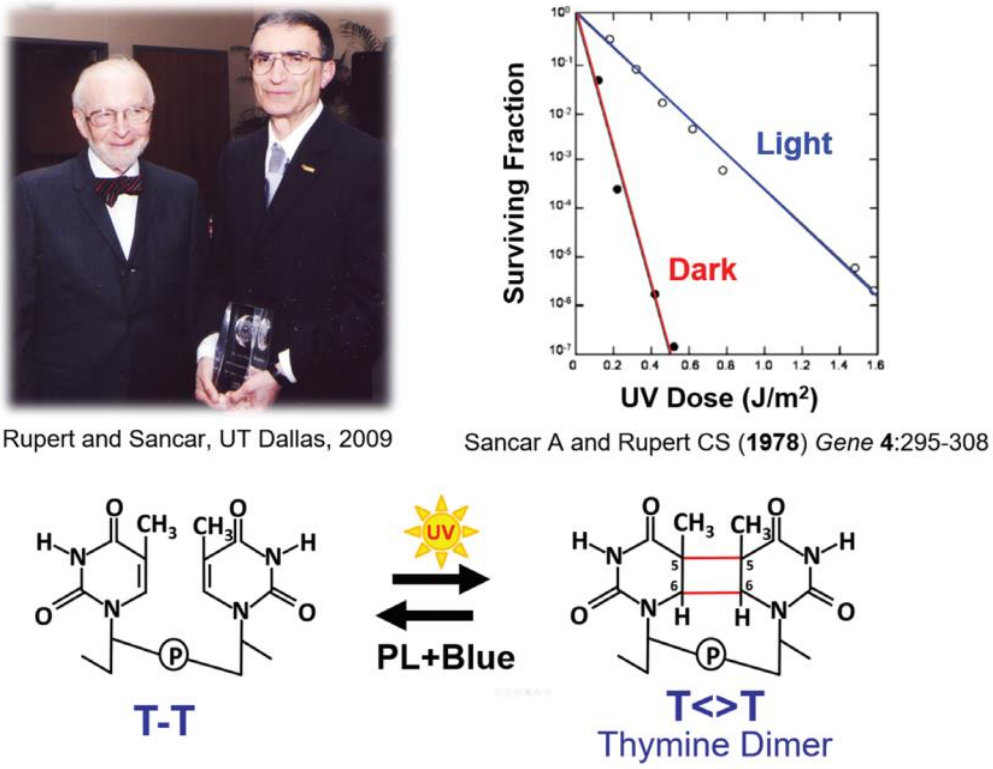

Figure 2.4 : DNA Photolyase gene discovery by Prof. Dr. Aziz SANCAR [1].

Figure shows the crystal structure of *E. coli* Photolyase. The strip diagram representation is given on the left, the surface potential representation is given on the right. Positively and negatively charged residues are highlighted in blue and red. The phosphodiester bond of the damaged thread is attached to the positively charged diagonal groove on the enzyme surface. The dashed box shows the hole leading to the FADH catalytic cofactor [1].

Figure 2.5 (left) shows the electron micrograph of the phr plasmid containing the Photolyase gene of *E.coli* bacteria. The enzyme was found to be bright blue when purifying (right). The blue color of the enzyme means it absorbs light. The enzyme does this by using methyltetrahydrofolate (folate) and the cofactor flavin adenine dinucleotide (FADH–), which absorbs two blue light. It has been discovered that the enzyme exhibits purple to orange colors depending on the redox state of the flavin cofactor. The purified photolyase enzyme shows a blue color due to the flavin neutral radical cofactor of the enzyme. Color ranges from sky blue to dark blue depending on enzyme concentration [1].

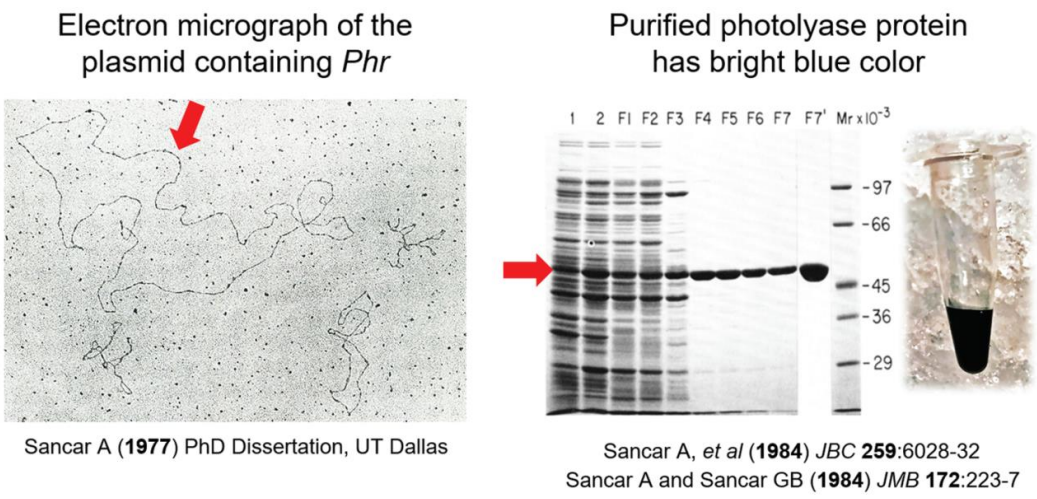

Figure 2.5 : Characterization and over production of DNA photolyase enzyme in *E.coli* [1].

In eukaryotes, UV radiation induces photoreactions that can cause serious biological consequences for mutagenesis or cell death if not repaired by disrupting the double helix structure of the DNA molecule [2, 66]. UV light from the sun damages DNA by stimulating photoisomerization of the sequential pyrimidine base present in the DNA. UVB (~ 295–320 nm) has been shown to play a more active role in the formation of the pyrimidine dimer in the DNA structure [67]. In single-celled organisms such as *E. coli, S. cerevisiae,* Photolyase is characterized by wavelengths of visible light (300-390 nm) that are not efficiently absorbed by nucleic acids or polypeptides in the UV or visible regions of the spectrum [68]. UVB radiation, the most energetic and mutagenic component of solar radiation, is directly absorbed by DNA and induces dimeric photoproducts between adjacent pyrimidine bases, namely cyclobutane pyrimidine dimers (CPDs) and pyrimidine (6-4PP) photoproducts [69]. Photolyases are DNA repair enzymes (photo-activation) that use light as an energy source for repairing UV-damaged DNA. To achieve this, it binds flavin adenine dinucleotide (FAD) and an additional chromophore, which generally functions as an antenna pigment, such as methyltetrahydrofolate (MTHF). With the photoactivation of the antenna molecule, the energy that enables electron transfer to the pyrimidine dimer is transferred to the fully reduced FAD (FADH), which causes the split in monomers [70]. Cyclobutane pyrimidine dimer (CPD) PHR binds flavin adenine dinucleotide (FAD) as a cofactor and repairs CPD lesions in double-stranded DNA [71]. The researchers realized that UV radiation facilitates electron injection from mitochondrial

transcription factor A to DNA using a photo-reactive thymine analog, 5-Bromouracil, to investigate electron transfer in DNA. They have also observed that this electron injection can lead to the repair of thymine-thymine dimer [72]. Many organisms have a rapid DNA repair system using photolyase which active in visible light convert DNA to the pyrimidine dimer formed by the transfer of the electron from the cofactor of a single UV-induced photoproduct [71]. Photolyase repairs UV-induced DNA damages of cyclobutane pyrimidine dimer (CPD) and pyrimidine-pyrimidone (6-4) photoproducts using blue-light as an energy source and it belongs to the cryptochrome/photolyase protein family (CPF) which perform different functions such as DNA repair, circadian photoreceptor, and transcriptional regulation [2, 73]. There are two different types of photolyases; These are classified as CPD photolyase and (6-4) photolyase according to the photo product class they repair. Although they are structurally similar, two photolyase is very evident in their actions against one or other type of photo product they repair [69]. With the 6-4 Photolyase-like preserved folded structure motif, the bifurcated electron transfer paths initially work as in CPD photolyase, and then a critical proton transfer is required to transfer hydrogen and then oxygen atoms between the two damaged bases. This proton comes from an active site histidine residue, and therefore the photolyase enzyme is part of the key repair additives [74]. Under physiological conditions, photolyase has adopted the optimized orientation of the photopigment to efficiently convert solar energy for the repair of damaged DNA [75]. Close relatives, cryptochromes have lost DNA repair functionality and often act as signal proteins; the growth and development of the plant are used as triggers for the initiation of flowering or the drag of the circadian rhythms in plants and animals [76]. Figure 2.6 shows homologous region of the photolyase and the cryptochrome genes.

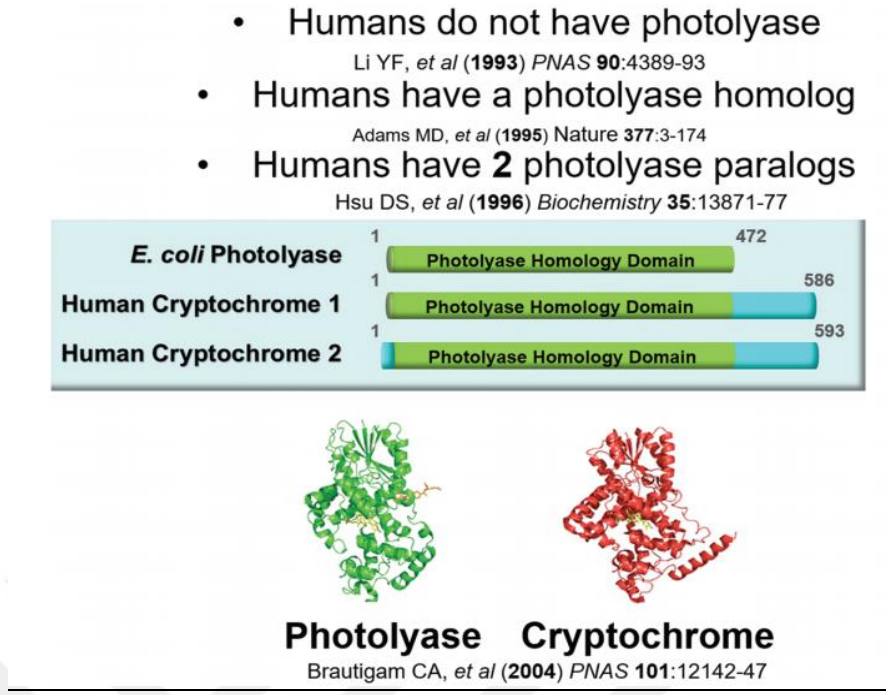

Figure 2.6 : Homologous region of Photolyase and Cryptochrome gene [1].

The human Cryptochrome gene functions as photoreceptors or integral components of the circadian clock by taking part in the regulation of the circadian rhythm [77]. CRYs are divided into I and II animal types, CRYs, and CRY-DASH photoreceptors (DASH: Drosophila, Arabidopsis, Synechocystis, Homo). BcCRY1 is a cyclobutane pyrimidine dimer (CPD) photolyase and does not have an important role in signaling as the main enzyme of photoreactivation. On the contrary, BcCRY2 is expressed as a photoactivation enzyme, but it fulfills regulatory functions by suppressing conjugation in white and especially black/NUV light [78]. Some studies determined that cryptochrome genes which belong to photosynthetic algae, where they may act not only in signaling but also as photolyases [76]. Animal cryptochromes (Photolyase-like) are thought to have evolved from the Photolyase gene, an ancestor associated with DNA repair. It provides circadian rhythm control by losing its gene repair function. Animal cryptochromes can be non-photoreceptive that provide direct light entry into the circadian clock or possibly act as transcriptional suppressors of the clock genes [79]. People with other DNA repair mechanisms, such as nucleotide excision repair (NER) pathways, which have been reported to repair UV-induced DNA damage, do not have photolyase. The researchers found that the Type II photolyase genes of the Shope-broma virus and Myxoma virus genome were transfected into the knock-out

E.coli bacteria, repairing the DNA of the virus gene with UV light damage by 70 %. In the same way, they found that the photolyase enzymes of the virus protect the virus genomes by working only in a cytosolic environment [80]. In 1940, Dr. Albert Kelner discovered that "visible light has a healing effect against UV damage" and called this phenomenon Photoreactivation [81]. Dr. Renato Dulbecco's "Photo-reactivation can be an enzymatic process dependent on light." recommended his hypothesis. Dr. Stan Rupert (Supervisor of Dr. Aziz Sancar) has confirmed this theory, which they announced "Photolyase" [82]. Photolyase is a flavoprotein [83]. The two chromophores in photolyase contain reduced FADH and Folate group cofactors [84]. Photolyase is stimulated by a regional free radical mechanism. It has been discovered that electron transfer occurs by absorbing light at 300-500 nm wavelength [2]. Pyrimidine dimers are molecular contusions formed by photochemical reactions from thymine or cytosine bases in DNA [85]. Ultraviolet light causes the pattern of covalent bonds with localized reactions in C = C double bonds [70]. These lesions change the structure of DNA and consequently inhibit polymerases and stop replication [86]. Photolyase performs different functions such as DNA repair, circadian photoreceptor, and transcriptional regulation. It belongs to the cryptochrome/photolyase protein family (CPF) [87]. Photolyase is responsible for repairing DNA damage caused by UV (cyclobutane pyrimidine dimer, CPD, and pyrimidine-pyrimidone (6-4) photoproducts) by activating the blue light wavelength from daylight [88]. This enzyme has two chromophores: a flavin adenine dinucleotide (FAD) as a cofactor and a photoanthenna such as a methyltetrahydrofolate (MTHF). FAD is required for the catalysis of DNA repair. To increase the repair efficiency of the enzyme, the second chromophore absorbs photons in the blue light spectrum and transfers energy to FADH [76]. Photolyase enzyme attaches to DNA and the enzyme-DNA complex is formed [89]. Thymidine dimers are monomerized after the enzyme activation is achieved by the absorption of visible light of the repair. Based on biochemical experiments, folate is like a solar panel that absorbs light and then transfers light energy to the flavin cofactor in the enzyme's core to catalyze it [90]. The DNA Phatolyase 3D structure shown in Figure 2.7.

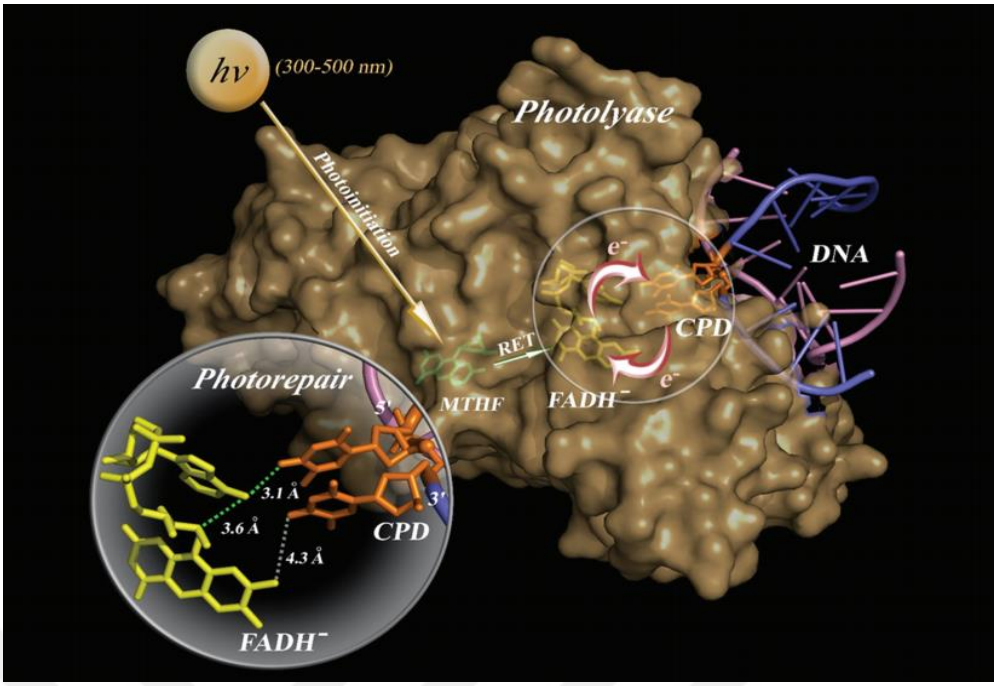

Figure 2.7 : DNA Photolyase enzyme 3D [1].

Photolyase binds DNA T<>T alters the backbone of the DNA. Upon binding to damaged DNA, ionic interactions between the positively charged groove on the photolyase surface and negatively charged DNA phosphodiester backbone the enzyme pulls the T<>T out from within the helix and into the core of the enzyme so that the T<>T is within Van der Walls contact with FADH– [91]. The enzyme makes ionic bonds with the phosphate residues of the damaged DNA strand and flips out the thymine dimer dinucleotide into the active site cavity so that the T<>T is within Van der Waals contact with FADH–. The catalytic reaction is proposed by the absorption of a photon (300–500 nm) by the folate (MTHF). The MTHF excited singlet state assigns the excitation energy to FADH– by Forster Resonance Energy Transfer (FRET). The excited FADH– divides the cyclobutane ring by cyclic redox reaction to convert T<>T to T-T and the repaired DNA alienated from the enzyme. All these photochemical reactions total 1ns. takes place in the process [92]. The import shows the distances among the designated atoms of FADH– and the cyclobutane pyrimidine dimer (CPD) [1]. Prof. Dr. Aziz Sancar discovered the working mechanism of DNA photolyase enzyme for the in vitro reaction of *E. coli* DNA photolyase, the reduction of the FAD radical cofactor by light, followed by the transfer of electrons from the induced singlet state of reduced FADH to the dimer [93]. DNA Photolyase gene comes from the photolyase/cryptochrome superfamily. Members of this superfamily, the

FAD-binding sites, and their antennas are functionally preserved. However, photolyase and cryptochrome genes have different functions [94]. The DNA Photolyase gene is not found in the human mammal genome. Instead, because cryptochromes are semi-reduced, they perform photomorphogenesis, circadian rhythm regulation, photo-magnetoreception. It cannot perform DNA repair [69]. Symptoms due to malaria disease occur when red blood cells containing parasites are synchronized to release parasites. Therefore, it is thought that Plasmodium parasites causing malaria must have internal circadian clocks to be synchronized in this way [3]. In recent studies, the malaria cell cycle and gene expression have been closely linked to daily rhythms, so the malaria parasite has also been shown to have an internal timekeeping mechanism, rather than just responding to host cues [95]. These enzymes have been used in multiple studies to determine their functions. However, the characterization of the DNA Photolyase gene of the malaria parasite and its effect on the development of the malaria parasite has never been investigated. Our aim in this study was to determine and characterize the function of DNA Photolyase in a rodent malaria parasite.

2.3 CRISPR-Cas9 Gene Editing Technology

The Cas9 nuclease of the *Streptococcus pyogenes* microorganisms is complementary to the twenty nucleotides of the 20-nucleotide long-chain RNA (sgRNA) and can bind to a target DNA sequence adjacent to a protospacer contiguous motif (PAM) shown in Figure 2.8. DNA double chain breaks induced by Cas9 are repaired in mammalian cells by non-homologous splice (NHEJ) or homology repair (HDR), thereby enabling targeted genome editing [96]. CRISPR-Cas9 has become one of the powerful and adaptable platforms of recent times in genetic engineering and once again emphasizes the importance of basic science research. CRISPR-Cas, based on the prokaryotic viral defense system, especially the Cas9-based Type II system, allows deletion or insertion to occur by binding to any desired DNA region with sgRNA [97]. CRISPR-Cas9, which provides acquired immunity against specific and exogenous genetic elements identified in the immune system of bacteria, can be adapted [98]. CRISPR and Cas9 genes in bacteria and archaea can regularly adapt to nucleic acid-based immune systems [99]. It has been demonstrated by genetic studies with *Streptococcus thermophilus* that Cas9 (also called Cas5, Csn1, or Csx12) is the only enzyme that cuts

target DNA in case gene clusters [100]. Non-coding trans-activating crRNAs (tracrRNAs) were uncovered that associate with crRNA, a key integral in the processing and genesis of crRNAs in CRISPR Type II systems, and simplify RNA targeting of Cas9 [101]. This binate RNA hybrid formed by Cas9 and endogenous RNAase III is needed for the process of transcription of the CRISPR sequence into mature crRNAs [102]. Studies have reported that at least three components (Cas9, mature crRNA, tracrRNA) are required for the CRISPR Type II system [103]. Researchers showed for the first time in 2011 that the type II CRISPR is a transferable system. Therefore, it has been shown that CRISPR intervention can be rearranged in different bacterial strains by transplantation of the type II CRISPR region from *Streptococcus thermophilus* to *Escherichia coli*. [104]. In 2013, two separate studies successfully engineered CRISPR systems from *Streptococcus thermophilus* and *Streptococcus pyogenes* for genome editing in mammalian cells. Thus, the CRISPR-Cas9 system was used in genome editing [105]. CRISPR activity lacks the existence of CRISPR-related (Cas) genes that are generally found contiguous to CRISPR sequences and encode proteins for immune response. These characteristic CRISPR sequences are created by counting non-repeating sequences acquired from the short section of foreign genetic material into repeating sequences [106].

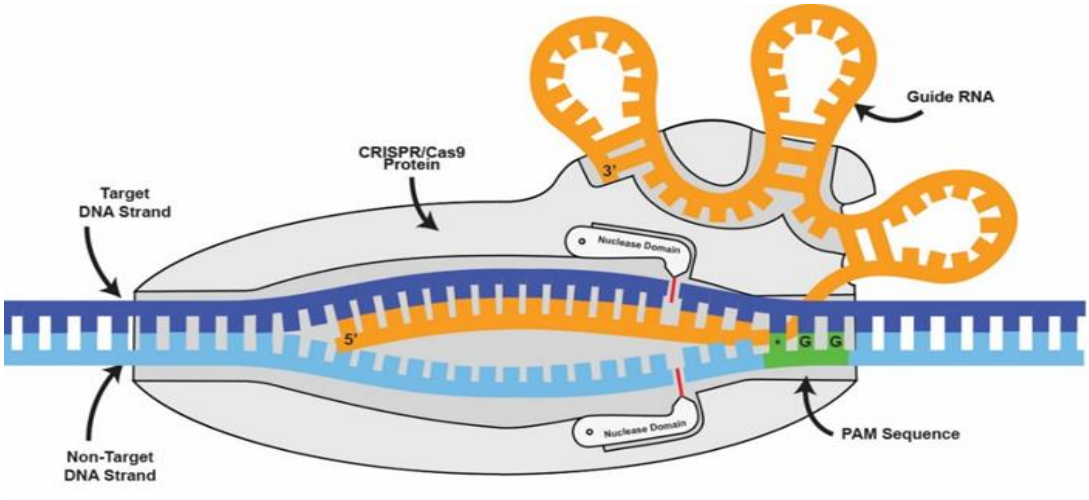

Figure 2.8 : CRISPR-Cas9 protein 3-step working mechanism.

(1) The PAM-carrying DNA region of the virus infecting the bacteria is inserted into the CRISPR locus with the repetitive regions, (2) CRISPR RNA (crRNA) biogenesis in which small crRNA sequences are formed by expressing and processing CRISPR

sequences, (3) Targeting the crRNA corresponding to the virus DNA by combining with Cas proteins and cutting the DNA.

CRISPR regions are the existence of conserved sequences that are called leaders fundament CRISPR according to the direction of transcription. CRISPR-Cas9 technology performs a function in the cell in three steps (Figure 2.1). The first step is the adoption where spacers from exogenous nucleic acid are arranged in the CRISPR region. In this step, the election of intervals is obstinate by the specific recognition of proto-spacing adjoining motifs (protospacer contiguous motif PAM) initiate in the invading plasmid and phage genomes [98]. PAMs are highly conserved sequence motifs consist of 2-5 nucleotides. PAM sequenced alien DNA spacer is inserted into the CRISPR region with repetitive genes. The absence of PAM recognition sequences in repeats in the bacterial CRISPR region eliminates the possibility of targeting and self-cutting of CRISPR Cas systems in the second step [107]. The last step is targeting. In this step, invasive nucleic acids are targeted using crRNA and Watson-Crick base pairing, and replication of viruses and plasmids is prevented by truncating homologous sequences with Cas nucleases [108]. Cas proteins are very diverse and interact with nucleic acids such as nucleases, helicases, and RNA binding proteins. Cas1 and Cas2 proteins play a role in adaptation and these proteins are found in all CRISPR-Cas systems [109]. The variety of Cas proteins, and the existence of multiple CRISPR regions make it difficult to classify CRISPR-Cas systems due to the transition between living things [110]. According to the organization of the CRISPR region and the content of Cas genes, CRISPR-Cas systems have three main types (I, II and III), and 11 subtypes (IA - IF, II-A - II-C and III-A - III-B). Because the Cas proteins are responsible for crRNA biogenesis and recognition and destruction of invasive nucleic acids, the molecular mechanism of each CRISPR type is different. In Type I, and Type III systems, endoribonucleolytic cleavage of repetitive sequences of pre-crRNAs to produce small mature crRNAs is based on the Cas6 nuclease family. In the Type I system, the crRNA molecule formed combines with Cascade and Cas3 proteins to cut foreign DNA, while in the Type III system, crRNA consisting of pre-crRNA forms a complex with Cmr / Cas10 or Csm / Cas10 proteins and Cas. Proteins in the complex cut foreign DNA. Type II system is the most studied and most illuminated system among these systems. In the Type II system, together with a second non-coding RNA (trans-activating CRISPR RNA (tracrRNA), crRNA forms a ribonucleoprotein

complex with endonuclease Cas9 and recognizes and cuts invading DNA [111]. Internal of the cell, the Cas9 system requires the enzyme RNaseIII along with crRNA and tracrRNA to cleavage the target DNA. All these requirements can be eradicated by the establishment of sgRNA, a combination of tracrRNA and crRNA, known as single-guided RNA (sgRNA). The crRNA in the generated sgRNA retains its guide role, and the secondary structure of the sgRNA was designed in accordance with Cas9 to cut the target site [112]. Cas9 has the HNH and RuvC nuclease domains needed to cut the double looped DNA, and the alpha-helical lobe that allows it to interact with the sgRNA [113]. Alongside the sgRNA consisting of 20 nucleotides, the PAM sequence is needed for the Cas9 protein to recognize the target DNA. The Cas9-sgRNA complex is acutely stable when constrained to DNA, and in vitro binding kinetics studies have shown that binding amid the Cas9-sgRNA complex and target DNA is virtually irreversible over a long duration of time [112]. The most important feature of the Cas9-based CRISPR system in gene editing is that it is programmable. The Cas9 enzyme can be directed to any region of the PAM sequence by changing the base sequence of the sgRNA. In addition to the use of Cas9 nuclease in genome editing, the catalytically inactive dCas9 (dead Cas9) enzyme, which cannot break down double-loop DNA, is also used to activate or suppress gene expression [114].

2.4 Photoconvertible Protein (mEos4b)

For decades, fluorescent proteins with phototransformation have revolutionized the field of cell biology. These fluorescent proteins change their excitation and emission spectra after exposure to light of a certain wavelength [115]. The application of these proteins in cellular motion, differentiation, cellular dynamics, protein-protein interactions, and a few others has made these proteins of particular interest. Therefore, in the thesis study, it was aimed to develop a new biological model system by integrating the mEos4b protein into the genome of the *Plasmodium berghei* parasite with the help of the CRISPR-Cas9 technique. This will be the first model system of this kind, to the best of our knowledge, in Turkey which will help in designing novel strategies to treat malaria as well as other life-threatening infectious diseases [115]. The beauty of phototransformable fluorescent proteins (PtFPs) is that some of the fluorescence properties can be controlled by light [116]. PtFPs which change from one color to another is known as photoconvertible fluorescent proteins (PcFPs) and the

PtFPs that irreversibly activated from non-fluorescence to fluorescence state are termed as photoactivatable fluorescent proteins (PaFPs). The first successful irreversible photoactivatable fluorescent protein reported was Pa-GFP. It was derived from Jellyfish (*Aequorea victoria*) GFP (wtGFP) by mutating Threonine 203 to Histidine [117]. Simulate Pa-GFP, scientists later developed red fluorescent photoactivatable fluorescent protein with several rounds of random mutagenesis. Pa-mCherry and Pa-mRFP1 were derived from DsRed and mRFP, respectively. When illuminated with purple light, both of those proteins are photo transformed into forms that emit brighter red fluorescence [4, 118].

Which after exposure to UV light photoconverts from green fluorescence (Excitation/emission of 505/516 nm) to red fluorescence (Excitation/emission of 569/581 nm). Another class of Pa-FPs is mEosFP which is a photoconvertible fluorescent protein switches from green to red fluorescence. Figure 2.9 explains the excitation and emission spectra of green to red mEosFP [119]. In the knock-out study, we ensured the deletion of the DNA Photolyase gene by integrating the photo-convertible mEOS4b gene with the plasmid. A wide variety of photoformable fluorescent proteins have been developed in recent years, including photoactive, photo-convertible, and photo-exchangeable fluorescent proteins. PtFPs that vary from one color to another is known as photo-convertible fluorescent proteins (PcFPs), and PtFPs that are irreversibly activated from non-fluorescence to fluorescent state are called photoactivatable fluorescent proteins (PaFPs) [4]. One class of Pa-FPs is mEosFP, which is a photo-convertible fluorescent protein. Describes activities in transgenic malaria parasite after UV light. Thanks to the EOS4b protein, the conversion of the green fluorescent protein to blue and red fluorescent protein under UV light observed and the characterization of the gene determined by examining the cytotoxic activity of the parasite in the developmental stage. Due to its color-changing properties, the class of fluorescent proteins (FP) such as EosFP, 2 DendFP, mcavRFP, and r-oRFP and others have become an important tool in the development of super-resolution microscopic techniques for imaging subcellular biological structures with unprecedented detail.

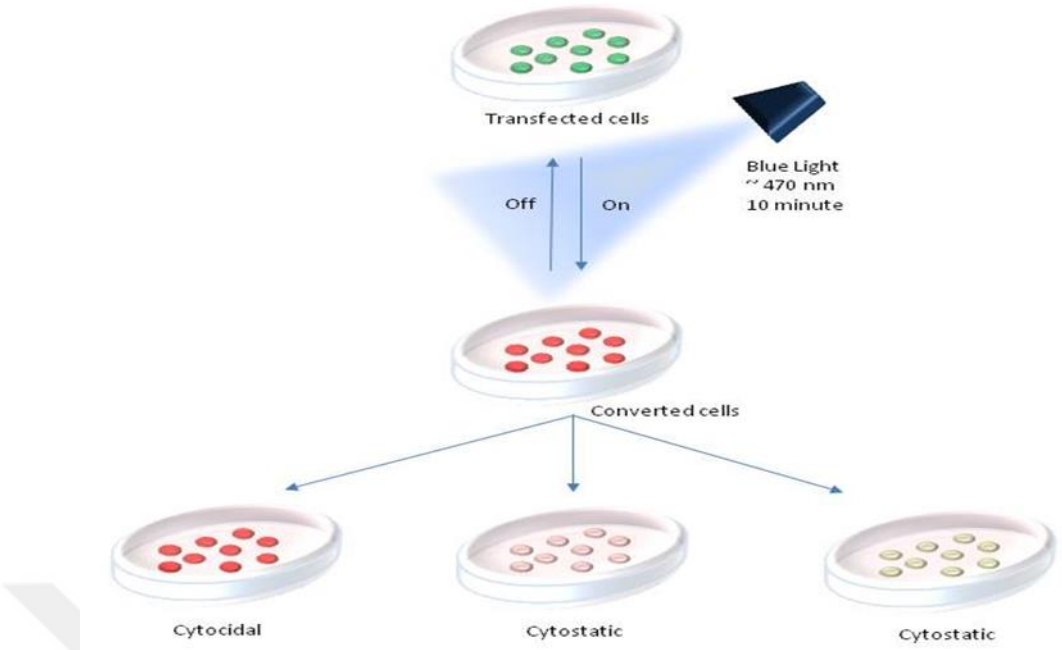

Figure 2.9 : mEos4b a phototransformable fluorescent protein.

Green-to-red (G/R) photo-transformable proteins form a GFP-like protein class that can undergo a light-dependent color transformation. The green form (emission at ~518 nm) is irreversibly converted to a red radiation form (emission at 582 nm) when exposed to UV or purple radiation [120]. The phenotype, which can be converted from green to red, appears to be caused by a common green ancestor with the migration of a knob-like fixation region crosswise from the active site to the fold of the beta-barrel. Allosterically linked mutation sites provide active conformational mobility through the epistasis [121]. Several other phototransformable fluorescent proteins have been discovered e.g; Kaede, PS-CFP2, Dronpa, etc and are being applied in numerous biological applications. The phototransformative property of these phototransformable fluorescent proteins has allowed researchers to highlight and tracking of subpopulations of cells, organelles and, also proteins in living systems. Additionally, phototransformable fluorescent proteins open new ways for superresolution fluorescence microscopy and optogenetics modifications of proteins [115]. Mutoh et al. showed in the mouse neonatal brain, the use of Kaede eased monitoring movement of a progenitor cell between different compartments while permitting visualization of the division of the same cell [122]. Karbowski et al. were able to visualize and quantify the fusion dynamics of mitochondria in healthy and apoptotic cells by engineering Pa-GFP tagged to a mitochondrial matrix protein [123]. PtFPs are helpful to the

understanding of insulin secretion. Baltrusch et al. explain the role of Pa-GFP or Dendra2 followed by photoactivation or photoconversion, respectively, in long-distance tracking of individual granules through the cytoplasm until their fusion with the plasma membrane and subsequent insulin release [124]. Photoconvertible fluorescent proteins like mEosFP, mEos2, Dendra2 are being used for plastid dynamics, tracking peroxisomes, and monitoring protein dynamics in cilia, mitochondrial dynamics, and in several other applications [125, 126]. Dronpa which is a photoswitchable fluorescent protein (PsFP) is used for manipulation of protein-protein interactions by light and monitoring protein exchange among different cellular compartments [127]. A plasmid vector was used as a donor vector for homologous recombination to repair the double strand breaks in our study. For thesis study phototransformable mEos4b fluorescent marker and a drug resistance marker hDHFR were used. CRISPR-Cas9 members were added to the AA20 vector. Additionally, CRISPR-Cas9 is designed with the Turq2 fusion protein for fluorescence detection. Donor plasmid DNA was placed in AA20 plasmid. In future work, this model system will be used to study the cytocidal and cytostatic activity of chemical compounds. The model system will also be used in the mechanical characterization of key molecular players to gain clear insight into the development of resistance to anti-malarial drugs that will help develop more precise chemotherapeutic strategies and successful treatment of malaria.

3. MATERIAL AND METHOD

3.1 Materials

3.1.1 Working places

Genetic engineering and cloning studies of this thesis were carried out in Dr. Bedia Laboratory (Istanbul University Department of Molecular Biotechnology and Genetic, Beyazıt). Mosquito, mouse, transfection experiments were performed at the Dr. Aly Laboratory (Bezmialem Vakif University Institute of Life Sciences and Biotechnology, Beykoz).

3.1.2 Devices

Analytical scales (Ohaus Pioneer, PA4102C - 0.01- 4100 g, USA, Ohaus Pioneer, PA413 - 0.001 - 410 g, USA, Sartorious, Quintix 224 - 1S, GERMANY) were used for weighing chemicals used for the preparation of stock, solution, medium, and media. Agarose gel casting apparatuses (Biorad, Mini subcell GT, USA, Biorad, Wide mini subcell GT, USA, GE Healthcare, HE99 X, USA) were used for gel electrophoresis. Autoclave (Eryiğit SPR55105, TURKEY) was used for sterilization of solids and liquids. Bench centrifuge (ThermoScientific, MicroCL21R, USA) was used to precipitate molecular materials in small liquids. A cooled bench centrifuge (Beckman Coulter, Allegra X30R, USA) was used to precipitate biological materials in large liquids under cold conditions. A confocal laser scanning microscope (Leica, SP8, GERMANY) was used for detailed imaging of the transgenic parasite. Electroporator (Lonza, Nucleofactor 2b, SWITZERLAND) was used to transform the prepared vector into the parasite. Freezer -20°C (ThermoScientific, FFGL2320V, USA) was used for the storage of DNA, enzymes, and primers. Freezer -80°C (ThermoScientific, 8940086V, USA) was used for storage of parasite blood stocks, competent bacterial cells. Gel documentation system (Vilber, Fusion Solo S, SOUTH KOREA) was used to detecting the size of the DNA in agarose gel, it was used to obtain data from the computer environment using UV light. Ice machine (Scotsman AF 80, USA) was used to eliminate the need for ice in processes related to transformation and DNA. A small

Incubator (ThermoScientific, Heraterm IMC 18, USA) was used for the growth of bacterial clones into the plates at 37 °C. Shaker Incubator (Infors HT, Multitron Standard, SWITZERLAND) was used for growing bacteria in 37 °C by shaking 180-260 rpm. CO2, N, O2 incubator (ThermoScientific, FORMA Steri-cycle İl60, USA) with shaker (Infors HT, S-30126075, SWITZERLAND) were used for *P. berghei* parasite growth into the blood culture in 37 °C for transfection. Heating block (ThermoScientific, DryBathStdrd 4-black, USA) was used for DNA isolation from the gel, pure water heating, etc. have been used in experiments. Light microscope (Nikon, Eclipse E100, JAPAN) was used to obtain parasite in Giemsa stained thin blood smear slides with 1000X objective. A magnetic stirrer (Biorad, Digital hot plate stirrer, USA) was used for dissolving mixtures. Microwave (Arçelik, MD674S, TURKEY) was for agarose gel preparation. Mosquito adults cage (BioQuip Products Inc, Collapsible Cage, USA) was used for mosquito feeding and production. PCR machine (BioRad, T100 Thermal Cycler PCR, USA) was used for amplification of insert DNA. pH-Meter (HANNA, Edge pH, ITALY) was used to calculate pH for specific solutions. Refrigerator (Liebherr Mediline, Schrank vorb Weiss, GERMANY) was used for storage of LB, TB media and plates, cultures. Biosafety Cabinet (ThermoScientific, Maxi safe2020 1.5, USA) was used to prepare solutions and cultures in sterile conditions. UV-Lamp (Esterilizador Kill Virus Sterilizer Lampara UV, China) was used to damage DNA for wild type and knock-out parasites. Vortex (Isolab, IP42, GERMANY) was used for primer, cut smart mix. Water bath (ThermoScientific, TSGP15D, USA) was used for transformation and incubation experiments. Flow Cytometry (Biorad S3e Cell Sorter, USA) was used to sort transgenic parasites and detect parasitemia percentage. A cell imaging system (Biotek Cytation 5 Elx 808, USA) was used for imagining transgenic parasites with blue, green, and red filters. Dishwasher (Smeg, 6W4060, ITALY) was used for clean solid materials. A double distilled water device (Sartorious, Arium comfort, GERMANY) was used for users to obtain pure water in molecular experiments and in the preparation of solutions. An electrophoresis device (Biorad, Power Pac Basic, USA) was used for determining the presence and size of DNA. Electrophoresis tank apparatus (Biorad, All Size, USA) was used for the run gel to which the electric current in the buffer. A vacuum (KNF, NO 22 AN.18, USA) was used to collect mosquitoes. Vacuum manifold (Qiagen, QIAvac 24 Plus, GERMANY) was used miniprep columns. A big incubator (HiPoint, 740FH, TAIWAN) was used to incubate mosquitoes. Spectrophotometers (Hitachi, U-

5100, JAPAN, BioTek, Eon, USA) was used to measure bacterial cell density. Mini centrifuge (FischerScientific, 05-090-100, USA) was used to collect small liquids into the bottom of the eppendorf tube or remove bubbles from PCR tubes. Nanodrop (ThermoScientific, 8000-Spectrophotometer, USA) was used to measure DNA concentration. A phase-contrast microscope (Leica, DM 2500 Led, GERMANY) was used to observe parasites in the blood cells.

3.1.3 Experimental stuffs

Lorem 8-well chamber slides (Labtek, Turkey) were used to for account the number of sporozoites. Cryo-freezing tubes (Nest, South Africa) used for frozen parasite bloodstock storage. Disposable cuvettes (Isolab, Germany) were used to measure cell density in the spectrophotometer. Electroporation cuvettes (BioRad, München) were used for transfection DNA into the parasite. Falcon blue cap (50 ml and 15 ml, Nest, SA) was used for general experiments. Glass slides (Isolab, Germany) was used for thin blood smears. Syringes and needles (BD Diskardit, Becton Dickinson) were used for mice injections and tail smears. Parafilm (Isolab, 100 x 38 mm, Germany) was used for LB plate storage. Pasteur pipettes (Isolab, Germany) were used for general experiments. PCR tubes (Isolab, Germany) were used for PCR reactions. Petri-dishes (Isolab, 90x17mm, Germany) were used for LB agar plates. Pipettes tips (with sterile filtered, Isolab Tips RNase/DNase/Endotoxin-free, Germany) 10, 20, 200, 1000 µl were used for molecular experiments. Pipettes (Eppendorf Research Plus, Merck KGaA, Darmstadt, Germany) 0.1-2.5 µl, 2-20 µl, 20-200 µl 100-1000 µl calibrated were used for molecular experiments. Serological pipettes (5 ml,10 ml, and 25 ml, Grenier Cell STAR, Merck, Germany) were used for general experiments. Sterile Filter (0.2 µm, 0.4 µm, ThermoScientific, USA) was used for ampicillin stock preparation. Sterile Filter (Millipore, Sterile filtration units, 500 ml, Merck, Germany) was used for transfection culture preparation. Filter paper (Whatman™ 3MM paper Whatman paper company, Merck, Germany) was used for egg dish insertion of mosquitoes. Eppendorf centrifuge tubes (Isolab 1,5, 2 ml, Germany) were used for more molecular experiments. Measure (Isolab 50 ml, 100 ml, 250 ml, 500 ml, Germany), per glass (Isolab, 50 ml, 100 ml, 600 ml, 1000 ml, Germany), Arlen nuçe glass with glass water inlet tube (Isolab, 500 ml, Germany), erlen glass (Isolab, 100 ml, 500 ml, 1000 ml, 2000 ml, Germany), bottle (Isolab, borosilicate glass, amber or transparent, screw cap, 100 ml, 250 ml, 500 ml, 1000 ml, Germany) were used for

general experiments. Digital thermometer, digital thermohygrometer, thermometer maximum/minimum – electronic (Isolab, Germany) were used for the hot room and incubator degree confirmation. Scissors, gloves (Isolab, Germany), magnetic fish (Isolab, 20x6 mm, 30x6 mm, 40x8 mm, 50x8mm), tube stand (Isolab, for 15, 50 ml, Germany), Alarm Watch (Isolab, Germany) were used for general experiments. Sterile toothpick (Montopack, USA) was used for pickup single bacteria colonies. Rack for minus twenty (Interlab, Turkey) was used for store enzymes. Minus twenty boxes, minus eighty boxes (Interlab, Turkey) were used for store reagents in eppendorf tubes.

3.1.4 Software

EndNote X9 (Clarivate Analytics, USA) was used for thesis reference writing. Clone Manager 8.0 (Sci Ed Central Software, USA) was used for primer designing.

3.1.5 Chemicals

For the mosquito feeding solution, 4-Aminobenzoic acid (SIGMA,100 g) was used as received. For the transfection experiments, Accudenz ® A.G. Cell Separation Media (Accudenz Accurate Chemicals, 500 g) was used as received. For the gel electrophoresis experiments, Agarose LE (Benchmark Scientific, 500 g) used as received. For frozen parasite stocks, Alsever's Solution (Sigma, Taufkirchen) was used as received. For the culture preparation experiments, Albumin from Bovine Serum (SIGMA, 50 g) was used as received. For the bacteria, selective culture preparation Ampicillin sodium salt for biochemistry (Biofroxx, 10g) was used as received. For the bacteria, culture plate preparation Bacto-agar (BD Diskardit, Becton Dickinson) was used as received. For the SOC medium preparation, Bacto-tryptone (BD Diskardit, Becton Dickinson) was used as received. For the SOC medium preparation, Bacto-yeast extract (BD Diskardit, Becton Dickinson) was used as received. For the competent cell stock preparation, Calcium chloride anhydrous (SIGMA Taufkirchen, 50 g) was used as received. For the molecular experiments Cell Culture Water Pyrogen Free (Biosera, 100 ml) was used as received. For the parasite, genomic DNA isolation Cellulose (SIGMA, 250 g) was used as received. For the parasite culture preparation, DMEM-medium (GibcoBRL, Karlsruhe) was used as received. For the TAE buffer preparation, EDTA Disodium Salt Dihydrate (Genaxxon, 500g) was used as received. For the gel electrophoresis Ethidium bromide (Sigma, Taufkirchen) was used as received. For the DNA extraction and sterilization Ethanol

Absolute (ISOLAB, 2.5 L) was used as received. For the culture experiments, FCS, certified (USA Gibco Invitrogen, Karlsruhe) was used as received. For the culture experiments, Gentamicin Sulfate (Lonza, 10 ml) was used as received. For the TAE buffer preparation Glacial Acetic Acid >99.0% (Isolab, 2.5 L) was used as received. For the staining of the slides, Giemsa (SIGMA, 1 L) was used as received. For the mosquito feeding Glucose (Merck, Darmstadt) was used as received. For the freezing solution preparation, Glycerol (Isolab, 1L) was used as received. For the miniprep buffer, preparation Guanidine hydrochloride (Glentham, 1 kg) was used as received. For the take blood from mouse heart Heparin (Braun, Melsungen) was used as received. For the adjusted pH Hydrochloric Acid %37 (Merck, 2.5 L) was used as received. For the visual staining slides under 1000X objective of light microscope Immersion Oil (Merck, 100 ml) was used as received. For the bacterial culture growth, LB Agar (Multicell, 500 g) was used as received. For the bacterial culture inoculation, LB Broth Miller (Merck, 500 g) was used as received. For the cell fixation on the glass slide Methanol %99.9 HPLC (Isolab, 2.5 L) was used as received. For the competent cell buffer, preparation Magnesium Chloride (Glentham,100 g) was used as received. For the mosquito dissection experiments, PBS Tablets (MP Biomedicals, LLC, 100 Tab) was used as received. For the DNA precipitation Potassium Acetate, 98 % (Glentham, 500 g) was used as received. For the miniprep buffer, preparation of Potassium Chloride (SIGMA,500g) was used as received. For the transfected parasite, selection Pyrimethamine (MP Biomedicals, LLC, 25 g) was used as received. For the parasite, genomic DNA extraction Saponin, from quillaja bark (SIGMA,25g) was used as received. For the DNA precipitation, Sodium Acetate Anhydrous (Glentham, 500g) was used as received. For the competent cell buffer, preparation of Sodium chloride (Merck, 500g) was used as received. For the prepared miniprep buffer, preparation Sodium Dodecyl Sulfate (SIGMA, 100g) was used as received. For the adjusted pH Sodium Hydroxide Pellets Pure %99 (Isolab, 1 kg) was used as received. For the adjusted pH, Sodium Hydroxide Solution (Titripor, 1L) was used as received. For the bacterial cell culture preparation, Terrific Broth (Multicell, 1 kg) was used as received. For the TAE buffer preparation Trisma Base, Primary Standard, and Buffer >99, crystalline (SIGMA, 1L) was used as received. For the parasite transfection culture preparation Tryptone (Biolife, 250 g) was used as received. For the parasite transfection culture preparation Tryple Express 1x (Gibco, 100 ml) was used as received. For the SOC medium preparation Yeast Extract (Biolife, 500g) was used as

received. For the mosquito dissection, sporozoite extraction, transfection culture preparation experiments RPMI 1640-medium (GibcoBRL, Karlsruhe) was used as received. For the mounting gel preparation, Hoesct (33342, Trihydroclorid, 10 mg/ml, Invitrogen, USA) was used as received. For the pyrimethamine solution preparation, DMSO (Isolab, 2,5 L, Germany) was used as received. For the mice experiments Ketamin(Ketasol, Richter pharma ag, Wells, Austria), Xylazine (5g, Merck, Germany), Rompun (%2, Bayer, Turkey) were used as received.

3.1.6 Stocks

3.1.6.1 Antibiotic stock

Ampicillin Stock Preparation: 1000 mg of ampicillin powder was added into a 15 ml falcon tube. The solution was prepared with double distilled water and completed to 10 ml. All supplies were wiped with %70 ethanol and placed into a biosafety cabinet. The ampicillin solution was sterilized by 0.22 µm filter and 15 ml syringe. The ampicillin solution was distributed 500 µl into the dark 500 µl centrifuge tubes. The ampicillin stocks were stored at minus twenty fridges. Working antibiotic dilutions are all 1:1000 from stock solutions in LB or TB medium.

3.1.6.2 Competent cell stock

Chemically Competent Cells Preparation: 25 µl of Top10 bacteria cell (from the company) was planted with a disposable spreader into two Petri dishes containing previously prepared ampicillin-free LB agar. Plates were incubated in a 37 °C incubator overnight. The colony was inoculated into 4 ml TB medium without ampicillin and placed into a shaker at 37 °C, 220 rpm for five hours. 3 ml of inoculation was inoculated into 250 ml of ampicillin-free Terrific broth into 260 rpm, 37 °C shaker for an hour. The optimal density (OD) value was measured at 600 nm every half an hour for bacterial culture. TB was used as a blank solution. Incolutaion was ended when the OD value reached 3.5. Experiments were settled into an ice pack. 250 ml bacterial culture was distributed into 5 pieces 50 ml falcon tube. Balances were adjusted and tubes were centrifugated at 4 °C, 300 rpm for 15 minutes. The supernatants were discarded and the pellet chilled 20 ml of $MgCl_2$ buffer. Cells were combined and distributed into 2 tubes. Tubes were balanced and centrifugated at 4 °C, 3000 rpm for 15 min. The supernatants were discarded and the pellets were chilled

with 25 ml of $CaCl_2$ buffer. The tubes were left on ice for 20 minutes. 50 Eppendorf tubes were labeled and placed into an ice pack. The cells are centrifugated at 4 °C, 3000 rpm for 15 minutes. The supernatant was discarded and the pellets were dissolved with 600 µl $CaCl_2$ with %15 glycerol solution. 50 µl cells distributed prechilled Eppendorf tubes. The stock competent cells were stored in a minus eighty freezer.

3.1.6.3 Frozen malaria parasite stock

• *P.berghei* ANKA WT-G2 900 µl Black6

• IY04 - bFOTO ko Tf3-G9 900 µl Sorted Black6

• IY05 - bFOTO tag Tf5-G3 900 µl Black6

Preparation of frozen stock: Previously frozen parasite blood was injected intraperitoneal into Black6 mouse. Heart puncture was applied when parasitemia reached % 30 into mouse blood. Collected blood distributed 300 µl into cryotubes and completed with 600 µl freezing solution to 900 µl. Blood stocks were marked and stored in a minus eighty freezer.

3.1.7 Solutions

3.1.7.1 Mosquito-breeding solution

• Mosquitoes breeding water (for larvae and pupae): 0.1 % Sea salt in ddH_2O.

• Sucrose adults feeding solution: 10 % Sucrose, 0.01% pABA, add ddH_2O.

3.1.7.2 Freezing solution

• Freezing-Solution (for blood parasites): Glycerol: Alsever's solution (1:9)

3.1.8 Media

3.1.8.1 Bacterial media

Terrific broth

Terrific Broth (TB) medium preparation: 23.8 mg of Terrific Broth was placed into a 1 L glass bottle. 400 ml double distilled water was added and the solution was mixed on a stirrer with magnetic fish. After dissolve the solution was completed to 500 ml with double distilled water. The solution was autoclaved at 121 °C, 15 minute liquid

mode. The sterile solution was cooled, and 515 µl 1000X ampicillin was added. LB Broth with ampicillin stored in a 4 °C fridge.

LB-agar

LB-Agar Preparation: 17.5 g Luria Bertani-Agar was added into a 1-liter glass bottle and completed to 500 ml with double distilled water. The solution placed on stirrer and heater machine agar was dissolved using magnetic fish. The solution was placed into autoclave machine liquid mode for 121 °C , 15 min. The sterile LB agar solution was stirred at low temperature for 10 minutes. 515 µl 1000 X ampicillin was added into the solution at 60 °C temperature in sterile conditions. The nutrient was distributed into plates equally, marked, and parafilm. Plates were stored in a 4°C fridge.

SOC medium

200 mg of Tryptone, 50 mg of Yeast Extract, and 58.44 mg of NaCl were mixed into 80 ml double distilled water. PH was adjusted to 7 by NaOH. The solution was completed to 100 ml. 10 mM, 100 ml MgCl autoclaved, 2 M, 5 ml of Glucose was autoclaved. 500 µl of $MgCl_2$ and 1 ml of Glucose were added to the mixture. The solution was distributed into 2 ml Eppendorf tubes and stored in a 4 °C fridge.

3.1.8.2 Parasite media

Plasmodium berghei transfection culture medium (total 175 ml for 1 culture):

149 ml of RPMI medium was mixed with 35 ml of (20%) FCS (heat-inactivated) and 50µl of Gentamycin. The mixture was filtered with a 500 ml filter bottle.

3.1.8.3 Mosquito dissection medium

3% of Bovine albumin serum was added in RPMI.

3.1.9 Buffers

3.1.9.1 Buffers for DNA purification and analysis

0.5 M EDTA Preparation:

93.06 g of EDTA (MW:372.24 g/mol) was added to the 1 L glass bottle. The powder chemical was dissolved with 400 ml ddwater. Solid NaOH pellet was added and pH was adjusted 8.0 during stirrer by magnetic fish. The solution was completed to 500 ml with ddwater.

50 X TAE Electrophoresis Running Buffer Preparation:

484 g Trisma Base powder was added into the 2L glass bottle and mixed with 1 L water. 200 ml 0.5 M, pH:8 EDTA solution was added to the mixture. 114.2 ml Glacial Acetic Acid was added into the solution under the hood. The mixture was completed to 2 L with ddwater.

1 X TAE Electrophoresis Running Buffer Preparation:

20 ml of 50 X TAE buffer was completed to 1 L with 980 ml ddwater.

% 1 Agarose Gel Preparation:

1 g agarose was mixed with 99 ml 1 X TAE buffer and placed into the microwave for 2:30 minutes. 4 µl EtBr solution was added to the mixture. The agarose gel was poured into the tank and the appropriate comb was placed according to the number of samples. After gel dry, the comb was removed and gel placed into the electrophoresis tank which was filled with 1X TAE buffer. Table3.1 shows amounts of %1 agarose gel preparations.

Table 3.1 : %1 Agarose gel reagents.

Volume of Gel (ml)	Agarose (mg)	EtBr (µl)	Comb (cell)
40	400	3	8-16
70	700	3.5	16
100	1000	4	16

% 0.9 Agarose Gel Preparation:

0.9 g agarose was mixed with 99.1 ml 1 X TAE buffer and placed into the microwave for 2:30 minutes. 4 µl EtBr solution was added to the mixture. The agarose gel was poured into the tank and the appropriate comb was placed according to the number of samples. After gel dry, the comb was removed and gel placed into the electrophoresis tank which was filled with 1X TAE buffer. Table3.1 shows amounts of % 0.9 agarose gel preparations.

Table 3.2 : % 0.9 Agarose Gel Reagents

Volume of Gel (ml)	Agarose (mg)	EtBr (µl)	Comb (cell)
40	360	3	8-16
70	630	3.5	16
100	900	4	16

PB Binding Buffer Preparation:

47.79 g of Gu-HCl were dissolved in 20 ml ddwater. 30 ml of isopropanol was added to the solution. The solution was completed to 100 ml with ddwater. The solution was sterilized via autoclave. This buffer was used only for DNA isolation with Qiagen miniprep columns.

PE Wash Buffer Preparation:

121.2 g of Tris-HCl were dissolved in 15 ml ddwater. The PH was adjusted to 7.5 with HCl. 80 ml of ethanol was added to the solution. The solution was completed to 100 ml with ddwater. The solution was sterilized via autoclave. This buffer was used only for DNA isolation with Qiagen miniprep columns.

P1 Suspension Buffer Preparation:

0.60 g HCl was added into 20 ml ddwater. pH was maintained to 8.0. 2 ml of (0,5 M) was added. The solution was completed to 100 ml with ddwater.

P2 Lysis Buffer Preparation:

0.79 g of NaOH was added into 20 ml ddwater. 1 g of SDS was added. The solution was completed to 100 ml with ddwater.

N3 Neutralization Buffer Preparation:

80 g of GuHCl was added into 100 ml ddwater. 17.664 g of Potassium acetate was added. 0.37 % Fuming HCl was added to adjust pH to 4.8. The solution was completed to 200 ml with ddwater.

QC Buffer Preparation for Gel Extraction:

300 mg of Trisma Base was mixed wih 81.29 g Guanidine thiocyanate and the mixture was completed to 50 ml with ddwater. pH was adjusted to 6.6.

3.1.9.2 Buffers for competent cell preparation

100 mM $CaCl_2$ Preparation:

5.55 g $CaCl_2$ powder was mixed with 494 ml ddwater. The solution was autoclaved. Stored in 4 °C fridge.

85 mM $CaCl_2$ with %15 glycerol preparation:

1.11 g of $CaCl_2$ powder and 20 ml of ddwater were dissolved in glass bottle. 15 ml glycerol was added. The mixture was completed to 100 ml with ddwater.

100 mM $MgCl_2$ Preparation:

4.76 g of $MgCl_2$ powder was mixed with 494 ml ddwater. The solution was autoclaved and stored in 4 °C fridge.

3.1.10 Molecular biological reagents

3.1.10.1 Enzymes

Klenow blunt end DNA polymerase (New England Biolabs, USA), T4-DNA-Ligase (NEB,USA), T4 Ligase Buffer (NEB, USA), BamH1-HF (NEB,USA), Cut Smart (NEB, USA), EcoR1-HF(NEB, USA), HindIII-HF(NEB, USA), Kpn1-HF(NEB, USA), Sac2(NEB, USA), Bbs1 (NEB, USA), T4 PNK(NEB, USA), Antartic Phosphatase (NEB, USA), Anthartic Phosphat Reaction Buffer(NEB, USA), Spe1(NEB, USA), Nhe1 (NEB,USA), Xho1 (NEB, USA), EcoRV (NEB, USA), q5 Reaction Buffer(NEB, USA), 1X dNTP mix(NEB, USA), q5 PCR enzyme (NEB, USA), Red enzyme mix for PCR(2X BioMix, Turkey).

3.1.10.2 Molecular biological kits

• QIAgen PCR Purification Kit QIAGEN, Hilden

• QIAprep Spin Miniprep Kit QIAGEN, Hilden

• HiSpeed Plasmid Maxi Kit QIAGEN, Hilden

• QIAamp DNA-Blood Mini Kit QIAGEN, Hilden

• QIAgen Gel Extraction Kit, Hilden

3.1.10.3 Molecular markers for gel electrophoresis

• 1 kb DNA-Ladder, GeneRuler, ThermoScientific

• Purple 6 x loading dye, NEB

3.1.11 Biochemical and cellular biological reagents

3.1.11.1 Pyrimethamine drug solution preparation

60 mg of Pyrimethamine drug was dissolved with 594 ml ddwater. 7 ml of DMSO was added to the drug solution. pH was adjusted to 3.30. The solution was stored in a dark bottle at room temperature.

3.1.11.2 1X Heparin preparation

42 mg of 10 X heparin was dissolved with 10 ml of RPMI. 1 ml of 10X was used for 1X heparin with 9 ml RPMI. The solutions were stored in fridge.

3.1.11.3 Blood sample preparation for Flow Cytometry

2.5 µl of mouse blood containing transgenic parasite was mixed with 2.5 µl 1X heparin solution. To prepare 1:200 dilution 495 µl of PBS solution were added. To prepare a 1:500 dilution 1245 µl of PBS solution was added.

3.1.11.4 Ketamine/ Xylasine preparation

600 µl of Ketasol was added into 400 µl of Rompun solution.

3.1.11.5 Mounting gel preparation

PBS solution was prepared with one tablet PBS into 200 ml ddwater. 25 ml Glycerol was added into a 50 ml sterile falcon tube. 25 ml of PBS solution was added into glycerol. 20.5 µl Hoesct was added into the mixture. The mounting gel was stored in dark conditions in a 4 °C fridge.

3.1.12 Biological materials

3.1.12.1 Experimental live organisms and cells

Bacterial Strains *(Escherichia coli)*

Stbl3 (Thermofischer, USA) was used for transformation of ligated plasmid vectors. XL10-Gold (Thermofischer, USA) was used for transformation of ligated plasmid vectors. Top10 (Thermofischer, USA) was used for transformation of ligated plasmid vectors. Omnimax (Thermofischer, USA) was used for transformation of ligated plasmid vectors.

3.1.12.2 Experimental animals

Mice: *Mus musculus*: BALB/c (Bezmialem Research Center), Black6 (Bezmialem Research Center) 6 weeks, female were used for transfection and light application studies.

Rats: *Rattus norvegicus:* Wistar (WIST), Sprague-Dawley (SD) 6 weeks, female were used as a donor for *P. berghei* parasite clonning.

3.1.12.3 Mosquitoes

Anopheles stephensi Nijmegen, Netherlands, *Anopheles stephensi* mosquitoes were raised under 14 h light/ 10 h dark cycle, 75% humidity, and at 28ºC or 20ºC, for uninfected and infected mosquitoes, respectively.

3.1.12.4 Parasite strains

Plasmodium berghei ANKA

3.1.13 Nucleic acids

3.1.13.1 Oligonucleotids

Plasmodium berghei strain ANKA genomic DNAs was used as templates for specific sequences amplification. All primers were obtained from Sentebiolab custom primers,

Right arm primers of Photolyase

nbFOTO_ko3 forward (HindIII)

5’ TGCCAAGCTTGATAATTTTAATGGAGCCAAGGATTGGGCAAAAG 3’

nbFOTO_ko4 reverse (KpnI)

5’ TCCGGTACCACCCAATATGCATTAATATTTTTCAAACCCCAT 3’

Left arm primers of Photolyase

nbFOTO_ko1 forward (Sac2)

5’ GGCCGCGGGTAGTAATAAAACATTGTGATTTGTGATAACAA 3’

nbFOTO_ko2 reverse (BamH1)

5’ TCCGGATCCCATGTTAACCAACATTTGGTTTTGTTTCATTCAT 3’

Tagging primers for Photolyase

mEos4b_test forward

5’ GTGAGTGCGATTAAGCCAGACATGAGGATCAAA 3’

mEos4b_test reverse

5’ ACGTCTAGCATTATCAGGCAATCCAGAATGAGC 3’

nbFOTO_+tag1 (Sac2) forward

5’GGCCGCGGAAATTTTGTATGTACCGAAAAAAAAGCCAAGGAGATCTTAGAAAATTTTTGCAAAAA 3’

bFOTO tag1 forward (Sac2)

5’GGCCGCGGCTATAAAGCCCAAAATACAAACTCACTTATCTTC 3’

bFOTO tag2_sgRNA reverse

5’TGATTAACAAATCGTCATTAAAATATTCTTTCCCGCTCGAAGCATGAATA 3’

bFOTO tag3_ sgRNA forward

5’TAACAAATATGCTCTGCAATTTCCTTCTATTCATGCTTCGAGCGGGAAAG 3’

bFOTO tag4 reverse (EcoR1)

5’TCCGAATTCGTTTAACTTCGTATCAATTTTCACCTCCTTATC 3’

bFOTO_5testF	5’ TACATACACTTACAAAGACGGGGAAATGTAACT 3’
bFOTO_3testR	5’ ATCACACAATTTGCACCCATATTAGTTATTCCT 3’
bFOTO_orfF	5’ GAATTCATGAAATAAAAACAGTTGTCTGTGATT 3’
bFOTO_orfR	5’ CTGCTAATTCTTTCTTGATTAACAAATCGTCAT 3’
mEos4b testR	5’ ATCAATTACAAAATGATGTCCGTTTACATTGCC 3’
nbFOTO_gRNA2+F	5’ TATTGAGCATGTGAATGGCAAATA 3’
nbFOTO_gRNA2+R	5’ AAACTATTTGCCATTCACATGCTC 3’

CAS9 plasmid primers

T2A- Turq2 forward (spe1)

5’GAAGGTAGAGGAAGCCTTCTAACATGTGGAGATGTAGAAGAAAATCCT
GGACCTACTAGTATGGTGAGCAAGGGCGAAGAACTATTTACT 3’

Turq2 reverse (Xho1)

5’TGGTGGCTCGAGTTACTTGTACAGCTCGTCCATGCCGAGAGTGAT 3’

Cas9_seq44 forward

5’ GCTATTAAGAAGGGTATTCTACAAACAGTA 3’

Cas9_p2a forward (afl2)

5’ GGTGGTCTTAAGAAAATGGACTATAAGGATCATGATGGAGAT 3’

Cas9_p2a reverse (afl2)

5’GGACTAGTGAGCATATAGAAAGCCATATTCAAC 3’

hDHFR test forward-17

5’GTGTTCTTTCTGATGTTCAAGAAGAAAAAGGTA 3’

hDHFR-T2A forward (Afl2)

5’ GGCTTAAGAAAATGGTTGGTTCACTAAATTGTATTGTTGCT 3’

hDHFR-T2A reverse (Xho1)

5’ TGCCTCGAGACTAGTAGGTCCAGGATTTTCTTCTACATCTCC 3’

Cas9_frag1 forward (EcoR1)

5’ GGGAATTCAAAATGGACTATAAGGATCATGATGGAGATTATAAG 3’

Cas9_frag1 reverse (EcoR5)

5’ TGCGATATCGCTAGCGGCGCCCTTGTCCACCACTTCCTCGAAGTT 3’

DHFR-T2A forward (EcoR1)

5’ GGGAATTCAAAATGGTTGGTTCACTAAATTGTATTGTTGCT 3’

DHFR-T2A reverse (EcoR1)

5’ TGCGAATTCAGGTCCAGGATTTTCTTCTACATCTCCACATGT 3’

Cas9_seq1F TACCATGAGAAGTACCCTACTATTTATCAT 3’

Cas9_seq2F GTCTGATGCTATTCTGCTGAGTGATATTCT 3’

Cas9_seq3F GATTCGCCTGGATGACCAGAAAGAGCGAGG 3’

Cas9_seq4F GCTGATTAACGGCATTCGGGATAAGCAGTC 3’

Cas9_seq5F GTGCCTTCTGAAGAGGTCGTGAAGAAGATG 3’

Cas9_seq6F GGGTCGGGATTTTGCTACTGTGCGGAAAGT 3’

Cas9_seq44F GCTATTAAGAAGGGTATTCTACAAACAGTA 3’

Cas9_p2a_afl2F
5’GGTGGTCTTAAGAAAATGGACTATAAGGATCATGATGGAGAT 3’

3.1.13.2 Transfection vectors

The plasmid was derived from the pBluescript plasmid that contains the ampicillin resistance marker. Besides, it contains the pyrimethamine-resistance marker DHFRU/ Ts from *P. berghei.* The expression of the selection marker is under the control of the endogenous 5’ and 3’ UTRs. Depending on the selection of the linearization enzymes, the original b3d plasmid was modified by endonucleases digestion, Klenow enzyme filling, and re-ligation. The newly-generated plasmid pbAA20 lacks the three restriction enzymatic sites BamHI, EcoRI, and EcoRV, which can instead be used as linearization restriction sites. The second vector used for the replacement (deletion) transfection strategy is the PbDHFR derived from the pUC19 that contains the ampicillin resistance gene. It contains the pyrimethamine and WR99210 drug resistance selection marker gene DHFR from humans under the regulation of *P.berghei* regulatory elements (5’UTR and 3’UTR). Using the AA20 vector generated by Dr. Ahmed ALY (AA), it was planned to design the DNA Photolyase knock-out/knock-in plasmid. The AA20 plasmid map given in Figure 3.1.

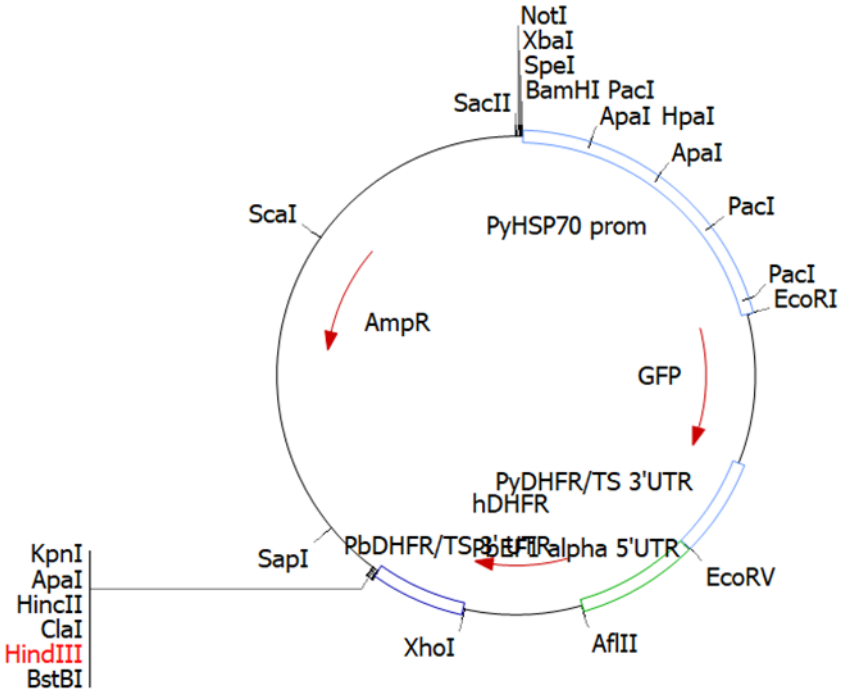

Figure 3.1 : AA20 Plasmid used for knock-out, knock-in vector.

The constructs informations are given in the table 3.3 below.

Table 3.3 : Transgenic vector names created by Ilknur Yilmaz (IY).

Vector Type	Vector Name	Digested Vector	Insert		
			Digested Insert	Restr. Enzymes	Insert Future
Knock-out	AA31	AA20	mEos4b	EcoR1-EcoRV	Label
KO	IY03	AA31	Right arm	HindIII-Kpn1	Homolog
KO	IY04	IY03	Left arm	SacII-BamH1	Homolog
KO	IY10	IY04	hDHFR-	Klenow-Nhe1-Xho1	Remove resistant
Knock-in	IY05	IY03	Pb. Photo overlap	Sac2-EcoR1	Gene Tag
Cas9	IY26	UK06	Pb. Photo sgRNA	Bbs1	Crıspr-Cas9

3.2 Method

The experiments were completed by following the work plan shown in Figure 3.2.

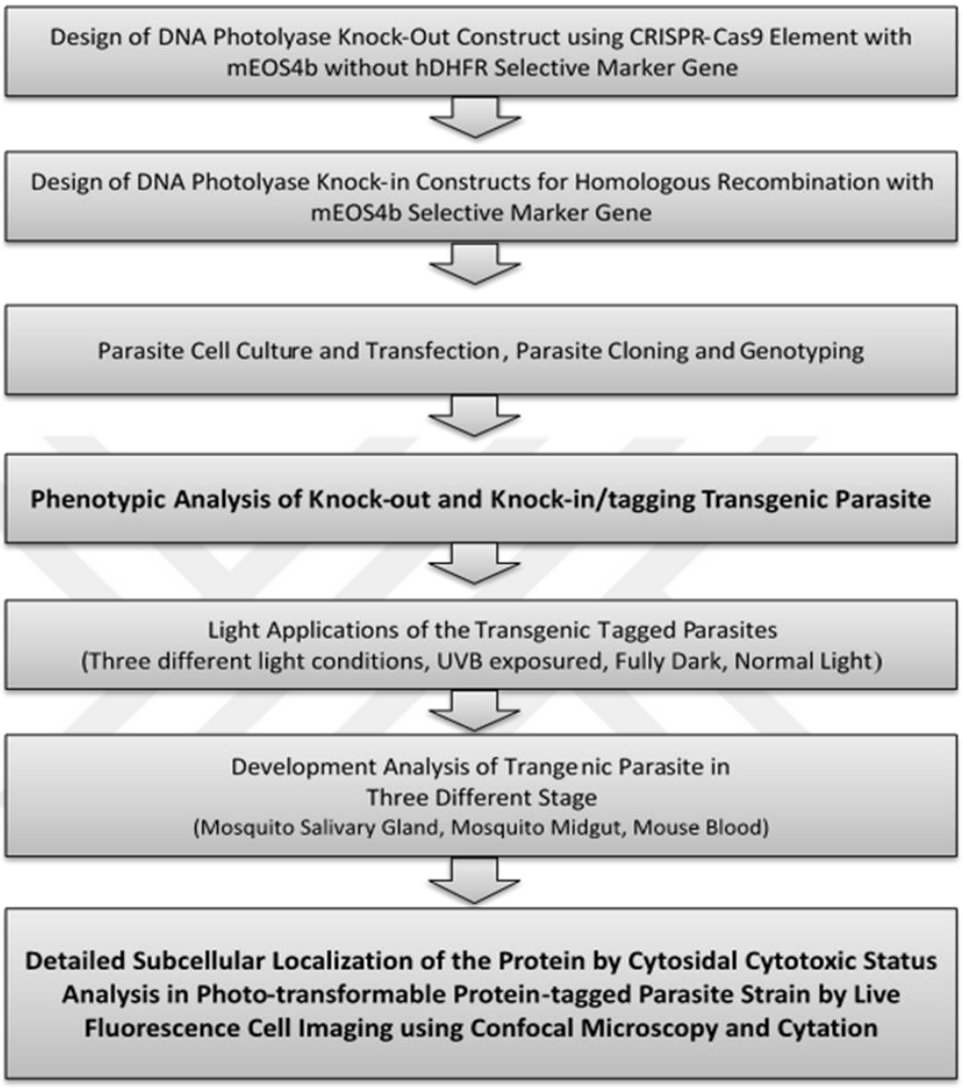

Figure 3.2 : Study plan.

The DNA Photolyase gene is found in some unicellular organisms, such as malaria parasites, in some vertebrate animals in plants but not in mammals and the human genome. In this study, we have designed knock-out knock-in plasmids using the CRISPR-Cas9 system. Rodent transgenic malaria parasite *P.berghei* which has produced by transfections of the plasmids into rodent malaria parasites detected the anomalies in the parasite development cycle in mosquito, mouse and the vital importance of the function of the gene for the parasite determined. With the possibility of blocking the development of gene deletion parasites, a gene inhibitor can be designed for the treatment of malaria-infected patients in the future, and the

reproduction of the parasite in the blood can be prevented. Gene targeting is a process in which different strategies may be applied to alter or eliminate the function of a gene. These modifications can be obtained through deletion, insertion, or replacement of endogenous sequences with alternative sequences. Recently, the CRISPR-Cas9 system has emerged as a precise and powerful tool for gene targeting. Targeted gene disruption is created by Cas9 protein directed by guide RNA (gRNA). Cas9 nuclease creates a double-strand break in the targeted gene sequence [128]. The experiment was initiated with a vector design. Cloning of the photolyase gene homologous arms flanking a cassette expressing a photo-transformable mEOS4b gene that can transform from green fluorescence to red fluorescence under blue light exposure was performed for the knock-out vector. Another vector expressing another Turquoise fluorescence marker (Turq2) is carrying the enhanced-specificity Cas9 gene and the U6 cassette that expressed the sgRNA of the Photolyase gene. The vectors were transfected into the rodent malaria parasite *Plasmodium berghei* ANKA strain. We used the drug resistance gene hDHFR to select the transgenic parasite by pyrimethamine drug administration in mice. Transgenic parasites were detected and sorted out by Flow cytometry. Diagnostic PCR was performed by isolating the parasite genome from the blood. The deletion and marking of DNA photolyase gene by using CRISPR-Cas9. *Plasmodium berghei* DNA Photolyase gene left arm and right-arm amplification, and integration of donor plasmid DNA with CRISPR-Cas9 technology, design, and synthesis of CRISPR-Cas9 elements, EOS4b marking with a fluorescent protein shown in Figure 3.3.

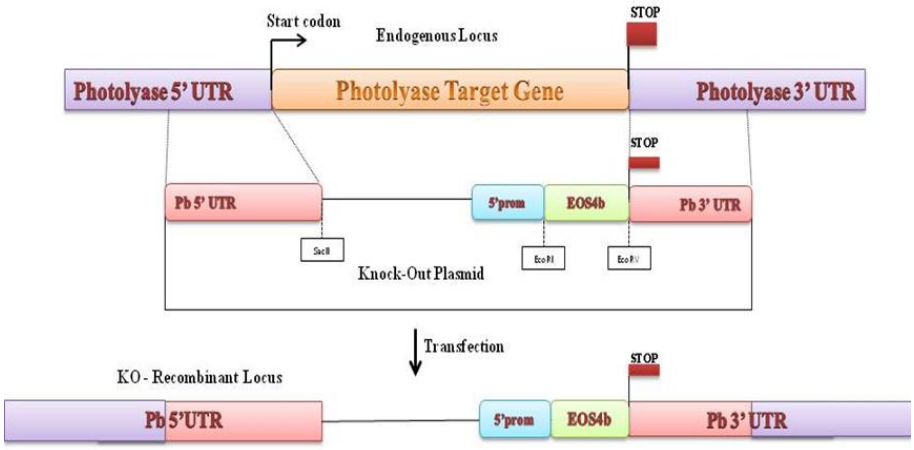

Figure 3.3 : Knock-out study construct.

Knock-in-tagging Study Construct *Plasmodium berghei* DNA Photolyase gene insertion into AA20 vector by using CRISPR-Cas9 and labeling with mEos4b fluorescent protein shown in Figure 3.4.

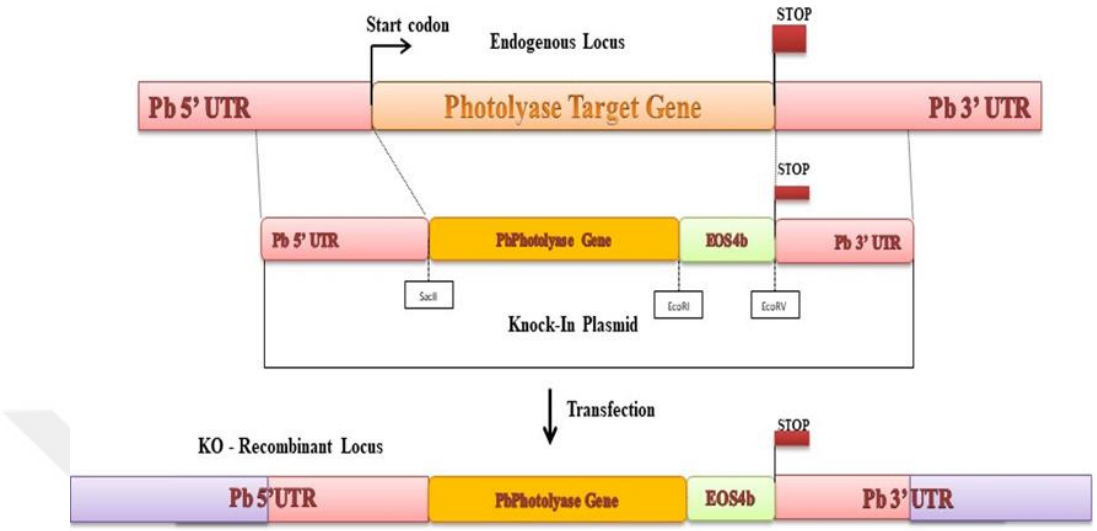

Figure 3.4 : Knock-in tagging study construct.

Design, synthesis and cloning of photoconvertible gene mEos4b:

Clone Manager software for the design and codon optimization of photo-transformable mEos4b gene sequences. One generation of primers was sent to integrate the right and left strands of the Pb Photolyase gene containing the restriction enzyme region sequences into the AA20 plasmid. For homologous recombination of the genetic double crossover, the left and right arms (5 'UTR and 3' UTR) inserts were amplified and cloned into the AA20 plasmid vector surrounding the GFP and hDHFR cassettes. The GFP region mEos4b was replaced with the amplified insert marker gene.

3.2.1 Amplification of the DNA sequences by PCR

The polymerase chain reaction (PCR) was used to amplify specific DNA sequences from *P. berghei* wild type or mutant genomic DNA. The specificity of the amplification is largely dependent on the careful selection of the primer sequences to be amplified, which will allow the specific binding to the template. Primers that are too short will increase the probability of unspecific primer binding. If too long, primers may not bind at a suitable annealing temperature. Therefore, the length of the primers was always selected between 20 and 40 bp. The total GC content is also an important factor that affects the specific binding of primers to their template. The melting

temperature formula Tm = 59.9 + 41 [%GC] – [675/ length of the primer] is an indicator of the right annealing temperature. In practical terms, several trials have shown that the GC content should be above 30%. The annealing temperature controls the primer binding specificity as well. Low annealing temperatures allow unspecific binding, which either precludes the extension of the primers or amplifies other unspecific target sequences. The specific annealing temperature in my experiments was typically confined to 55°C. The amplification success, as well as specificity, can be tested on standard 1% agarose gel electrophoresis. Two PCR method was used for PCR of inserts that are red enzyme PCR and q5 PCR. For knock-out vector of Photolayse gene inserts were amplified with Red enzyme PCR. The general method and device program of PCRs made with the red PCR enzyme mix is given in Figure 3.5.

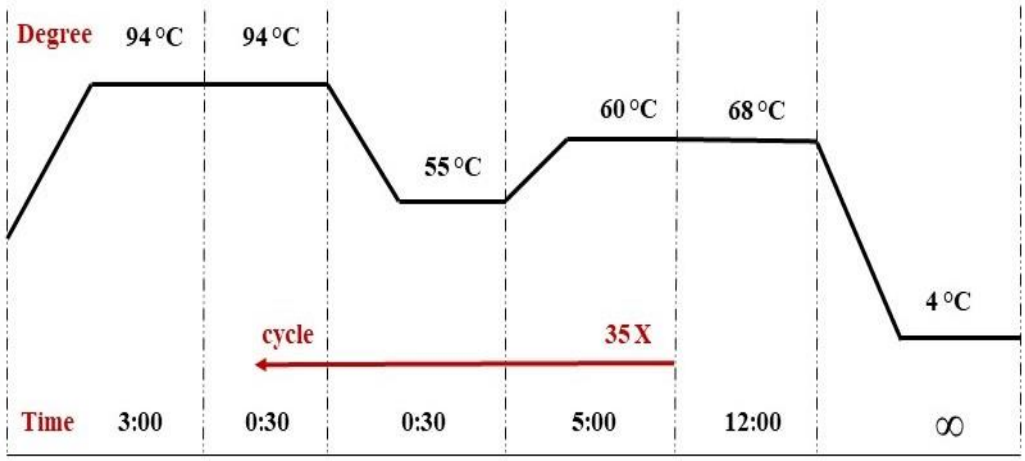

Figure 3.5 : Red enzyme PCR program.

Denaturation of plasmid DNA (3 min, 94°C), elongation period (30 sec 94°C, 30 sec 55°C, 3-10 min 60°C) for 30-35 cycles. Each cycle consists of denaturation, annealing, and extension steps. The final extension (8-12 min 68°C).

The standard reaction components throughout the experiments were mixed as follows:

0.5-2 µl Template DNA

0.5-1 µl Primer forward (100 µM)

0.5-1 µl Primer reverse (100 µM)

25 µl Red Enzyme Mix

ddH_2O complete to 50 µl

The red enzyme PCR reaxtions for Photolyase Knock-Out Vector:

Left Arm Insert PCR reax (Sac2-Bamh1)
Pb ANKA Genomic DNA…. 1 µl
Primer1 Forward: Sac2…….1 µl
Primer2 Reverse: BamH1…..1 µl
Red Enzyme: 25 µl
ddwater: 22 µl
Right Arm Insert PCR reax (Hind III, Kpn1)
Pb ANKA Genomic DNA…. 1 µl
Primer1 Forward: HindIII…….1 µl
Primer2 Reverse: Kpn1…..1 µl
Red Enzyme: 25 µl
ddwater: 22 µl

Preparation of sgRNA:

sgRNA Primer Forward 100µM……..1 µl

sgRNA Primer Reverse 100 µM…….1 µl

T4 ligase buffer ……..1 µl

T4 PNK enzyme……..1 µl

ddwater……..10 µl

PCR programme for sgRNA

37 °C ……..30 min

95 °C ……5 min

Ramped down to 25 °C slowly (0.1 °C /sec)

25 °C ……..30 min

Placed into ice package. 1:300 diluted with water.

The q5 enzyme PCR reaxtions for Photolyase Knock- In Vector:

For Knock-in vector of Photolayse inserts were amplified with high accuracy q5 PCR. The programme was shown in Figure 3.6.

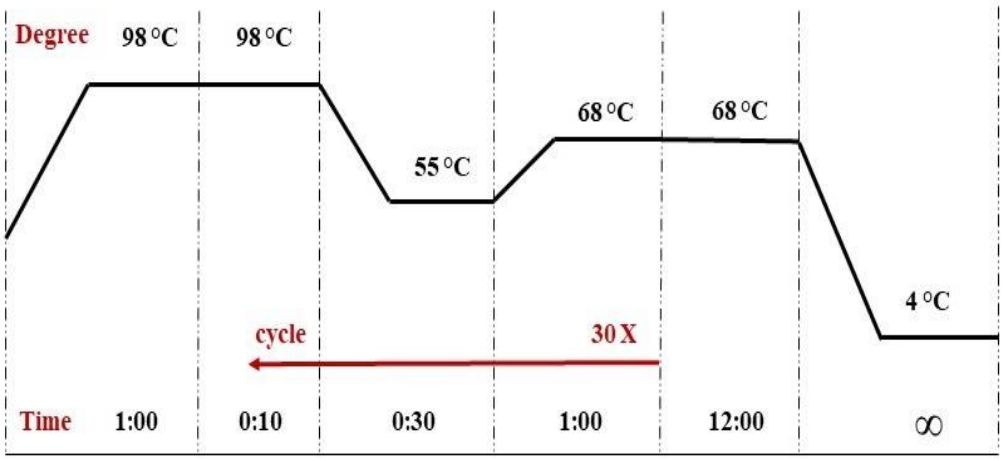

Figure 3.6 : Q5 PCR program.

Denaturation of plasmid DNA (1 min, 98°C), elongation period (10 sec 98°C, 30 sec 55°C, 1 min 68°C) for 30-35 cycles. Each cycle consists of denaturation, annealing, and extension steps. The final extension (8-12 min 68°C).

The standard reaction components throughout the experiments were mixed as follows:

0.5-2 µl Template DNA

2.5 µl Primer forward (100 µM) 1:10 diluted

2.5 µl Primer reverse (100 µM) 1:10 diluted

1 µl 1 X DNTP

10 µl Q5 Reaxtion Buffer

0.5 µl Q5 Enzyme

ddH_2O complete to 50 µl

To prepare knock-in vector *Plasmodium berghei* DNA photolyase gene was produced via overlap PCR. 4 primer designed, 2 for half of the length of the DNA Photolyase gene and 2 for another half of the gene produced with q5 PCR. For final DNA

photolyase full length 1. And 4. The primer was used with the first two PCR products as a template see Figure 3.17.

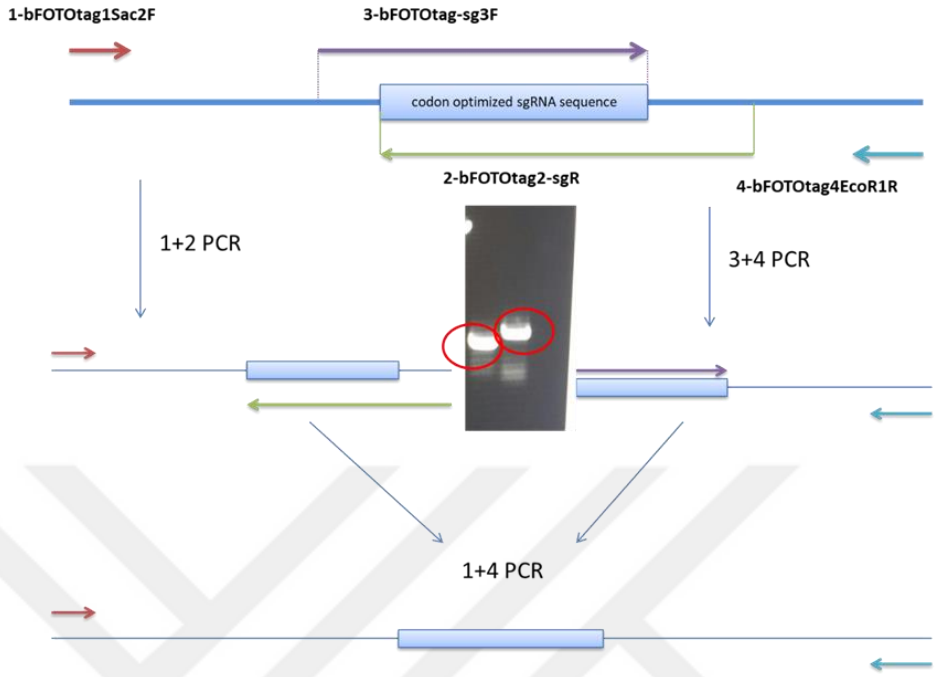

Figure 3.7 : Overlap PCR for Pb DNA Photolyase gene.

The usage of the PCR amplification throughout the experiments can be classified into three categories:

1. Amplification of DNA fragments for cloning in plasmid vectors

For this application, primers are designed to contain additional specific restriction sites, which will facilitate the cloning into target plasmid vectors. The elongation step at the end of the PCR aims at completing the ends of the primers, to increase the subsequent endonuclease digestion efficiency. The template, in this case, is mostly wild type genomic DNA. The amplified sequences need to be purified with the kit (Qiagen), and eluted in sterile ddH_2O, before proceeding with the enzymatic digestion.

2. Amplification of DNA fragments for verifying the transfection success

For this application, additional restriction sites can typically be omitted. The resulting amplified DNA fragments verify the integration of the foreign DNA sequence into the endogenous locus. Therefore, master mixes of all components except for template DNAs of the tested strains are prepared for each primer combination separately. To verify the presence or absence of the tested DNA sequences, wild type genomic DNA

and circular transfection plasmid vector are included as template controls, in addition to the genomic DNA from transfected parasite populations. The extra elongation step of the PCR reaction, a very low number of transcripts.

Diagnostic PCR for knock-out and knock-in genomic DNA:

Plasmodium berghei WT genomic DNA was used as a control. IY10 Tf (1^{st} generation) and IY10 Tf4 (4^{th} generation) two genotype were used for Knock-Out genomic DNA template. IY05 Parental (1^{st} generation) and IY05 Par3 (3^{rd} generation) two genotype were used for Knock-in genomic DNA template. 0.5 µl of genomic DNA were added into the PCR tubes. Three region were sellected for aplications for all templates;

1- 5' UTR Primers (5' Test Forward- HSP70 Reverse)
2- 3' UTR Primers (5' Test Forward- 3'Test Reverse)
3- Open reading frame Primers (orf Forward- orf Reverse)

Red enzyme PCR reaction was proceed with red enzyme PCR program.

3.2.2 Analysis and purification of the DNA molecules

3.2.2.1 Analysis of DNA molecules by agarose gel electrophoresis

Agarose gel electrophoresis is now widely used to characterize and separate DNA molecules. It depends on the electric mobilization of the negatively charged DNA molecules through the pores of the agarose gel, which in turn is dependent on the length of the molecules, transported through the gel (i.e. short DNA fragments move faster within the gel than longer ones). The gel is prepared from 0.8-1% agarose in 40–100 ml 1X TAE buffer. After boiling for 1 minute and cooling down to 50 60°C, ethidium bromide is added and mixed well (10µg/100ml) before pouring the gel solution. The agarose DNA electrophoresis is normally run for 1 hour at 90 V. Ultraviolet light is used to visualize the separated DNA molecules. A gel documentation system saves a picture of the gel for further analysis of the results. To facilitate the determination of molecular sizes, a 1kb DNA marker (NEB) is loaded on lateral lanes.

3.2.3 Purification of the DNA by the PCR purification kit

This method is used to purify and/or concentrate DNA molecules on a small scale. In general, digestion reaction and PCR amplified sequences for cloning are purified by this method. For a detailed description of procedures and reagents, see the Qiagen PCR purification Kit manual.

3.2.4 Purification of the DNA by the ethanol precipitation

This method is used to purify and/or concentrate DNA molecules in a smaller volume than the starting one. This method is used with high solution volumes and/ or large amounts of DNA molecules. After the addition of sodium acetate (pH 4.8) to the solution, the DNA is precipitated by ice-cold 100% ethanol. Sodium acetate and cold ethanol are added 0.1x and 2x to the starter solution volume, respectively. After 30 minutes incubation at -80°C, the precipitated DNA is harvested by centrifugation for 20 to 30 at maximum speed minutes at 4°C. The DNA is then washed with 70% cold ethanol and again centrifuged for 10 minutes at full speed also at 4°C. Afterward the pellet is left to be air-dried at room temperature and finally eluted in the appropriate volume of ddH_2O or TE buffer.

3.2.5 Determination of the DNA concentration

For further processing of the DNA preparation, the concentration of DNA solution must first be determined. In addition to the empirical estimation on agarose gel electrophoresis, a mass spectrophotometer is used to determine the concentration of DNA in solutions. The nanodrop is used for the calculation of DNA concentration. Figure 3.8 shows an example of nanodrope results.

According to the graph in Figure 3.8, nanodrop measurement results for ng/µl unit A260 is 2,873, A280 is 1,551, nm 1 abs. is 2.866, A260/280 is 1.85, A260/230 is 2.34. The concentration is 143.6 ng/µl.

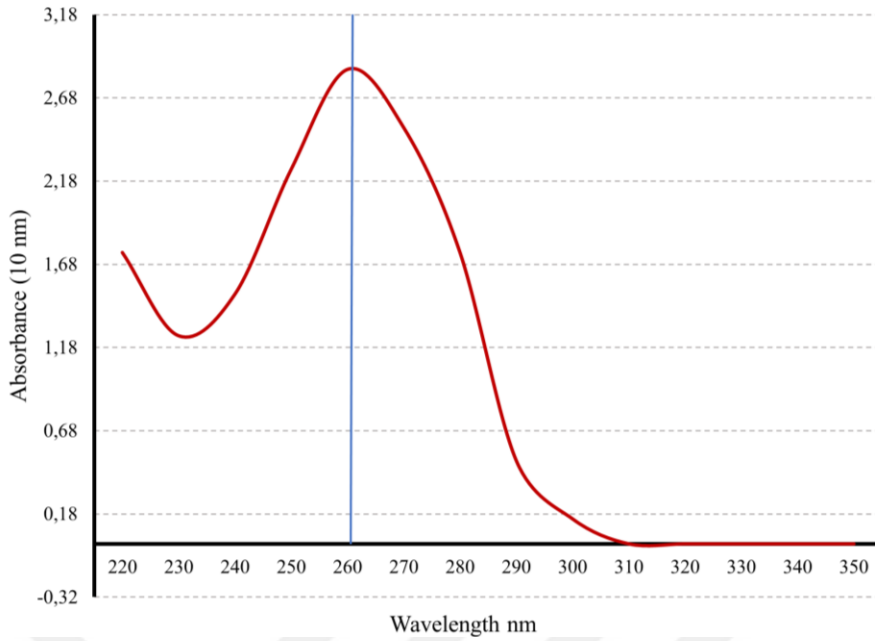

Figure 3.8 : An example for nanodrop result of DNA concentration.

The optical density at 260nm (OD260) is used for calculation of DNA solutions by the following formula: (OD260 x dilution factor x 50) /1000 = DNA concentration in ng/µl. For example, an OD260 measurement of 1.0 corresponds to a DNA concentration of 50ng/µl.

3.2.6 Digestion of inserts after PCR purification

Cloning starts with the preparative digestion of both the DNA fragments and the vectors with the respective enzymes. Typically, a restriction reaction with one enzyme unit is sufficient to digest 1µg DNA under optimal conditions. One unit of endonuclease enzyme corresponds to the amount of enzyme required to digest 1 µg of λ DNA in an hour at 37°C in a total reaction volume of 50 µl. For more details, see NEW England Biolabs endonuclease enzyme catalog. Optimal conditions include incubation for 2-20 hours at 37°C and use of the proper enzyme buffer. The standard endonuclease digestion reaction used for cloning consists of the following: 1-2 µg DNA 1-2 U/ml restriction enzyme BSA (bovine albumin serum; needed for many enzymes for optimal digestion), Enzyme buffer, ddH_2O. This scheme is applied for most digestion reactions of DNA fragments or plasmid vectors. Digestion with two restriction enzymes can be done in one reaction vial if one suitable enzyme buffer for both enzymes is available. After digestion with the respective enzymes, all DNA

molecules must be purified with the PCR purification kit (Qiagen), and eluted in warm ddwater, before proceeding with ligation.

3.2.6.1 Left arm of PbDNA Photolyase gene insert digestion and purification

64 µl of purified PCR KO 1-2 product was mixed with 8 µl of Cut smart and 2 µl of Sac2, BamH1 digestion enzymes. The reaxtion was completed to 80 µl with pyrogen free pure water. The soultion was incubated in 37 °C for 1 and half hour. Second time 2 µl of same digestion enzymes added into the reaction. And it is incubated for additional an hour. The reaxtion was stopped at 85 °C for fifteen minutes. Purified with qiagen PB (5X) and PE (750 µl) buffers with it's colums. Eluted with 40 µl of pure water. The concentration was measured using nanodrop.

3.2.6.2 Right-arm of PbDNA Photolyase gene insert digestion and purification

64 µl of purified PCR KO 3-4 product was mixed with 8 µl of Cut smart and 2 µl of HindIII, Kpn1 digestion enzymes. The reaxtion was completed to 80 µl with pyrogen free pure water. The soultion was incubated in 37 °C for 1 and half hour. Second time 2 µl of same digestion enzymes added into the reaction. And it is incubated for additional an hour. The reaxtion was stopped at 85 °C for fifteen minutes. Purified with qiagen PB (5X) and PE (750 µl) buffers with it's colums. Eluted with 40 µl of pure water. The concentration was measured using nanodrop.

3.2.7 Gel Extractions

3.2.7.1 Gel extraction and digestion of Pb Photolyase overlap PCR product (iy05)

Overlap PCR products were loaded on 0.9 % agarose gel. The gel was run at 90 V for an hour. Upper band was taken into 2 ml Eppendorf tubes. The tubes were measured. 3X concentration QC buffer (gel extraction kit) was added into the gels. The tubes were kept at 56 °C incubator for 10 minute. The tubes were vortex each 3 minute during 10 minute incubation. After gel is melted 1 X concentration of 100% isopropanol was added and the solutions passed through qiagen columns. DNA purified and eluted with 90 µl of warm ddwater. The insert DNA was digested with Sac2, EcoR1. Please see the digestion protocol above.

3.2.7.2 Gel extraction and digestion of MKO1 mEos4b gen region (iy03)

MKO1 vector which contain mEos4b gene was digested with EcoR1 and EcoR5 restriction enzymes. The reaction was loaded on 0.9 % agarose gel. The gel was run at 90 V for an hour. Upper band was taken into 2 ml Eppendorf tubes. The tubes were measured. 3X concentration QC buffer (gel extraction kit) was added into the gels. The tubes were kept at 56 °C incubator for 10 minute. The tubes were vortex each 3 minute during 10 minute incubation. After gel is melted 1 X concentration of 100% isopropanol was added and the solutions passed through qiagen columns. DNA purified and eluted with 40 µl of warm ddwater.

3.2.8 Digestion and dephosphorylation reactions of plasmids

3.2.8.1 Digestion and dephosphotylation of AA20 Vector

85 µl of AA20 plasmid was mixed with 10 µl of Cut smart and 3 µl of EcoR1, EcoR5 digestion enzymes. The reaxtion was completed to 100 µl with pyrogen free pure water. The soultion was incubated in 37 °C for 1 and half hour. Second time 1.5 µl of same digestion enzymes added into the reaction. And it is incubated for additional an hour. The reaxtion was stopped at 85 °C heat inactivated mixture in addition to 5 µl of Phosphatase enzyme. The solution was incubated in 37 °C incubator for an hour. 1.5 µl of Phosphatase enzyme was added in solution and incubated for another an hour. The mixture was heat inactivated in 85 °C for 15 minutes. Purified with qiagen PB (5X) and PE (750 µl) buffers with it's colums. Eluted with 40 µl of pure water. The concentration was measured using nanodrop.

3.2.8.2 Digestion and dephosphotylation of AA31 Vector

85 µl of AA31 plasmid was mixed with 10 µl of Cut smart and 3 µl of Hind3, Kpn1 digestion enzymes. The reaxtion was completed to 100 µl with pyrogen free pure water. The soultion was incubated in 37 °C for 1 and half hour. Second time 1.5 µl of same digestion enzymes added into the reaction. And it is incubated for additional an hour. The reaxtion was stopped at 85 °C for fifteen minutes. 12 µl of Antartic Phospate Buffer was added into heat inactivated mixture in addition to 5 µl of Phosphatase enzyme. The solution was incubated in 37 °C incubator for an hour. 1.5 µl of Phosphatase enzyme was added in solution and incubated for another an hour. The

mixture was heat inactivated in 85 °C for 15 minutes. Purified with qiagen PB (5X) and PE (750 µl) buffers with it's colums. Eluted with 40 µl of pure water. The concentration was measured using nanodrop.

3.2.8.3 Digestion and dephosphotylation of IY03 Vector

85 µl of IYO3 plasmid was mixed with 10 µl of Cut smart and 3 µl of Sac2, BamH1 digestion enzymes. The reaxtion was completed to 100 µl with pyrogen free pure water. The soultion was incubated in 37 °C for 1 and half hour. Second time 1.5 µl of same digestion enzymes added into the reaction. And it is incubated for additional an hour. The reaxtion was stopped at 85 °C for fifteen minutes. 12 µl of Antartic Phospate Buffer was added into heat inactivated mixture in addition to 5 µl of Phosphatase enzyme. The solution was incubated in 37 °C incubator for an hour. 1.5 µl of Phosphatase enzyme was added in solution and incubated for another an hour. The mixture was heat inactivated in 85 °C for 15 minutes. Purified with qiagen PB (5X) and PE (750 µl) buffers with it's colums. Eluted with 40 µl of pure water. The concentration was measured using nanodrop.

For Knock-In

85 µl of IYO3 plasmid was mixed with 10 µl of Cut smart and 3 µl of Sac2, EcoR1 digestion enzymes. The reaxtion was completed to 100 µl with pyrogen free pure water. The soultion was incubated in 37°C for 1 and half hour. Second time 1.5 µl of same digestion enzymes added into the reaction. And it is incubated for additional an hour. The reaxtion was stopped at 85 °C for fifteen minutes. 12 µl of Antartic Phospate Buffer was added into heat inactivated mixture in addition to 5 µl of Phosphatase enzyme. The solution was incubated in 37 °C incubator for an hour. 1.5 µl of Phosphatase enzyme was added in solution and incubated for another an hour. The mixture was heat inactivated in 85 °C for 15 minutes. Purified with qaigen PB (5X) and PE (750 µl) buffers with it's colums. Eluted with 40 µl of pure water. The concentration was measured using nanodrop.

3.2.8.4 Digestion and dephosphotylation of IY04 Vector

85 µl of IYO4 plasmid was mixed with 10 µl of Cut smart and 3 µl of Nhe1-Xho1 digestion enzymes. The reaxtion was completed to 100 µl with pyrogen free pure

water. The soultion was incubated in 37 °C for 1 and half hour. Second time 1.5 µl of same digestion enzymes added into the reaction. And it is incubated for additional an hour. The reaxtion was stopped at 85 °C for fifteen minutes. 12 µl of Antartic Phospate Buffer was added into heat inactivated mixture in addition to 5 µl of Phosphatase enzyme. The solution was incubated in 37 °C incubator for an hour. 1.5 µl of Phosphatase enzyme was added in solution and incubated for another an hour. The mixture was heat inactivated in 85 °C for 15 minutes. Purified with qiagen PB (5X) and PE (750 µl) buffers with it's colums. Eluted with 40 µl of pure water. The concentration was measured using nanodrop.

Klenow Application

5.5 µl of digested IY04 was mixed with 1.5 µl of Klenow enzyme, 2 µl of T4 Ligase buffer, 1 µl of dNTPs and the reaction was completed to 20 µl with 10 µl of ddwater. The reaction was kept in room temparature for 40 minutes. Heat inactivated at 85 °C 15 minute and purified with Qiagen purification kit. The DNA was eluted into 40 µl ddwater.

3.2.8.5 Digestion and dephosphotylation of UKO6 Vector

88 µl of UKO6 plasmid was mixed with 10 µl of Cut smart and 1.5 µl of Bbs1 digestion enzyme. The reaxtion was completed to 100 µl with pyrogen free pure water. The soultion was incubated in 37 °C for 1 and half hour. Second time 0.5 µl of same digestion enzymes added into the reaction. And it is incubated for additional an hour. The reaxtion was stopped at 85 °C for fifteen minutes. 12 µl of Antartic Phospate Buffer was added into heat inactivated mixture in addition to 8 µl of Phosphatase enzyme. The solution was incubated in 37 °C incubator for an hour. 2 µl of Phosphatase enzyme was added in solution and incubated for another an hour. The mixture was heat inactivated in 85 °C for 15 minutes. Purified with qiagen PB (5X) and PE (750 µl) buffers with it's colums. Eluted with 40 µl of pure water. The concentration was measured using nanodrop.

3.2.9 Designing CRISPR-Cas9 vector

The high-fidelity CRISPR-Cas9 elements designed and introduced into high-efficiency transfection vectors in Figure 3.9. The codon-optimized Cas9 endonuclease and sgRNA sequences are ordered from a gene synthesis company. The AA20 vector

(Dr. Aly at Tulane University developed these transfection plasmids) be used for the introduction of the synthesized sequence. Another improved AA20 plasmid used for the introduction of knock-in donor DNA for homologous recombination. UKO6 vector is include U6 promoter scaffold U6 terminator, HSP70 promoter, Cas9 and HSP70 UTR. In addition it has Turg2 marker gene with hDHFR sellective gene. Only the Cas9 plasmid contains the hDHFR (human dihydrofolate reductase) cassette which is used as a positive selection marker conferring the resistance against the well-known antimalarial drug Pyrimethamine. Pb Photolyase gRNA dimer was produced and inserted into UKO6 cassette.

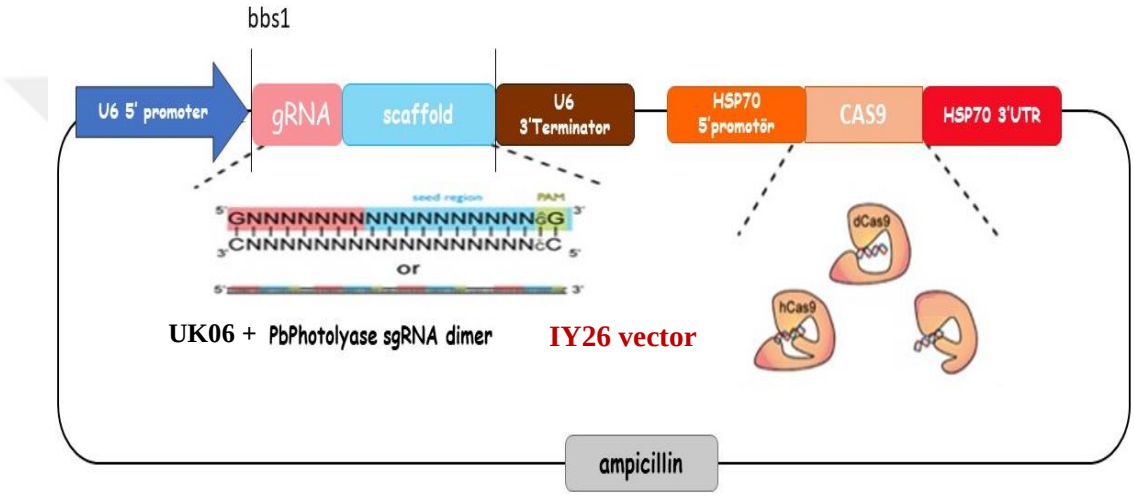

Figure 3.9 : Designed UK06 Cas9 expression vector for Photolyase knock-out.

3.2.10 Ligations

T4 ligase enzyme and ligase buffer is used for ligation of the digested DNA 5' to 3' ends at room temperature for 2-4 hours. The standard ligation reaction consists of the following: 1.5 µl plasmid vector 7 µl amplified DNA target sequence 1 µl ligase buffer 0.5 µl ligase enzyme. Afterwards, the ligation reaction is kept on room temperature, and is not purified before transformation into competent bacterial cells. Digested AA20 vector was ligated with digested iy03 (mEos4b) insert for AA32. Digested AA32 vector was ligated with digested iy02 (right arm) insert for IY03. Digested IY03 vector was ligated with digested iy01 (left arm) insert for IY04. Digested IY04 vector was ligated into itself (no hDHFR) for IY10. Digested IY03 vector was ligated with digested iy05 (Pb photo with left arm) for IY05. Digested UK06 vector was ligated with gRNA dimer for IY26.

3.2.11 Transformation of recombinant plasmid vectors

Ligated plasmids are transformed into the heat-shock transformable *E. coli* strain Stbl3, Omnimax, XL10 Gold. The principle of plasmid acquisition by heat shock depends on the opening of pores in the plasma membrane of the bacteria following rapid temperature elevation to 42°C. β-mercaptoethanol facilitates this permeabilization process and therefore is added to the pre-incubated competent cells, followed by the addition of ligated recombinant plasmids. The initial volume of the bacterial cells suspension determines the volume of both β-mercaptoethanol and ligation reaction mixture and normally the amounts used are 40 µl, 0.68 µl, and 2 µl, respectively. For a detailed description of the transformation protocol, see the stratagene XL-10 Gold competent cells transformation manual. The bacterial cells containing the recombinant plasmids are selected on agar plates containing ampicillin, to which the cells that contain the recombinant plasmid are resistant. Following the spreading of all of the transformation suspension on LB-agar plates and incubation at 37°C for 16-20 hours, single colonies growing on the LB-agar plates are picked up to be cultured separately (Exmp. Figure 3.10). Thereafter, recombinant plasmids are isolated and tested further.

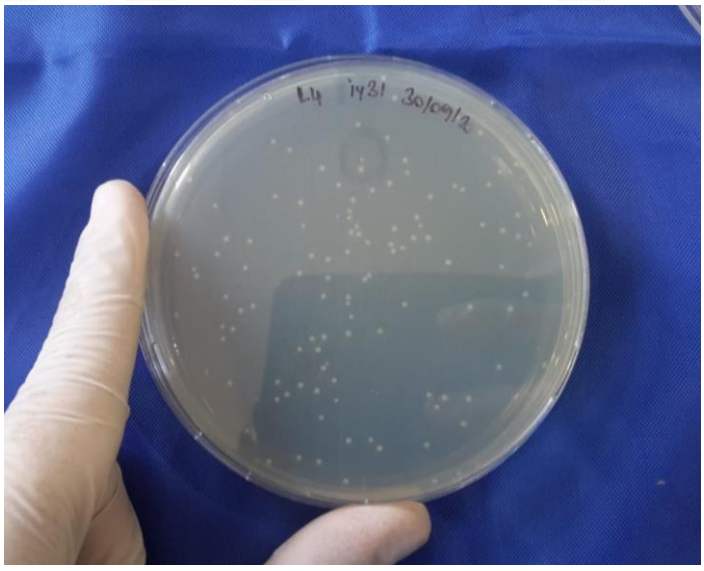

Figure 3.10 : *E.coli c*olony image for AA31 transgenic stbl3 cells.

3.2.12 Isolation of the recombinant plasmids

In order to screen for recombinant plasmids among the isolated single colonies, the colonies are re-suspended in 5 ml LB containing ampicillin and are cultured at 37°C

for 16-20 hours in a shaking incubator. The isolation of the plasmids from the bacterial cells follows the principle of alkaline lysis of the bacterial cell wall and plasma membrane. Next, proteins, lipids and genomic DNA are precipitated with acetic acid. Circular plasmids are not precipitated and therefore remain in the soluble supernatant fraction after centrifugation. The QIAprep Spin Miniprep Kit (Qiagen) was used to isolate the recombinant plasmids from 3 ml of the overnight bacterial mini culture. The plasmids were finally eluted in 50 µl ddH_2O. For a detailed description of the isolation procedures, see the Qiagen QIAprep spin miniprep manual. The recombinant plasmids are then tested by digestion with the appropriate restriction enzymes. The digestion reactions are then loaded onto a 0.8-0.9% agarose gel and separated by gel electrophoresis. The bacterial cell line containing the right recombinant plasmids is cultured and spread onto ampicillin LB-agar plates for further high scale DNA purification of the recombinant plasmids by Qiagen HiSpeed Plasmid Maxi DNA Kit. Eventually, the recombinant bacterial cell line is preserved for long-term storage by mixing 500 µl 30% glycerol with 500 µl of freshly inoculated bacterial cell suspension from freshly streaked LB-agar plate. Afterwards the vials can be stored in fluid nitrogen or in the -80°C freezer.

3.2.13 Large-scale DNA preparation of recombinant plasmid vectors

To obtain large amounts of plasmid DNA from the recombinant bacterial cell line, large-scale cultivation of a 250 ml LB maxi culture is needed. Inoculation of the maxi culture from numerous re-suspended colonies is done from a freshly streaked LB agar plate of the recombinant bacterial cell line. After incubation for 16-20 hours in a shaking incubator at 220 rpm at 37°C, the bacterial cells are harvested and lysed. The same alkaline-lysis and acidic precipitation principle described above is also applied here. The HiSpeed Plasmid Maxi Kit (Qiagen) was used to isolate the recombinant plasmids, which were eluted in 1ml TE buffer. For a detailed description of the maxi DNA preparation, see the Qiagen HiSpeed Plasmid Maxi Kit manual.

3.2.14 Transfection of *Plasmodium berghei* parasites

3.2.14.1 Transfection culture preparation

Pyrimethamine-sensitive 200 µl of frozen stock *P. berghei* blood stage parasites (Pb ANKA) are injected inter-peritoneally into Wistar Rats (100-150g). After 3 to 4 days,

the parasitemia should be between 2 and 3% with almost no or very few gametocytes. The rats are bled via heart puncture with heparinized-syringes, and the blood from one rat is added to pre-warmed 10 ml transfection culture medium containing 250µl heparin in PBS. After centrifugation for 8 minutes at 1000 rpm (with no brake) at room temperature, the erythrocytes pellet is re-suspended in 50 ml transfection culture medium and then added to pre-warmed 100 ml culture medium in a flask. The flask with the 150 ml transfection culture is shaken for 15-16 hours at 77-80 rpm at 37°C in a mixed-gas incubator. The gas mix was 10 % O_2, 5 % CO_2, and 85 % N_2. During this time, nearly all erythrocytic stages mature and turn into to late schizonts. The quality of the infected erythrocytes must be checked by smearing a drop of the transfection culture and microscopical examination.

3.2.14.2 Isolation of the mature schizonts

The late schizonts are collected from the overnight culture using a density gradient, in PBS. Four 50 ml falcon tubes are filled each with 35 ml transfection culture. Underneath each culture fraction 10 ml density gradient solution is carefully pipetted. After centrifugation for 25 minutes at 1000 rpm (with no brake) at room temperature, the schizont-infected erythrocytes are concentrated in a ring phase between the culture medium and the remaining erythrocytes (ring-trophozoite stages infected erythrocytes, and uninfected erythrocytes). This ring of schizonts is carefully collected and centrifuged for 10 minutes at 1000 rpm (with no brake). The resulting 100µl pellet should contain mainly pure schizonts. The quality of the culture was controlled by a Giemsa stained smear. Accudenz stock solution was added to PBS to make a density gradient. Culture suspension prepared and added 60% Accudenz/PBS gradient at the bottom of each tube including culture. Then, tubes centrifuged for 25 minutes at 200g in a swinging rotor. The ring of schizonts (~5ml) at the phase interface of each tube collected with a Pasteur pipette to a new falcon tube. After adding a culture medium, tubes centrifuged for 10 minutes at 200g in the swinging rotor. The supernatant discarded. Schizonts pellets collected together.

3.2.14.3 Preparation of transfection plasmids

60-70 µg of the plasmid to be transfected is digested with the respective linearizing enzyme and incubated for at least 2 hours at 37°C. Afterwards, the linearized construct

is purified by ethanol precipitation and eluted in 300 µl sterile PBS. This solution is ready for electroporation.

3.2.14.4 Electroporation

100 µl schizont pellet is mixed with 300 µl transfection plasmid in a pre-cooled cuvette. Electroporation is done with a 800 V and 25 µFD electric pulse. Thereby, 108 electroporated schizonts will liberate 109 merozoites, some of which will acquire the linearized plasmids during the electric pulse. Thereafter, the transfected merozoites are quickly injected intravenously in two Wistar rats (50-60 g).

3.2.15 Positive selection of recombinant parasites

Pyrimethamine drugs are used to select for the recombinant parasite strains that express the mutated, drug resistant form of *P.berghei* dihydrofolate reductase (DHFR). Treating the infected animals with pyrimethamine (in addition to WR99210 in case of the human DHFR resistance marker) results in clearance of the drug-sensitive asexual stages and will select for the resistant transfected parasites. To a lesser extent, parasites that carry undigested transfection plasmids (episomal transfection), or parasites that were mutated spontaneously within their endogenous DHFR locus, can be selected for. The parasitemia of the infected rats is examined by daily blood smears beginning from day 1 post transfection. The animals are injected interperitoneally with pyrimethamine (25mg/kg animal weight) if any blood stage parasites during the first days after the transfection are detected. Normally, asexual stages are undetectable at day 3 post transfection after pyrimethamine treatment, whereas gametocytes can be detected till days 4 or 5 post transfection. Afterwards all blood stage parasites are undetectable for 2 to 4 days. During this period no pyrimethamine treatment is applied to the animals.

3.2.16 Long-term storage of blood stage parasites

After the confirmation of transgenic parasite via diagnostic PCR the blood of infected mouse was store in minus eighty fridge for future injections. Each infected Balb/c mice gives 1 ml blood by heart puncture. The blood was shared 250 or 300 microliters. The blood was mixed 1:3 ratio of freezing solution (750 or 600) in cryotubes and tag with the name of parasite and generation number of clonning.

3.2.17 Isolation of parasite genomic DNA from infected blood

In order to avoid contamination with the rodents' leukocyte and thrombocyte genomic DNA, self-made columns are assembled to separate efficiently the erythrocytes from the rest of the blood. The column is assembled from an opened 5 ml syringe (for mice blood), or from a 20 ml syringe (for rats blood) and filled with a cotton pad, cellulose powder and glass beads. The column is washed with PBS before use. Thrombocytes and leukocytes bind strongly to the glass beads and cellulose powder, respectively. The erythrocytes are eluted from the column with PBS and centrifuged for 8 minutes at 1500 rpm at room temperature. The erythrocyte pellet is resuspended in 0.2% Saponin/ PBS, which disrupts the plasma membrane of the erythrocytes and thereby releases the parasites into the medium. Lysis is followed by centrifugation for 8 minutes at 3000 rpm. The parasite pellet is re-suspended in 1 ml PBS and centrifuged for 3 minutes at 7000 rpm in a bench centrifuge at room temperature. This washing step is repeated until the supernatant is clear with no apparent hemoglobin contamination. Thereafter, the QIAamp DNA-Blood Mini Kit (Qiagen) was used to isolate and purify the genomic DNA of the parasites in a volume of 150-200 µl ddH_2O. For a detailed description of the procedures and the reagents used, see the Qiagen QIAamp DNA-Blood Mini Kit manual.

3.2.18 Parasite cloning

In a typical Plasmodium transfection experiment, the selected resistant population contains the recombinant and a proportion of resistant wild type or episomally transfected parasites. Therefore, reselection for the recombinant clonal population is done by limited dilution. This involves serial dilutions of the parasite population to obtain an end dilution that contains statistically one single parasite. The following formula was used to calculate the number of parasites needed to be injected per rodent from uninfected blood: 7×10^6 (total number of erythrocytes per µl blood) x parasitemia x 10^{-2} parasites = number of parasitized erythrocytes per µl blood. A series of six subsequent ten-fold dilutions were made with fresh isolated infected blood and RPMI. Thereby, the last dilution contains only one parasite in a volume of 10 to 90 µl. By injecting these single-parasite dilutions intravenously in a number of mice, patent mice are obtained within 8 to10 days post-infection. Bleeding of the patent mice by heart puncture and genotyping the asexual parasite clones results in the selection of

pure recombinant parasite lines. This stage called first generation of transgenic parasite. This experiments repeat by re-infecting the recipient naive mice via dilutions of donor blood. The generation number increase with each repeat of injection to new naive Balb/c mice. The desired parasite clone is then tested in the phenotypical analysis of the respective genotype. Similarly, more than one blood parasite in a defined volume can be obtained by applying the same formula. Intravenous injection of defined numbers of blood stage parasites is used in the phenotypical analysis of asexual blood parasites to screen for differences between clones.

3.2.19 Parasite genotyping

Transgenic parasites were genotyped with oligonucleotide primers to confirm mEos4b integration into the *P. berghei* genome. Integration at 5 ends, the genomic sequence was determined by PCR amplification using primers connected to the integration site at the 5 'end. 3'-end integration was determined by PCR using primers annealed in the integration site at sequence 3 'end.

The oligonucleotides are;

PbFOTO_5' F primer- mEos4b_testR

mEos4b_test F- PbFOTO_3' R

mEos4b_test F – mEos4b_testR

3.2.20 Phenotypical analysis of the parasites

After genetically engineered parasites are obtained, these parasites must be analyzed throughout their life cycle for any behavioral or morphological differences to the wild type parasites. This behavioral and morphological analysis requires the simultaneous use of the wild type parasite as controls. The methods for the phenotypical analysis depend largely on the stage being studied.

3.2.21 Mosquito breeding

Anopheles stephensi mosquito eggs were brought from abroad in a 50 ml falcon tube in water. Eggs were distributed in trays filled with drinking water. 1 mg of powdered fish meal was dispensed into each tray. The trays were kept in a warm room. A day later, the larvae hatched. The feeding continued with fish food. Figure 3.11 shows the

mosquito larvae and pupae we have produced in the left picture tray. The picture on the right shows the mosquito pupae collected from the tray into the beaker.

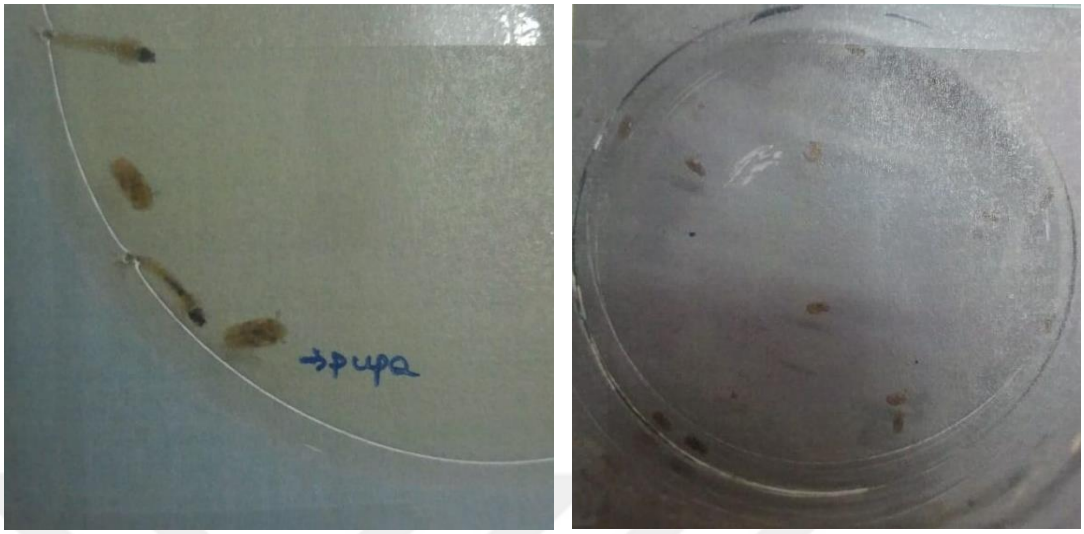

Figure 3.11 : Pupa collection.

When the larvae turned into pupa form, pupae were collected in a small flask with sterile disposable plastic pipettes with some water. Cones were placed in the sterilized mosquito cage. When the mosquitoes became adults, the dish was carefully removed from the cage. The feeding of mosquitoes was provided by leaving cotton pads containing sucrose solution on the cage. Figure 3.12 shows the egg plate we laid inside the mosquito cage and the black mosquito eggs collected in it. White filter paper was placed inside the plate and filled with a small amount of drinking water. Adult *Anopheles stephensi* mosquitoes are observed inside the plate and on the walls of the cage. Mosquito eggs cluster together in the water on the plate.

Figure 3.12 : Mosquito cage with eggs into dish.

Adult mosquitoes were collected in two cages. Colony cage 2 old uninfected BALB / c mice were fed with their blood by fainting. After feeding, a plate was placed in the cage, and some water was left in it. The eggs collected on the plate were distributed on trays and fed in the warm room in water for the next mosquito generation. Adult mosquitoes in the colony cage were terminated by spraying 70% ethanol. Mosquitoes in the infection cage were fed mice infected with transgenic malaria parasite by fainting and lying on the cage. After being fed with blood, they were placed in the large incubator and kept until the extraction process with cotton containing only water. The eggs in the collected colony cage were distributed to trays filled with water and fed with fish food. Figure 3.13 shows the mobile mosquito larvae in the water-filled facility.

Figure 3.13 : Larva and pupa of *Anopheles stephensi* mosquitoes.

3.2.22 Phenotypical analysis of the midgut oocysts

The morphology of *P. berghei* strain ANKA wild type blood stages have been already described. The replication and growth rates of the parasites are determined by screening microscopically the parasitemia in daily blood smears of the infected animals. Calculating parasitemia along the course of infection could display any differences in the ability of the asexually replicating parasites to grow normally inside their host erythrocytes.

3.2.23 Midgut extraction for oocysts observation

Sexual stage parasites are gametocytes that originate from intra-erythrocytic asexual parasites. The process that generates gametocytes is termed gametocytogenesis and is monitored through optical observation of the developing mature gametocytes in peripheral blood of mice. On the other hand, the process that results in fertile gametes within the midgut of blood feeding female mosquitoes is termed gametogenesis. The critical parameter to measure the capacity of the parasites to undergo this vital process is the male gamete exflagellation. Exflagellation is a process by which eight motile

gametes emerge from one microgametocyte upon activation. The motile gametes search for the female gamete to fertilize it and form the zygote. Therefore, the phenotypical analysis of this important feature is an indicator of the transmission efficiency to the invertebrate vector. Figure 3.14 shows the infection of mosquitoes with PbPhoto (-) transgenic parasites. Pure BALB/c mice were infected with Photolyase knock-out frozen blood stock. Mosquitoes were fed infected mice. The mosquito salivary gland and midgut were dissected for the parasite oocyst and sporozoite forms. 2 BALB/c mice were infected with Pb photo knock-out parasite by injecting IP. The mice were injected with 150 µl of Ketamine/Xylazine mixture IP.

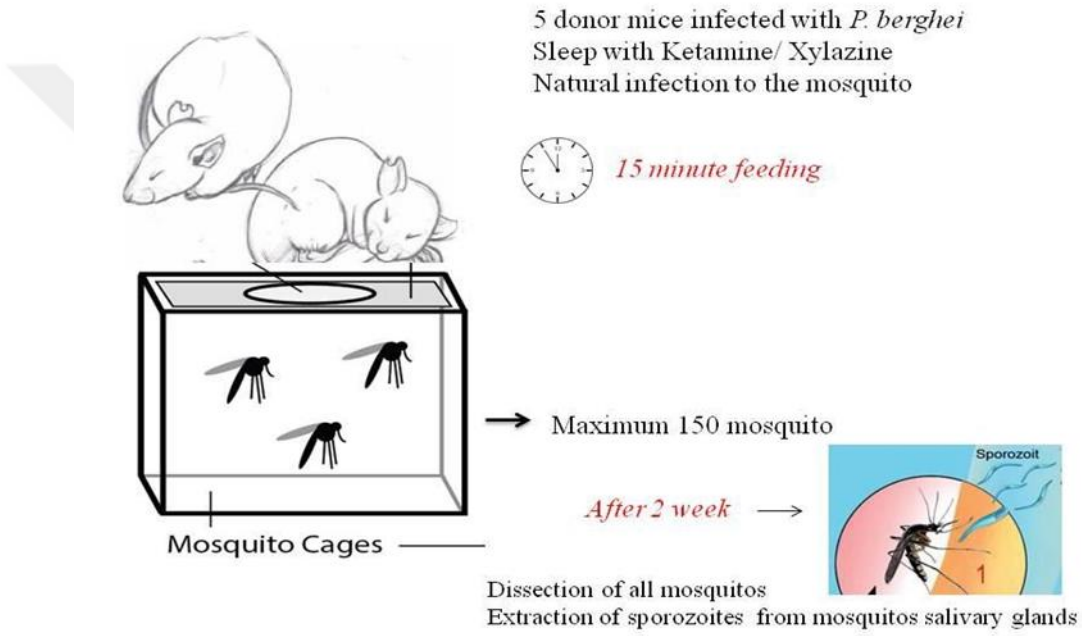

Figure 3.14 : Mosquito infection.

Anopheles stephensi mosquitoes, which were constantly cloned before, were bred in a cage of 150. The knocked-out mice were laid on the cage and the mosquitoes were fed with blood. The mice were resuscitated and resumed in normal living conditions. 10 piece of infected mosquitoes were collected in a 15 ml falcon tube which has 1 ml of %70 Ethanol. The mosquitoes were places into 1 X PBS solution. The mosquito's head was separated from abdoman and midgut was extracted. The midgusts of mosquitoes were laid on a glass slide and covered. The oocyst were observed under flurescent microscope.

3.2.24 Isolation and determination of sporozoite numbers

The mean oocyst sporozoite number per infected mosquito midgut is an important qualitative and quantitative tool to measure the completion of oocyst development and the proper production of sporozoites. Starting from day 14 post mosquito feeding, the female mosquitoes are dissected and the isolated whole midguts are collected in a test tube with dissection medium, with a minimum total of 10 isolated midguts. The whole midguts are then thoroughly mechanically grinded to free the sporozoites from the oocysts in the medium. The sporozoites are then measured in a Neubauer counting chamber after ten fold dilution of the oocyst sporozoites suspension. Afterwards, the total number of oocyst sporozoites in the suspension and the mean oocyst sporozoites number per infected midgut are calculated. In protein extraction probes, the probes are washed at least 3 times with RPMI to avoid extensive contamination with the bovine albumin serum, contained within the dissection medium. Washing is done by centrifugation for 2 minutes at 7000 rpm at 4°C, followed by discarding the supernatant and re-suspension in new RPMI medium. Alternatively, the sporozoites are dissected and isolated in RPMI medium, to completely avoid contamination with BSA. The midguts were placed on glass slide and covered with cover sleep for confocal examinations.

3.2.25 Exflagallation assay

Infected mouse one drop of blood was taken with needle from mouse tail. The blood was covered with lamella on glass slide and waited for 10 minute. The inversion microscope was settled 4X lambda pH1 and blood cells were observed. The microscope settle with 40X labda pH2 filter and sporozoites were observed between blood cells by shaking the cells.

3.2.26 Determination of salivary gland sporozoite numbers

Salivary gland sporozoites are isolated from salivary glands of female mosquitoes starting from day 15 post mosquito feeding. Salivary glands are collected in dissection medium in a test tube and incubated on ice. Thereafter, the salivary glands are grinded thoroughly to release the sporozoites into the medium. Because of the contamination with mosquito debris, the sporozoites are washed twice with dissection medium after spinning down for 2 minutes at 800 rpm at 4°C. After this gentle centrifugation, the sporozoites are recovered from the supernatant, which now is less contaminated with

debris materials. The combined supernatants are then suitable for calculation of sporozoite numbers and for further sporozoite phenotypical analysis. After counting in a Neubauer chamber the total sporozoite number and the mean sporozoite number per female mosquito can be determined. The sporozoites were placed on glass slide and covered with cover sleep for confocal examinations.

3.2.27 General phenotypical analysis of rats with sporozoites

3.2.27.1 Intravenous injection of rats with sporozoites

Susceptible Wistar rats are infected with sporozoites through the intravenous route of infection by injection of defined amounts of sporozoites through the tail veins. Before injection, the sporozoites are incubated on ice within the dissection medium for at least one hour, in order to be activated. Starting from day 3 post sporozoite infection, daily blood smears of infected rats are screened for the presence of blood stage parasites. The time till the first detection of any blood stage parasite is termed the pre-patent period.

3.2.28 UVB studies

Pb WT and IY04 enfected mice were bled for parasite culture bloods. The bloods were incubated in 37 °C via 30 minutes UVB (298 nm) irradiation. The blood was IV injected into three BALB/c mice for WT and knock-out parasites. Parasitemia pecentages were calculated by taking blood smears every 24 hour from mouse tail. The smears were stained with Giemsa and examined 1000X objective of light microscopy. The results were compared with the negative control (Pb WT). Parasite cells expressing the EOS4b fluorescent protein will began to produce a red glow when exposed to UV or blue light for a minimum of 30 minutes while they are radiating green. UVB study performed is schematically represented in Figure 3.15.

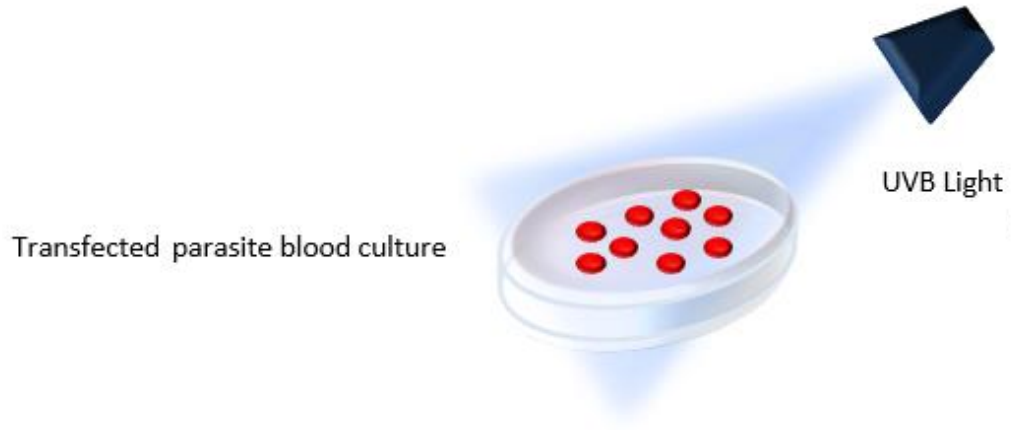

Figure 3.15 : The UVB application study after parasite transfection.

3.2.29 Confocal microscopy studies

Confocal microscopy to detect photoconversion: After the confirmation of mEos4b integration into the parasite genome, the photo-transformable feature of mEos4b was confirmed by confocal microscopy.

Confirmation of mEos4b genetic integration, and its cellular localization: We performed fluorescence microscopy for the cellular localization of mEos4b protein. Briefly, cells are mounted on a glass slide with a 50% glycerol mounting medium in PBS along with Hoechst stain. Slides are incubated for one hour in dark and then the conversion of fluorescence states (green fluorescence to red fluorescence) are observed by exposing the cells to blue light for 5-10 minutes. The images were captured using Confocal Laser Scanning Microscope Leica TCS SP8 at a specific wavelength.

3.2.30 Dark- light studies

Intraperitoneal injection with *P. berghei* strain was performed for 2 Wistar rats as donors. The blood culture was produced a parasite culture for 16 hours. The generated parasites were used in molecular studies to produce knock-out and labeled knock-in in the gene of interest. Genetically modified DNA by electroporation was transfected into the corresponding microorganism. Mouse infections and transgenic rodent malaria parasitemia study. In the sub-items of this assays, for rats and mouse procedures, intra-peritoneal injection of frozen blood stocks, microscopic examination with a drop of

blood from the tail, and ultimately, blood collection with the uptake. Figure 3.16 shows the animal study performed.

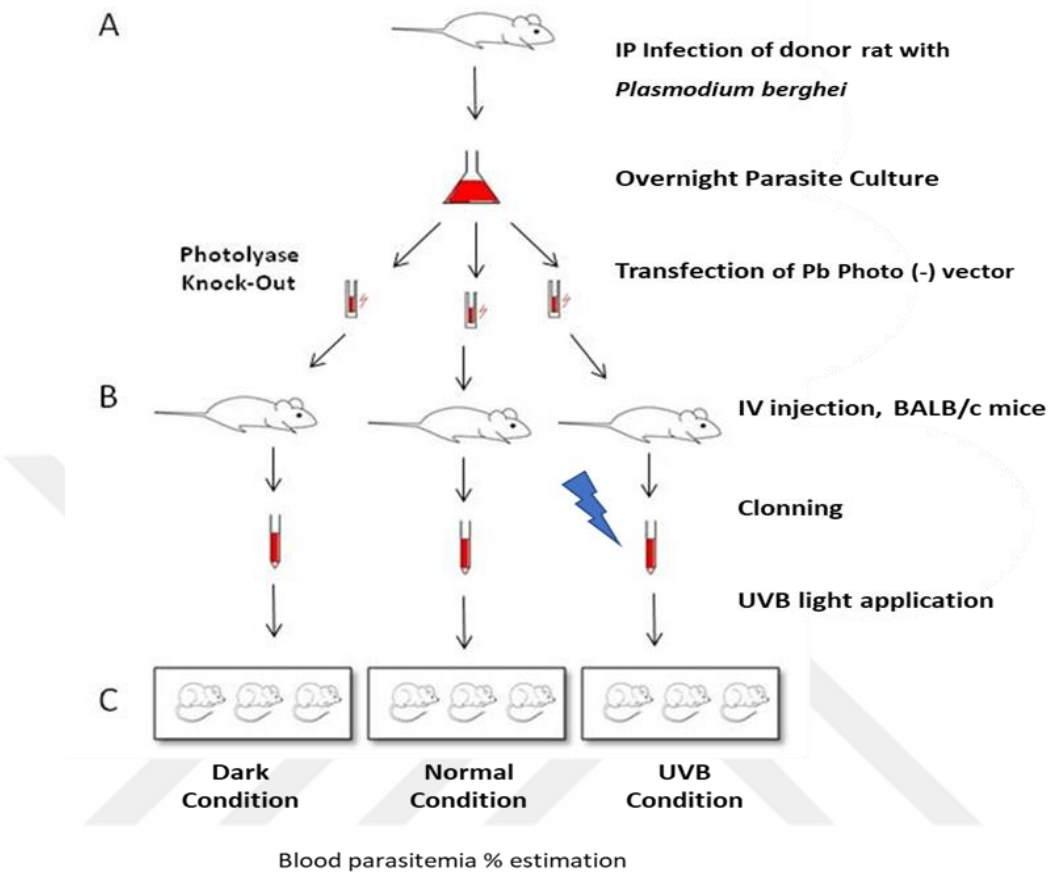

Figure 3.16 : Animal study **A.** Two Wistar rat has been used as donor for *berghei* parasite development for trasfection parasite culture. **B.** Three Balb/c mice as been used for each Knock-out, Knock-in strain for parasite genotyping via drug sellection. **C.** Three Balb/c mice used for each transgenic strain under three light applications.

Same amount has been used for wild type parasite as a control. UVB was applied on parasite blood culture on the conditions 30 minute, 37 °C incubation period. After validation of the designed knock-out vectors by sequencing, transfection was performed using two Wistar rats as *P. berghei* cloning donors. After detecting a high rate of parasitemia in rat blood, 5 ml of blood was taken from the heart. The culture was prepared in a sterile environment with blood RPMI and pen strep. The culture was shaken overnight in the Carbon Nitrogen and oxygen incubator. The schizont form the malaria parasite was isolated and combined with vectors. Transfection was performed with the Lonza nucleofection device. Blood transfers for the cloning study were performed three times in a row using Black6 and BALB/c mice. The parasite genome

was obtained and vectors were verified by diagnostic PCR. KO, WT parasites exposed to Knock-out, Wild type and UVB were injected into three Balb-c mice each. The PB WT and Knock-out mice were kept under completely dark or normal light conditions and blood was taken from dry blood under normal daylight conditions, and thin smears were taken Daily between 24 hours, and the rate of parasitemia after Giemsa staining was monitored by light microscopy.

3.2.31 Parasitemia pecentage calculations

To calculate the parasite percentage, a drop of blood was taken from the infected mouse tail and a thin smear was made. 3.5 ml of concentrated Giemsa dye was completed to 50 ml with ddwater. The top of the slide was covered with methanol. It was fixed for 1 minute. The slide was purged of methanol with distilled water. It was stained with diluted Giemsa for 15 minutes. The slide was purged of giemsa with distilled water. The slide was viewed under a light microscope with an immersion oil under 1000 X objective.

Red blood cells infected with the malaria parasite were scanned. The area with the infected cell was selected as the first area and all red blood cells in the area were counted. The number of infected cells in 30 different areas was determined, including the infected cells in the first area, on the same route. The percentage of parasitemia was calculated by the following formula.

Parasitemia Percentage (%) =
(All infected blood cells in 30 field / First Field Blood Cells x30) x100
Example:
First Field All Blood Cells: 500
Infected blood cells in 30 fields: 35
Parasitemia Percentage = (35/ 30x500)x100 = % 0.23

4. RESULTS AND DISCUSSION

With the CRISPR-Cas9 system, we aimed to create the rodent malaria parasite *Plasmodium berghei* DNA photolyase gene deletion and replace the gene with the new fluorescent photoswitchable marker EOS4b gene in the background. We designed the improved specificity Cas9 endonuclease (plasmid with very low non-genome targets, designed and developed by Dr. Ahmed ALY) by optimizing the sgRNA sequence codon. In our study, this plasmid was created to carry the Cas9 and sgRNA cassettes. The other plasmid was designed and implemented to carry the homology arm to be integrated into the chromosomal locus. The Cas9 plasmid contains an hDHFR (human dihydrofolate reductase) cassette resistant to Pyrimethamine, a well-known antimalarial drug to be used as a positive selection marker. We were able to create the Knock-out Photolyase vector containing the EOS4b gene. Targeted insertion of the mEos4b gene was accomplished by a dual genetic transition strategy driven by homologous recombination. *P. berghei* genomic DNA (gDNA) was used as a template to replicate the 5'UTR and ORF 5 'end fragments. The amplified fragment was inserted into the transfection plasmid AA20 between SacII and BamHI restriction enzyme sites. Fragments from the 3'UTR and 3 'end of ORF were duplicated from *P. berghei* gDNA as a template and placed between the KpnI and HindIII restriction sites in the AA20 plasmids. The fragments cloned for mEos4b were designed not to interfere with the coding sequences of any upstream or downstream neighboring gene, and the structure of these fragments was controlled by sequencing to ensure that unknown 5 'or 3' promoter signals were not altered. The final plasmid was linearized with SacII and Kpn1 before transfection. Transfection of *P. berghei* parasites with the Lonza Nucleofector II device was performed on parasite cultures from donor mice. HDHFR was used as the selection marker of transfected parasites.

4.1 Gel Results

4.1.1 PCR gel results of Photolyase knock-out inserts

Plasmodium berghei DNA photolyase gene sequence was obtained from the plasmodb website and ordered by designing forward and reverse primers adding Sac2, BamH1 restriction enzyme cut sequences for the left homologous arm in the Clone Manager program. Left arm wild type *P. berghei* genomic DNA was used as template and left arm of the gene was amplified by red enzyme PCR method. Figure 4.1 shows the result of gel electrophoresis of the PCR product. The sample was loaded into 1% 40 ml agarose gel and DNA was run at 90 V for 1 hour. Compared to the sample DNA ladder, it was determined that the left arm was the same size of 1 kb as the DNA sequence length. Left-arm amplification was successfully performed.

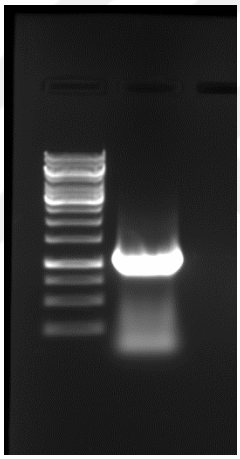

Figure 4.1 : PCR gel result of *Plasmodium berghei* DNA Photolyase 5' UTR (left arm).

Plasmodium berghei DNA photolyase gene sequence was obtained from the plasmodb website and ordered by designing forward and reverse primers adding HindIII, Kpn1 restriction enzyme cut sequences for the right homologous arm in the Clone Manager program. Left-arm wild type *P. berghei* genomic DNA was used as template and the left arm of the gene was amplified by the red enzyme PCR method.

Figure 4.2 shows the gel electrophoresis result of the PCR product. Sample was loaded into 1%, 40 ml agarose gel and DNA were run at 90 V for 1 hour. Compared to the sample DNA ladder, it was determined that the right arm was the same size 1.1 kb as the DNA sequence length. Left arm amplification was successfully performed.

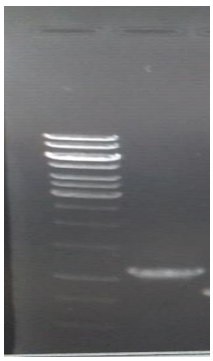

Figure 4.2 : PCR gel result of *Plasmodium berghei* DNA Photolyase 3' UTR (right arm).

mEos4b gene integration was obtained via red enzyme PCR. *Plasmodium berghei* Photolyase knock-out 3rd generation and 4th genomic DNA and wild type *P. berghei* genomic DNA was used as template. Right and the left arm of the gene was selected to introduce with mEos4b gene forward or reverse test primers. For 5' region a forward primer selected with mEos4b_test reverse primer. For 3' region a reverse primer selected with mEos4b_test forward primer. For confirmation of DNA Photolyase gene deletion open reading frame forward and reverse primers selected from coding sequence. Gel was run at 90 V for one hour. Gel results indicates existence of mEos4b gene in knock-out vector with left and right arm of Pb Photolyase gene. Open reading frame exist only in the wild-type genomic DNA.

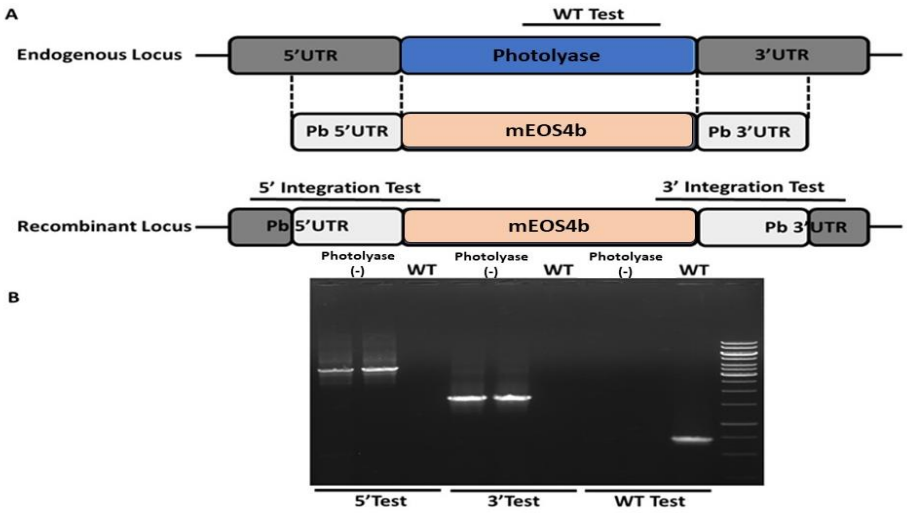

Figure 4.3 : PCR gel result of mEos4b gene integration into the knock-out vector. A) Scheme for expected mEos4b integration. B) Gel result for 5' Test (5'Forward primer with mEos4b R primer), 3' Test (mEos4b F primer with 3' R primer) and PbPhoto open reading frame.

4.1.2 PCR gel results of Photolyase knock-in inserts

In order to integrate the knock-in *Plasmodium berghei* DNA Photolyase gene and mark it with mEos4b, the gene was generated with overlap PCR method by changing the sgRNA sequence of the DNA Photolyase gene via codon optimization.

As shown in Figure 4.4, a forward primer (1) was designed in the clon manager program by adding the Sac2 restriction cut enzyme sequence to the beginning of the start codon. A reverse primer was chosen from the middle of the gene. (2) Another forward primer (3) with sequences similar to the reverse primer and its continuation was chosen. Finally, the last reverse primer (4) was designed by adding the EcoR1 restriction sequence before the stop codon of the gene. Since the expression of the DNA photolyase gene is important, the gene was amplified with high accuracy using q5 PCR. Primer 1 and Primer 2 were paired to replicate half of the gene. Primers 3 and 4 were again amplified with q5 to generate the other half of the gene. Using 1-2 and 3-4 PCR products as template, the whole Pb Photolyase gene was amplified by q5 PCR with primers 1 and 4.

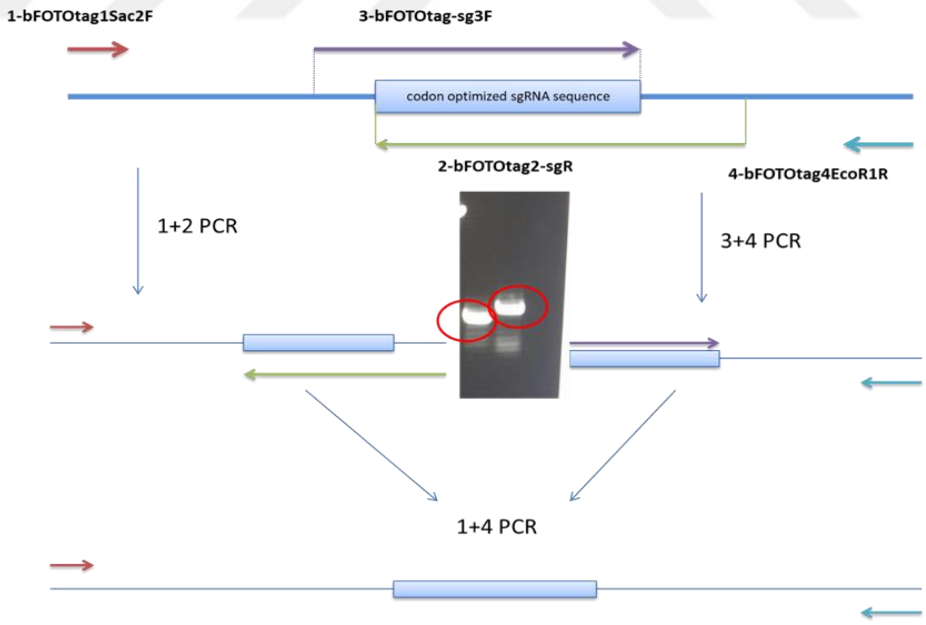

Figure 4.4 : The scheme of overlap PCR for *Plasmodium berghei* DNA Photolyase gene amplification.

Figure 4.5, 1-2 shows the result of 3-4 PbPhoto q5 PCR gel. The products were run in 100 ml 1% agarose gel at 90 V for 1 hour. The correct size 600 bps band was obtained

according to the DNA ladder. Q5 PCR products were used for overlap PCR. In the gel sequence, the first two bands indicate q5 1-2. The weak radiation of the bands shows that the products produced with q5 at 68 °C Extention are not sufficiently reproduced. The two bright bands next to it are the product of q5 1-2. This time the PCR was generated with 64 °C of extention. The next two bands are the red enzyme PCR product, amplified for control. The band brightness to be expected is as for the red enzyme. The q5 PCR was produced several times in the 64 °C PCR program for the product at sufficient concentration for cutting. The two bands to the left of the ladder indicate product q5 3-4. The correct band size, 650 bps 3-4, 68 °C of extention could be reproduced with q5 PCR program. It did not give products at 64 °C.

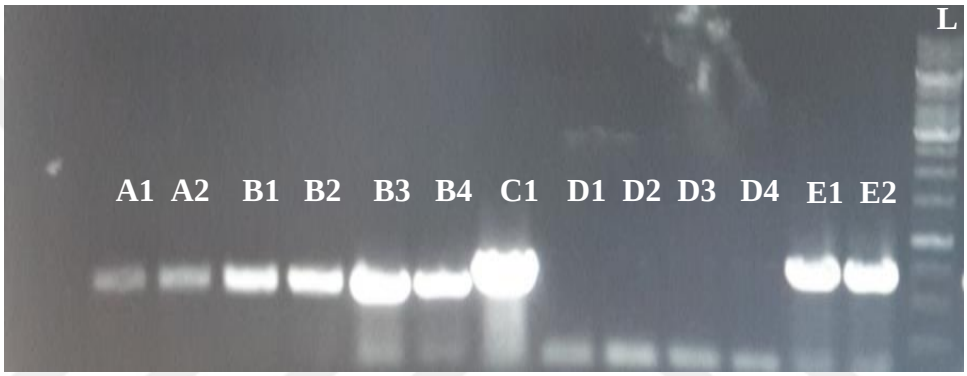

Figure 4.5 : Q5 PCR result of 1-2 insert and 3-4 insert. L: DNA Ladder, A: Q5 PCR products of 1-2 insert at 68 ^{o}C extension, B: Q5 PCR products of 1-2 insert at 64 ^{o}C extension, C: Red enzyme PCR product of 3-4 insert as control, D: Q5 PCR products of 3-4 insert at 64 ^{o}C extension, E: Q5 PCR products of 3-4 insert at 68 ^{o}C extension.

Finally, using 12-34 PCR products as a template, the Pb Photolyase gene was produced using q5 PCR 68 ^{o}C extension shown in Figure 4.6. The gene was isolated and purified from the corresponding size 1.2 kb band gel. Thus, we report that we have successfully completed gene amplification with overlap PCR.

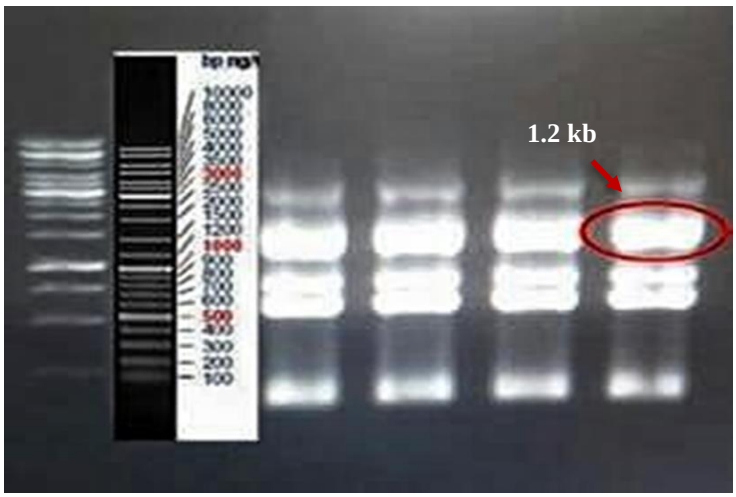

Figure 4.6 : Q5 Overlap PCR result of *Plasmodium berghei* DNA Photolyase gene.

4.1.3 Test digestion gel results of smallscale DNA productions

Plasmids of selected colonies that were inoculated using the Qiagen miniprep kit were isolated and then test cuts were made with Hind III and Kpn1. The cutting reactions, totaling 20 µl, were mixed with 4 µl of 6X Loading dye and loaded onto 100 ml of 100 ml agarose gel with 1%. It was run at 90 V for 1 hour. Figure 4.7 shows the gel result. The gel result shows us that 6 miniprep DNAs have the desired insert DNA (AA31 e PbPhoto right arm insertion). M1, M2, M4, M5, M6, M7 minipreps were evaluated as positive according to the gel result.

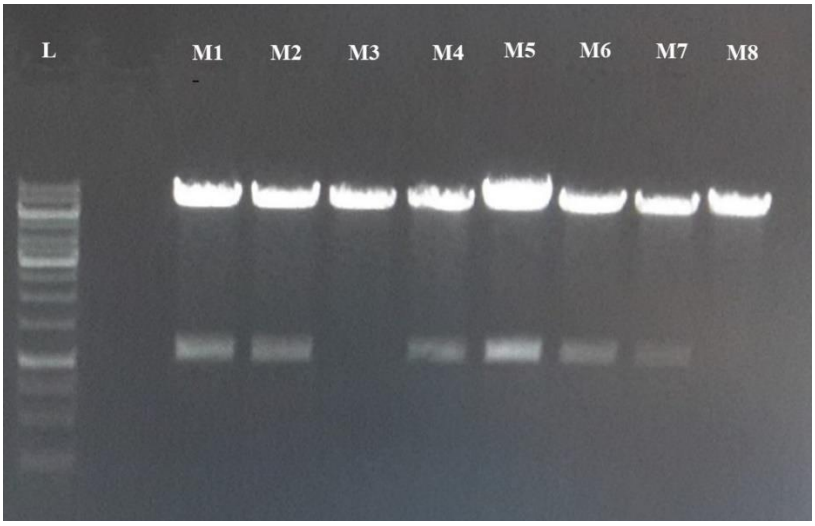

Figure 4.7 : Test digestion gel result of IY03 minipreps.The minipreps were cut with HindIII-Kpn1 restriction enzymes.

Similarly, minipreps DNA were isolated and cut with Sac2 and BamHI restriction enzymes and were run in agarose gel. According to the gel result shown in Figure 4.8, the IY03 vector came together with the left arm iy01 insert to form the knock-out pre-vector. M2, M3, M4, M5, M6, M9, M11, M13, M14 minipreps were evaluated as positive according to the gel result.

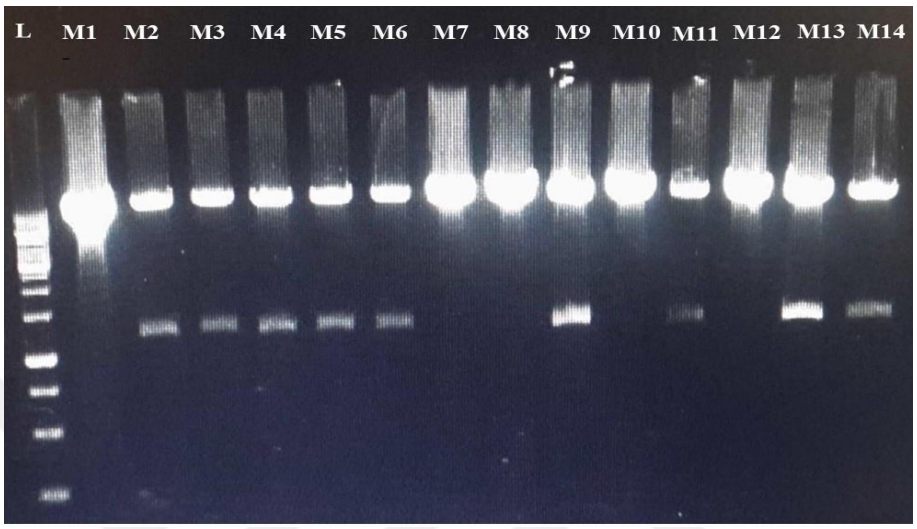

Figure 4.8 : Test digestion gel result of IY04 minipreps. The minipreps were cut with Sac2-BamH1 restriction enzymes. L: DNA Ladder, M: Miniprep

4.1.3.1 Test digestion result for knock-out construct

Three different digestion reactions were performed to IY10 knock-out vector, respectively. Reactions are first Sac2-BamHI, Second HindIII-KpnI, Third Sac2-KpnI. Figure 4.9 shows the gel results according to the reaction order. Band sizes are the same as expected; 1.1 kb for the first two digestions with sac2-bamh1 and hind3-kpn1, and 3 kb for the third digestion with sac2-kpn1. The gel result shows that the knock-out vector was completed successfully.

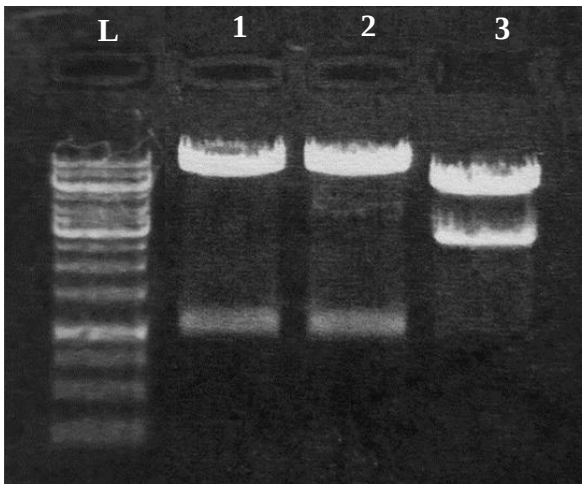

Figure 4.9 : Test digestion gel result of PbPhoto(-) construct. L: DNA Ladder 1) Sac2-Bamh1 digestion of IY10 vector, 2) HindIII-Kpn1 digestion of IY10 vector, 3) Sac2-Kpn1 digestion of IY10 knock-out vector.

4.1.3.2 Test digestion result for knock-in construct

IY05 Pb Photo (+) miniprep and maxiprep DNA were allowed to react with the restriction enzymes Sac2-EcoR1. As a result of the gel shown in Figure 4.10, after the DNA ladder, IY05 miniprep Sac2-EcoR1 cutting result, IY05 maxiprep Sac2-Ecor1 cutting result showing a band of 1.2 kb size confirms to the expected dimensions. Our knock-in vector has been found suitable for transfection.

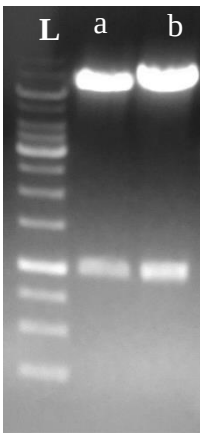

Figure 4.10 : Test digestion gel result of PbPhoto (+) a) miniprep (small scale DNA production) and b) maxiprep (large scale DNA production) of IY05 vector. L: DNA Ladder.

4.1.3.3 Test digestion result for sgRNA construct

The designed sgRNA primers were inserted in the form of dimerized gRNA and inserted into the UK06 Cas9 vector. Figure 4.11 shows the gel results of IY26 miniprep plasmids cut with bbs1 enzyme. Samples on the gel were loaded from left to right after ladder minipreps with bbs1 cut and uncut side by side. In the cut with Bbs1, the miniprep plasmid should be the same size as the uncut miniprep plasmid. Since the band sizes of the gel result are the same, I can say that our vector contains the gRNA insert. If gRNA is inside there is no cut of bbs1 because the recognition site for bbs1 was abolished. M2, M3, M4 and M6 minipreps were evaluated as positive according to the gel result.

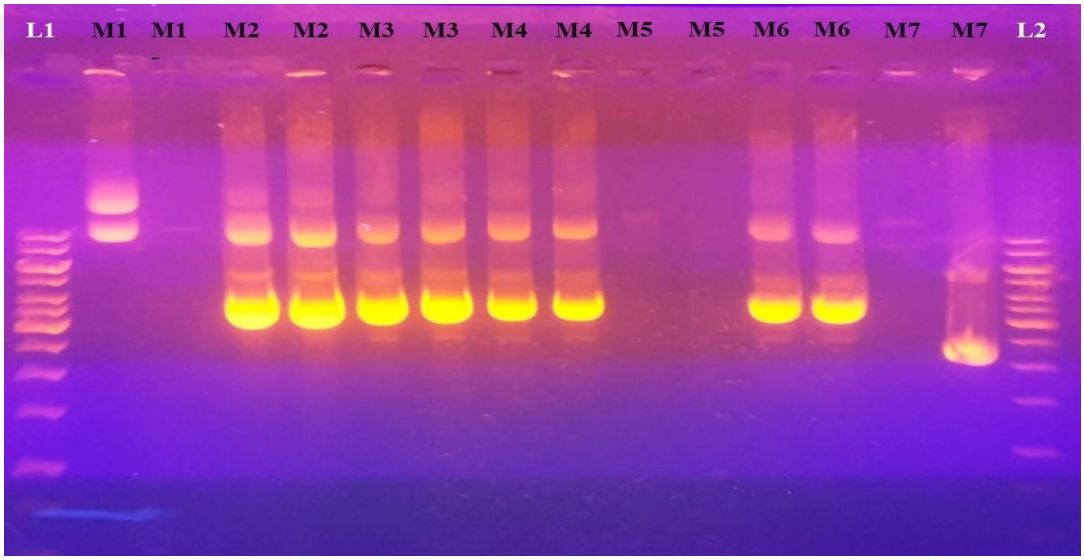

Figure 4.11 : Test digestion results of IY26 (gRNA+ Cas9) minipreps. L: DNA Ladder, M: Miniprep (small scale DNA product of one colony).

4.1.4 Diagnostic PCR gel result of knock-out parasite genomic DNA

Targeted deletion of the DNA Photolyase gene into *P. berghei* parasite with CRISPR-Cas9 technology. The diagnostic PCR for PbPhoto (-) confirmation gel picture indicates 5'UTR and 3'UTR of Pb DNA Photolyase gene integration into the knock-out vectors. Thus we confirm CRISPR-Cas9 targeting was successfully completed for DNA Photolyase gene deletion. You can see the results of the knock-out parasite genome diagnostic PCR in Figure 4.12. The sample order in the gel was determined as 3rd generation knock-out genomic DNA, 4th generation knock-out DNA, and wild-type DNA. The first two bands show the 5' UTR region, the left arm of the photolyase

gene integrated into the knock-out genome. Not available in WT genome. The two bands in the middle indicate that the 3' UTR region is present in the knock-out genomes and not in the wild type genome. The band seen to the right of the gel indicates the wild-type open reading frame region. ORF is not available in knock-out vectors.

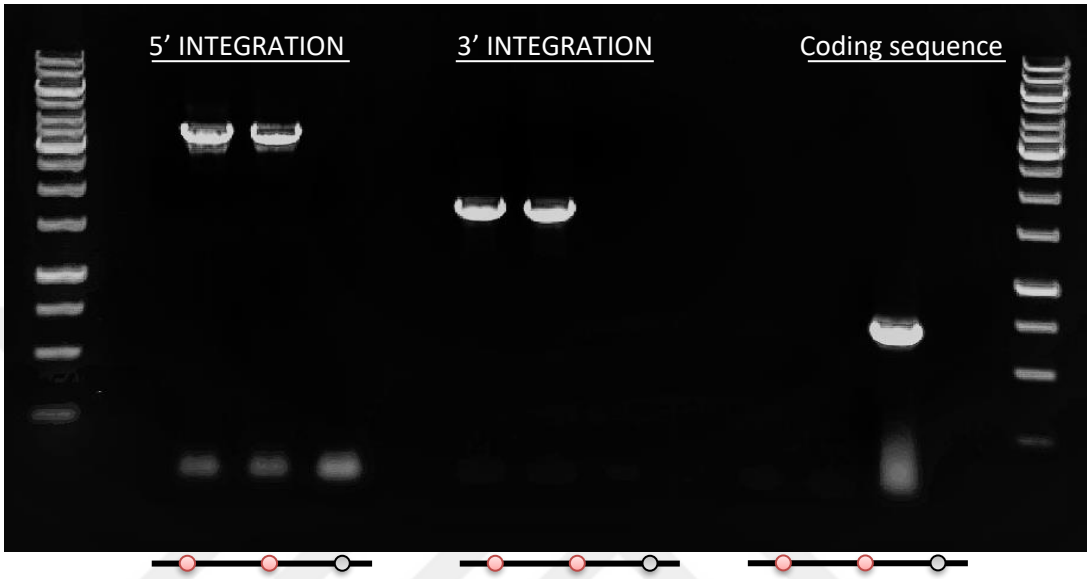

Figure 4.12 : Targeted deletion of the DNA Photolyase gene into *P. berghei* parasite with CRISPR-Cas9 technology. Gel result of diagnostic PCR. (Pink dot shows knock-out parasite genomes, grey dot showes Pb WT genome)

4.1.5 Diagnostic PCR gel result of knock-in parasite genomic DNA

Targeted insertion of the DNA Photolyase gene into *P. berghei* parasite with CRISPR-Cas9 technology. The diagnostic PCR for PbPhoto (+) confirmation gel picture indicates 5'UTR and 3'UTR of Pb DNA Photolyase gene integration into the knock-in vectors. Thus we confirm CRISPR-Cas9 targeting was successfully completed for DNA Photolyase gene insertion. You can see the results of the knock-in parasite genome diagnostic PCR in Figure 4.13. The sample order in the gel was determined as 3rd generation of knock-out genomic DNA, 3rd generation knock-in DNA, and wild-type DNA. The first two bands show the 5' UTR region, the left arm of the photolyase gene integrated into the knock-out and knock-in genomes. Not available in WT genome. The two bands in the middle indicate that the 3' UTR region is present in the knock-out and knock-in genomes and not in the wild type genome. The band seen to the right of the gel indicates the wild-type open reading frame region. ORF is not available in knock-out vector but available in knock-in and wild-type genomes.

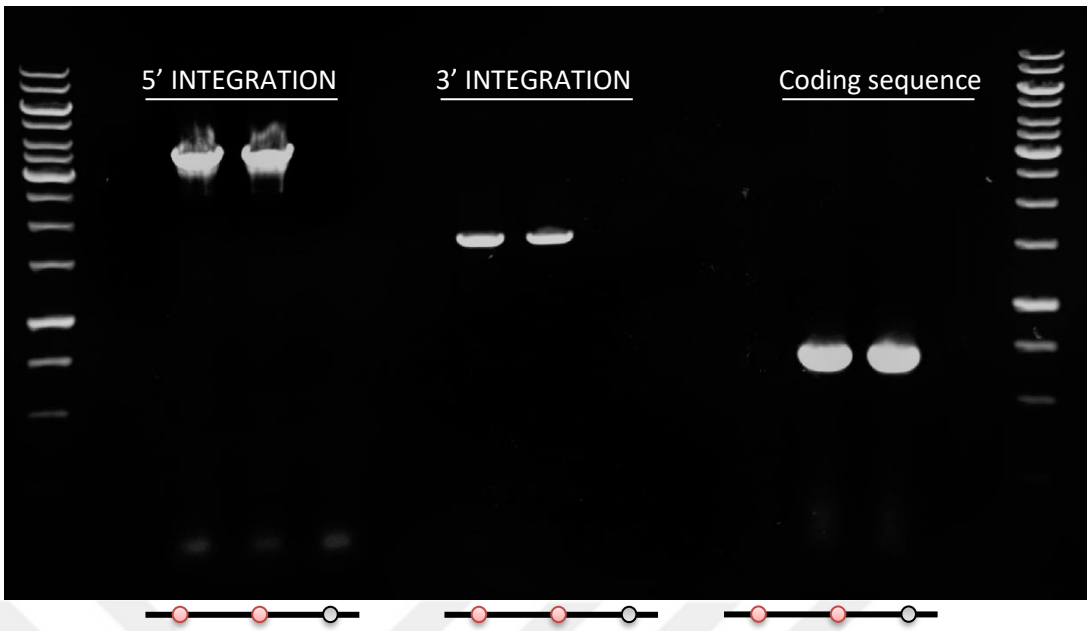

Figure 4.13 : Targeted insertion of the DNA Photolyase gene into *P. berghei* parasite with CRISPR-Cas9 technology. Gel result of diagnostic PCR. (Pink dot shows knock-out and knock-in parasite genomes, grey dot showes Pb WT genome)

4.2 Nanodrop Concentration of Vectors and Inserts

DNA concentrations were measured using the nanodrop device. 1.5 µl of water was loaded as a blank. The measurement was made by loading the same amount of DNA. Measurement results are given in Table 4.1-4.4. According to the measurement results, it was determined that the samples were pure because the DNA purity (A260/A280) was about 2. Miniprep results generally range between 100-300 ng / µl.

Table 4.1 : Results for digested inserts.

Insert Name	Rest.Enzyme Name	A260 ng/µl	A260/280
iy01	Sac2-BamH1	208.2	1.9
iy02	Hind III-KpnI	219.2	2
iy03	EcoR1-R5	69.25	1.98
iy05	Sac2-EcoR1	77.34	2.01

Table 4.2 : Results for digested vectors.

Vector Name	Rest.Enzyme Name	A260 ng/µl	A260/280
AA31	Sac2-BamH1	360	1.9
IY03	Hind III-KpnI	630	2
IY04	EcoR1-R5	250	1.98
IY04	Sac2-EcoR1	220	2.01
IY04	Nhe1-Xho1	189	2

Table 4.3 : Results for maxipreps.

Vector Name	Features	A260 ng/µl	A260/280
AA31	AA20(eos4b)	360	1.88
IY03	Right arm	630	1.98
IY04	Left arm	427	1.98
IY10	(-) hDHFR	869	2
IY05	Pb Photo	575	2.4
IY26	gRNA	500	2

Table 4.4 : Results for linearized precipitated DNA.

Vector Name	Features	A260 ng/µl	A260/280
IY10	KO	1148	1.98
IY10	KO	1128	2.05
IY05	KN	1942	1.85
IY05	KN	1194	2

4.3 Flow Cytometry Results of Transgenic Parasites

4.3.1 FACs result for Photolyase knock-out parasites

2.5 µl of blood was collected from the tail of the infected mouse to determine the presence of knock-out parasites after transfection. It was diluted 1:250 with PBS. Green luminescent parasite cells were detected using flow cytometry device. In Figure 4.14, the graphic R3 shows all blood cells in the flow on the left and the infected blood cells emitting a green glow in the selected region of R2 on the right.

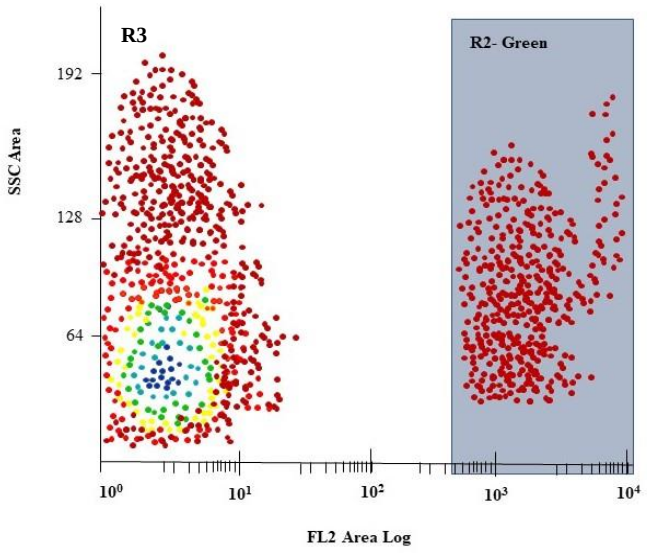

Figure 4.14 : Flow cytometry result for PbPhoto(-) parasites.

The red dots seen in R2 indicate that the transfection was a positive and the parasites had a knock-out vector. According to the FACs result, 7.694 transgenic parasites were counted in 224.993 blood cells. For the cloning and genotyping studies of transgenic parasites, parasites were sorted in 100% efficiency and enrich mode by the FACs device. The values are shown in the Table 4.5. At around 449.445 parasites we transfected only in PBS were made ready for injection into the new BALB/c mouse.

Table 4.5 : FACs sort statistics for PbPhoto(-) IV injection.

Statictics	**Left Sort**	**Right Sort**
Sort Logic	R1&R2	-
Mode	Enrich	None
Current Target	1	2
Sort Count	449.445	0
Sort Volume-ml	2.5094	0
Abort Count	0	0
Sorts Per Second	1275	0
Aborts Per Second	0	0
Sort %	% 3.41	% 0
Abort%	% 0	% 0
Efficiency	%100	% 0
	Event Rate	Total Events
	38267	13.188.217

4.3.2 FACs result for Photolyase knock-in parasites

2.5 µl of blood was collected from the tail of the infected mouse to determine the presence of knock-out parasites after transfection. It was diluted 1:250 with PBS. Green luminescent parasite cells were detected using flow cytometry device.

In Figure 4.15, the graphic R3 shows all blood cells in the flow on the left and the infected blood cells emitting a green glow in the selected region of R2 on the right. The red dots seen in R2 indicate that the transfection was a positive and the parasites had a knock-in vector. According to the FACs result, 5.890 transgenic parasites were counted in 172.572 blood cells counted.

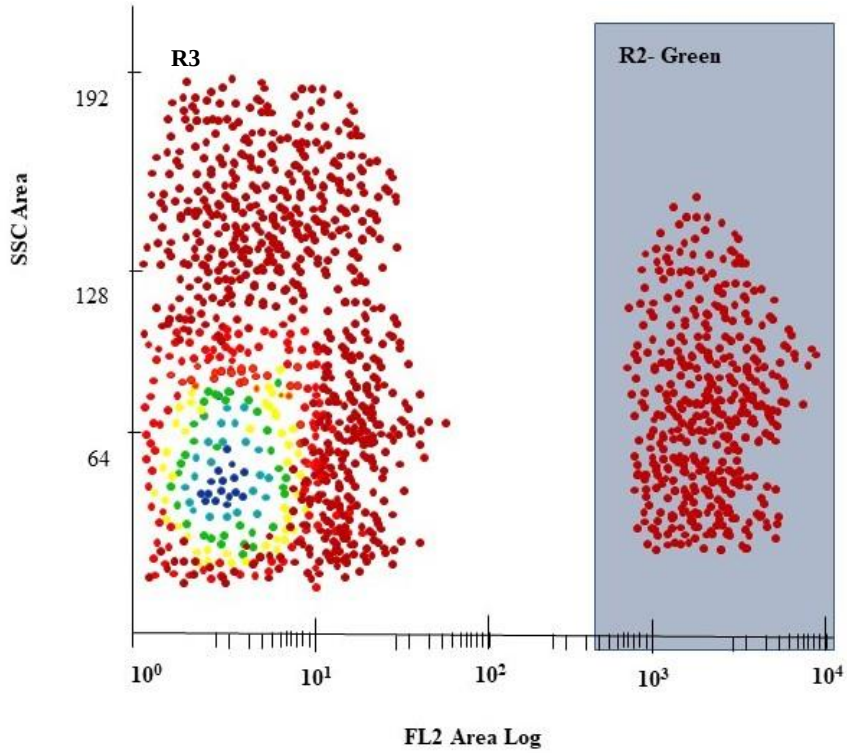

Figure 4.15 : Flow cytometry result for PbPhoto(+) parasites.

4.4 Light Microscopy Results for Knock-Out Parasites

Blood was taken from the tail of mice infected with knock-out parasites and a thin smear was made on the slide. Blood cells were fixed by covering them with 100% methanol for 1 minute. The cells were stained by completing 50 ml with 3.5 ml Giemsa ddwater and pouring on the slides for fifteen minutes. Parasites stained with Giemsa were viewed with immersion oil in a 1000X objective, and the parasites were imaged. Wild type *P. berghei* trophozoite cells marked with Giemsa staining are shown in the picture in figure 4.16. The ring-shaped parasite image is a pink-purple colored parasite nucleus, and the hollow part in the middle is a parasitic vacuole with an annular membrane around the cytoplasm membrane.

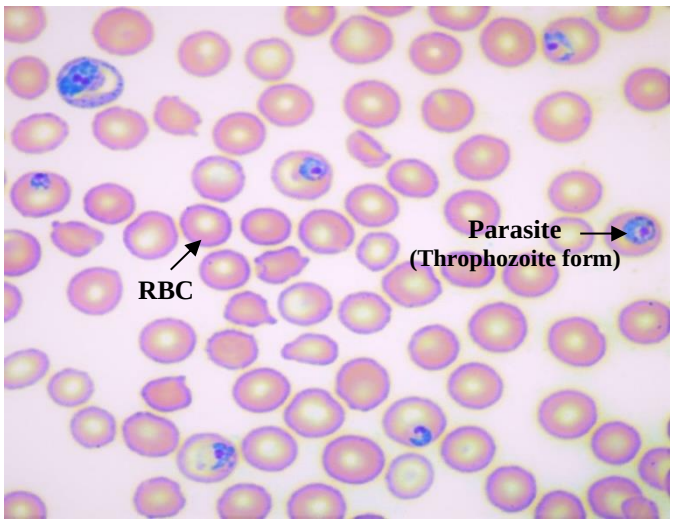

Figure 4.16 : Giemsa stained PbWT (Plasmodium berghei wild-type) throphozoite form of parasite enfected blood cells thin smear result under light microscopy.

The image of DNA Photolyase Knock-out *P. berghei* parasites is shown in Figure 4.17. Only the pink-purple nucleus is shown, the vascular membrane has shrunk and is almost invisible.

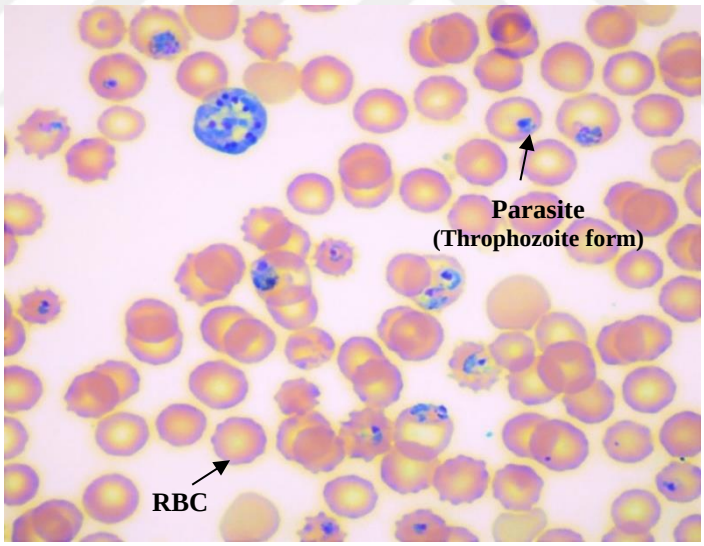

Figure 4.17 : Giemsa stained PbPhoto(-) throphozoite form of parasite enfected blood cells thin smear result under light microscopy.

4.5 Confocal Fluorescent Microscopy Results

4.5.1 Confocal fluorescent microscopy results for knock-out parasites

4 µl of blood was drawn from the tail of mice infected with the knock-out parasite. The mounting gel containing 10 µl of hoesct was added to the blood cells and the cells

were covered with a coverslip. Knock-out parasites carry the green fluorescent protein mEos4b. Unless the parasite interacts with the blue light, the green-luminescent protein is clustered in the parasite's cytoplasm to the size of the parasite. Figure 4.18 shows that the parasites have the marker gene and the gene is successfully expressed in the confocal microscope. The figure shows squares of blood cells with bright-field, blue-light fluorescent DAPI, red-light fluorescent, and green-light fluorescent filters applied.

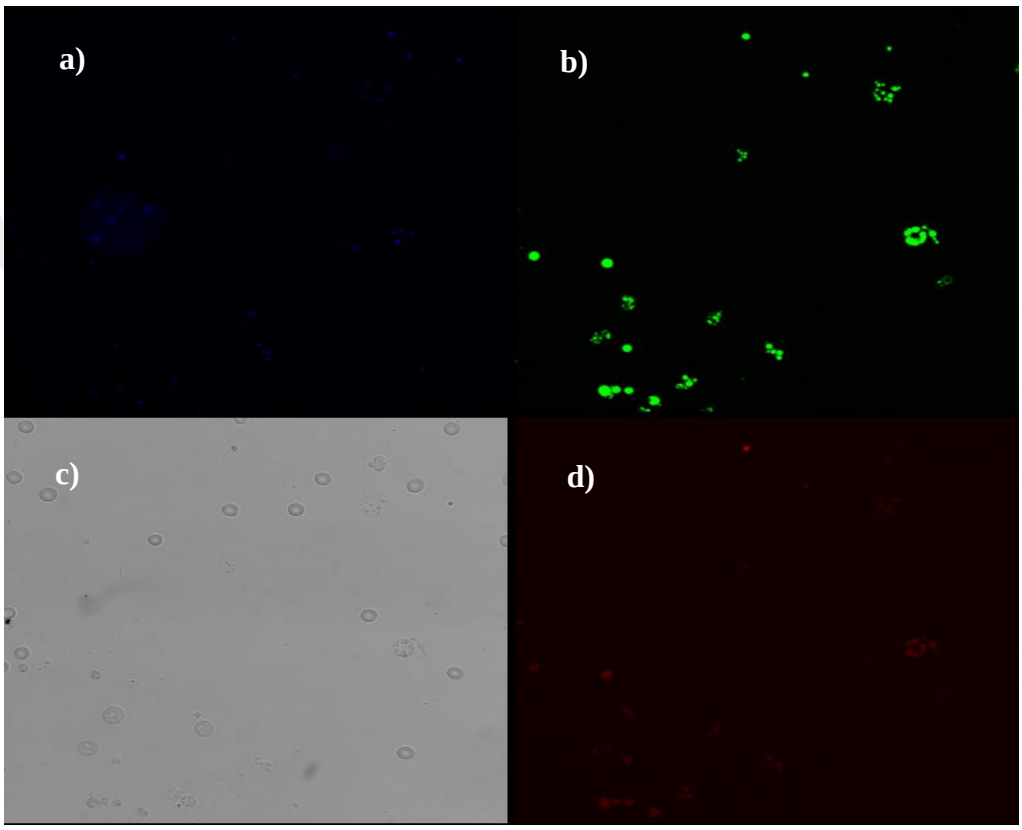

Figure 4.18 : Confocal fluorescent result P. berghei DNA Photolyase knock-out parasites. a) 40X, DAPI, b) 40X, GF, c) 40X, Bried-field, d) 40X, RF

4.5.2 Confocal fluorescent microscopy results for knock-in parasites

In knock-in parasites, the *P. berghei* DNA Photolyase gene is labeled with the mEos4b marker gene. It is known that the photolite ship gave green glow by explaining the marker gene at the same location. Figure 4.19 shows the bright field, DAPI, and green light fluorescence results. Bright field image shows 8 parasites in one of the 4 blood cells. When the parasite cells that give a green glow are examined carefully, it is understood that the protein of the marker gene, Photolyase enzyme, is expressed in the parasite nucleus.

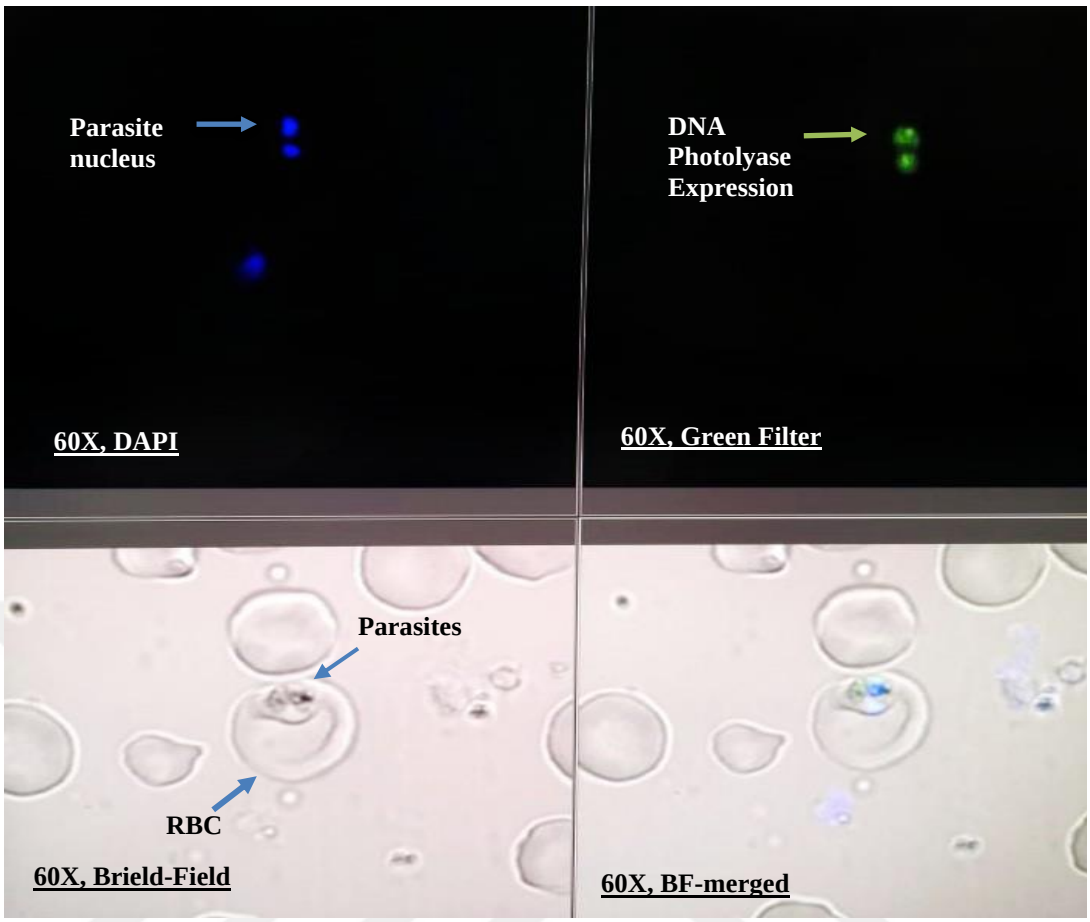

Figure 4.19 : *P. berghei* DNA Photolyase knock-in-tagging parasites.

Observation of the DNA photolyase enzyme, which acts as a restorative of the DNA pyrimidine dimer, in the nucleus where the DNA is located shows that we have successfully achieved the functional characterization of the gene.

4.5.3 Confocal fluorescent microscopy results for mEos4b model

Knock-out parasites that we marked with the mEos4b photo-transformable gene were first detected by checking the bright field and green glow in confocal microscopy. The first green glow of the parasites identified in Figure 4.20 is given at the top of the figure. The gene was excited by giving blue light to living parasites in the blood cells in the lambda in the confocal microscope for one minute. When looking at the same parasites with a green light filter, it was noticed that they did not glow green, and it is shown at the bottom of the figure that red fluorescent proteins are active when the red filter is held.

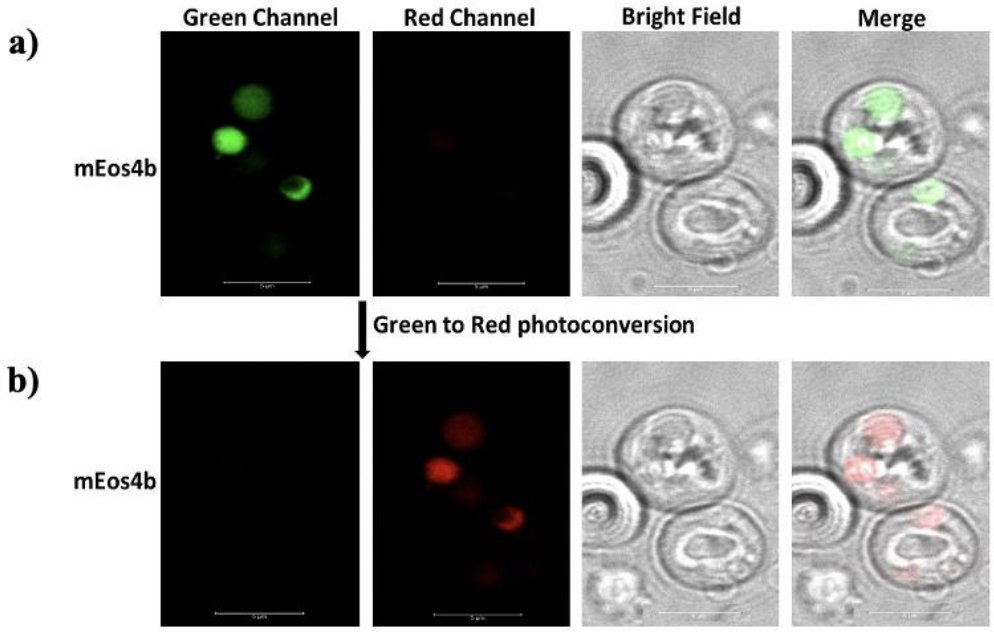

Figure 4.20 : PbPhoto(-) parasites a) before and b) after one minute of blue light application.

Bright field, DAPI, GFP, RFP confocal images of mouse blood cells infected with malaria parasite are given in the picture, respectively. The image of parasites in blood cells selected from another area before blue light application is shown in Figure 4.21. In knock-out parasites, mEos4b proteins appear to glow green.

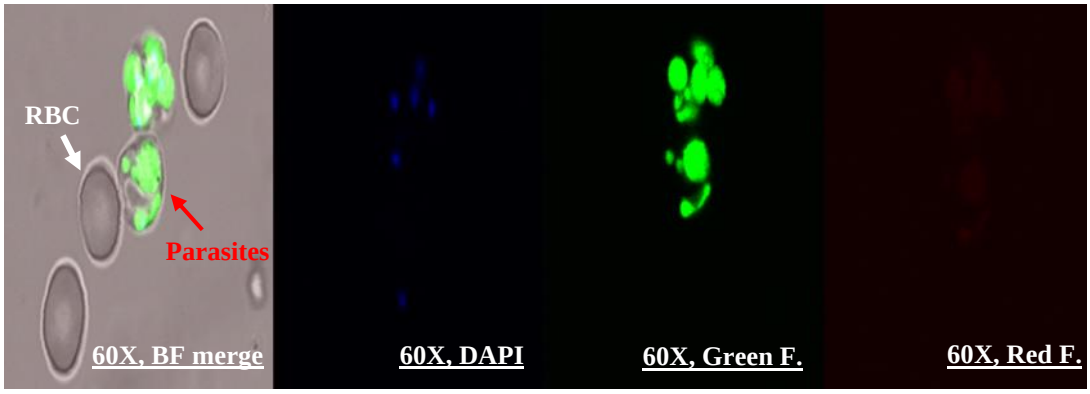

Figure 4.21 : PbPhoto(-) parasites before blue light application. Blood cells captured with brield-field, DAPI, green and red fluorescence.

The image of the excited parasite cell mEos protein 30 seconds after the application of blue light for one minute is shown in Figure 4.22. After 30 seconds, green and red fluorescence is at the same rate. With the disappearance of the blue light, the parasites

that make red glow start to glow green again. Thus, phototransformation of the mEos4b gene in the parasite was verified using the confocal microscope.

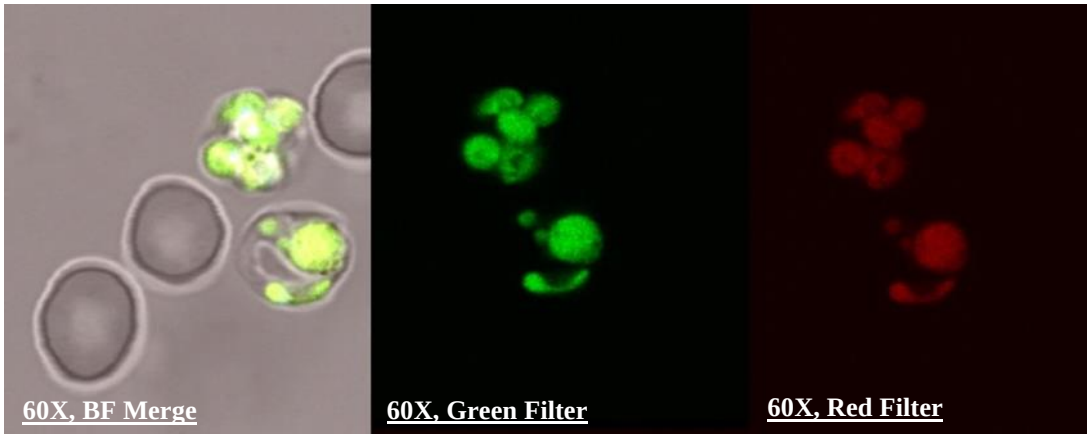

Figure 4.22 : PbPhoto(-) parasites after 30 seconds of blue light application blood cells captured with brield field, green and red green and red fluorescence.

4.6 Results of Mosquito Studies

Anopheles stephensi mosquitoes were grown in mineral drinking water at 75% humidity under a 14 h light / 10 h dark cycle. A minimum of 150 was collected in cages. BALB / c mice infected with PbPhoto (-) were fed with blood and infected. Midgut and salivary gland extractions were performed with infected mosquitoes in 1 X PBS.

Sporozoites extracted from the mosquito salivary gland were placed on a glass slide and covered with a coverslip. A green fluorescence image was taken with the Biotek Cytation 5 device. Sporozoites producing mEos 4b protein are shown in Figure 4.23. There was no change in the size and structure of sporozoites.

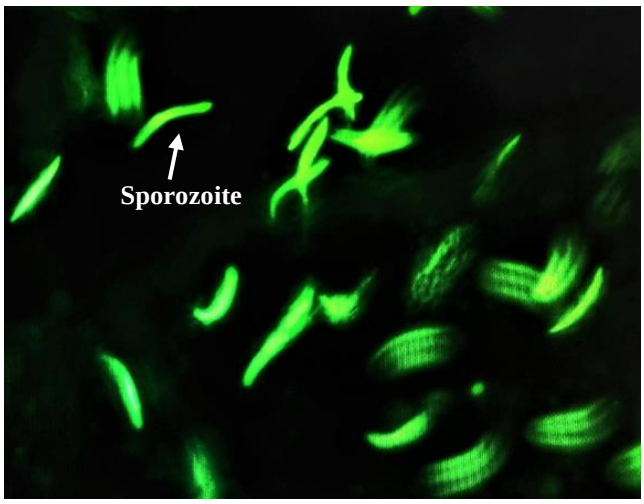

Figure 4.23 : Pb Photolyase (-) sporozoites exctracted from a *Anopheles stephensi* mosquito salivary gland.

The image of oocysts in the abdominal cavity of mosquitoes infected with the Photolyase knock-out parasite labeled with the *P. berghei* mEos4b gene is given in Figure 4.24. Parasitic oocysts with gene deletions were found to be normal as in the wild type. The photolyase gene deletion did not cause a change in the stages of parasite mosquito development. 150 mosquitoes were dissected.

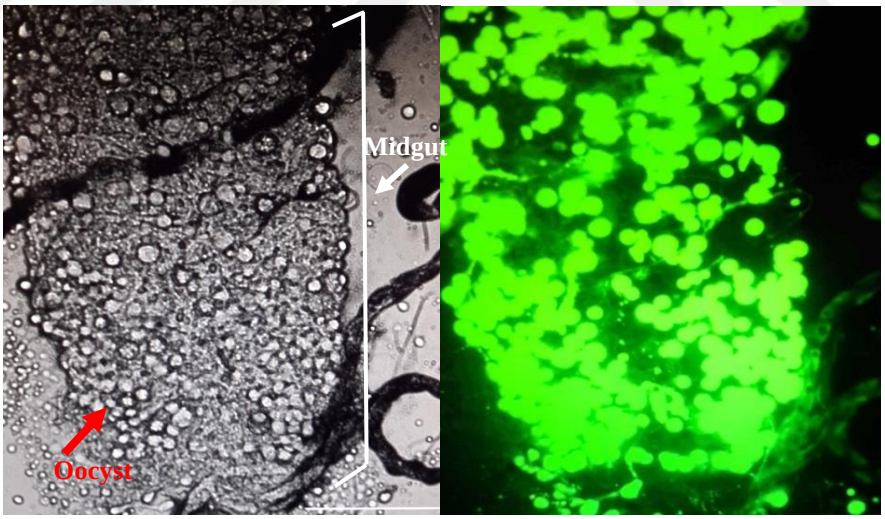

Figure 4.24 : Pb Photolyase (-) oocysts in midgut of a *Anopheles stephensi* mosquito.

The sporozoites were counted under the inversion microscope. *P. berghei* WT sporozoite count is 8.400.000 per 420 µl. Pb. Photo (-) The number of 150 mosquito sporozoites was found to be 8.399.950. The results show that the DNA photolyase deletion has no effect on the life cycle of the parasite in mosquitoes.

4.7 Results of Mouse Studies

BALB/c mice were infected by IV injection of 1 million parasites WT-KO and KN parasites prepared in 150 µl RPMI solution. (Three BALB/c were used for each parasite species. PbWT parasites were selected as controls for blood-stage development. The mice were placed under dark and light conditions. Three mice were infected with UVB treated (30 minutes) 1 million parasites. One drop of blood was collected from the tail 24 hours after infection and the slide was sampled by thin smear. Tail blood was taken at 24-hours intervals every day. Parasitemia percentage was calculated by counting the parasites in the inversion microscope after Giemsa staining. Tables 4.6 show the daily (November 18, 2020 - November 30, 2020) parasitemia percentages of mice affected by normal-dark-UVB light. The results are also shown in the Figure 4.25 and 4.26. Since 30 minutes of UVB application killed the parasites, the UV experiment did not result as desired.

Table 4.6 : Animal normal light- dark, UVB light study parasitemia (%) results. (Red- Green: WT, Blue- Black: KO).

Mouse Tag	18-21 November	22 November	23 November	24 November	25 November	26 November	27 November
Normal Light							
Red 4	-	0.1	0.22	0.9	1.3	7.5	alive
Red 5	-	0.2	0.24	0.98	2.2	8.3	alive
Red 6	-	-	0.03	1.35	3.7	10.6	died
Blue 4	-	0.01	1.11	0.75	1.9	0.8	died
Blue 5	-	0.06	0.54	0.90	1.76	1.7	alive
Blue 6	-	0.02	0.11	0.8	1.45	1.6	died
Completely Dark							
Red 1	-	0.04	0.2	0.3	3.2	0.12	died
Red 2	-	-	0.06	3.2	1.65	3.48	died
Red 3	-	-	0.04	3.33	3.48	8.3	died
Blue 1	-	0.005	0.1	0.3	0.35	0.9	alive
Blue 2	-	0.01	0.5	0.9	0.84	0.48	alive
Blue 3	-	0.01	0.01	0.9	0.48	1.08	alive

Table 4.6 (continue): Animal normal light- dark, UVB light study parasitemia (%) results. (Red- Green: WT, Blue- Black: KO).

Mouse Tag	18-21 November	22 November	23 November	24 November	25 November	26 November	27 November
UVB Light (30 min)							
Green 1	-	-	-	-	-	-	alive
Green 2	-	-	-	-	-	-	alive
Green 3	-	-	-	-	-	-	alive
Black 1	-	-	-	-	-	-	alive
Black 2	-	-	-	-	-	-	alive
Black 3	-	-	-	-	-	-	alive

Targeted deletion of DNA Photolyase in *P. berghei* has an important effect on blood-stage parasite development. The graph shows the average blood-stage parasitemia (% infected erythrocytes out of >5000 cells counted) in groups of three BALB/c mice per strain in Figure 4.25. The strains are wild type (WT) *P. berghei* parasites under normal light conditions and Pb Photolyase knock-out parasites under the normal light conditions. This experiment confirmed that the deletion of PbPhoto (-) lead to a statistically significant reduction in blood-stage parasitemia compared to WT under normal light conditions.

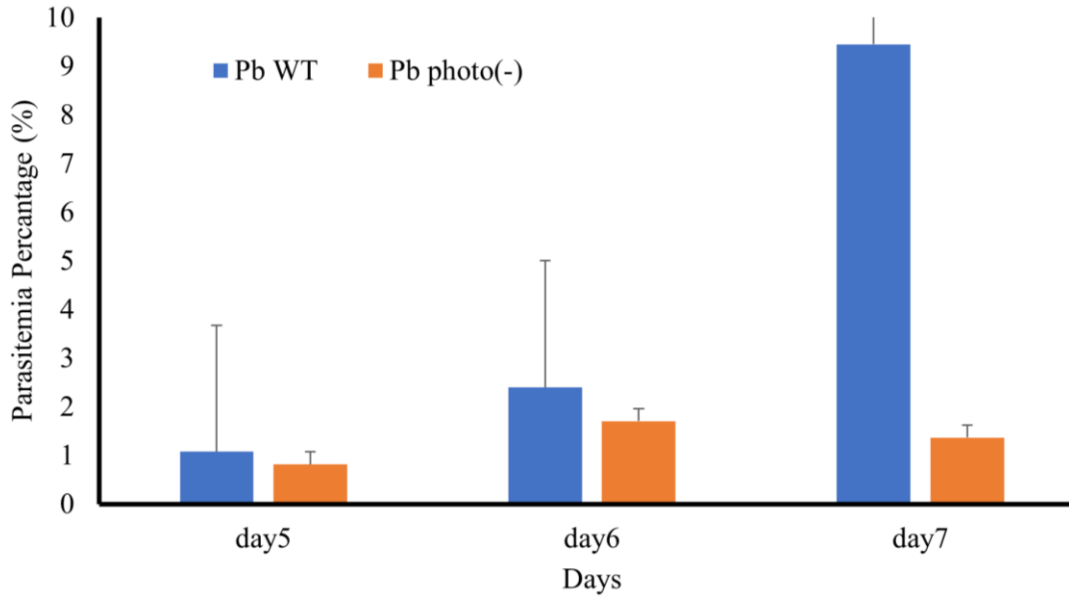

Figure 4.25 : Parasitemia percentage of PbWT vs. PbPhoto(-) light condition.

Targeted deletion of DNA Photolyase in *P. berghei* has an important effect on blood-stage parasite development. The graph shows the average blood-stage parasitemia (% infected erythrocytes out of >5000 cells counted) in groups of three BALB/c mice per strain in Figure 4.26. The strains are wild type (WT) *P. berghei* parasites under completely dark condition and Pb Photolyase knock-out parasites under the completely dark conditions. This experiment confirmed that the deletion of PbPhoto (-) lead to a statistically significant reduction in blood-stage parasitemia compared to WT under dark conditions. Besides, it was observed that the wild type *P. berghei* malaria parasite breeding under normal light conditions decreased by half in dark conditions.

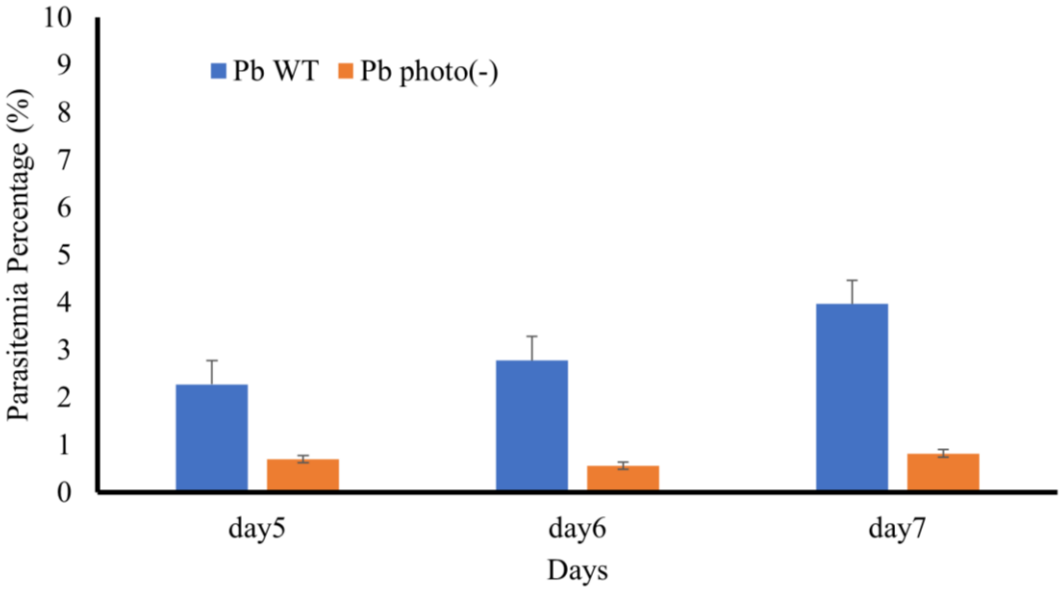

Figure 4.26 : Parasitemia percentage of PbWT vs. PbPhoto(-) dark condition.

5. CONCLUSION

Rodent malaria parasite *Plasmodium berghei* DNA Photolyase gene knock-out and knock-in vectors were designed. Designed knock-out and knock-in vector cloning studies were performed at 99.9 % accuracy, and the vectors were produced purely in the desired amount in multiple copies. DNA Photolyase gene deletion and gene insertion were successfully performed with CRISPR-Cas9 technology and the deletion was confirmed by diagnostic PCR. In addition to diagnostic PCR confirmation, the vectors were sequenced via a sequencing company. The sequencing results were matched 99.9 % with designed vectors. The presence of the marker gene mEOS4b, which I added to the knock-in and knock-out vectors, was detected by applying blue light for one minute to infected cells examined under confocal microscopy. The mEOS4b photoconvertible marker gene transformed from green to red after exposured to blue light, showed that the transfection of the vectors we created to *P. berghei* parasites were accomplished successfully. It has been determined that the mEos4b gene integrated vector, which we can use in future studies, can lead as a model in many cytotoxicity studies. With the gene deletion, no defect in parasite development was observed in mosquito stages but only in blood stages, there was a defect in the development of synchronous blood stages compared to the wild type. The DNA Photolyase knock-out parasites failed to recover after UV light exposure similar to *P.berghei* wild-type parasites. In the normal light mouse study, parasite blood-stage growth was significantly lower in knock-out parasites than wild-type parasite growth. In the completely dark condition mouse study, the growth of knock-out parasites occurred at a lower rate compared to knock-out mice that breed in normal light. Thus, it has been determined that the DNA Photolyase gene plays a vital role in the successful realization of parasite reproduction and replication at the blood stage. Mice infected with PbWT visibly displayed signs of the disease within fourteen days, while mice infected with the PbPhoto (-) knock-out parasite did not show phenotypic signs of the disease. In the advanced stages of the disease, shivering, inability to socialize, limited mobility, and stagnation in eating and drinking were observed in control mice. Social activity, eating, drinking, and movements were observed as normal in transgenic DNA

Photolyase gene knock-out mice, which had a high rate of parasitemia in the blood. They showed no phenotypic signs of malaria. On the contrary, it was not different from a normal mouse without disease. They also survived one week longer than mice infected with the wild-type parasite. The rate of parasitemia in mice in complete darkness, infected with the wild-type Plasmodium berghei parasite, was less than the rate of parasitemia in mice under normal light. Thus, we initially confirmed that light plays an important role in the DNA Photolyase gene functioning and reproduction of the malaria parasite. In the confocal image of the knock-in transgenic parasite, the mEos4b green light protein fluorescence was observed only in the parasite nucleus. It is thought that the enzyme localization takes place in the nucleus so that the photolyase enzyme provides genome repair. Since the photolyase gene is not found in humans, if an inhibitor for the parasite photolyase gene is designed, the reproduction of the parasite in the blood stage can be slowed down. Application of the UVB experiment with exposure times of 10 seconds and 30 seconds result in primer dimers in the exon or intron in the parasite DNA. Thus, parasite development can be stopped at a certain stage or the function of an unknown gene can be determined. Therefore a more in-depth investigation is needed to detail the molecular function of the DNA photolyase in the malaria parasite and in other pathogenic microorganisms.

REFERENCES

[1] **Sancar, A.** (2016). Mechanisms of DNA Repair by Photolyase and Excision Nuclease (Nobel Lecture). *Angew Chem Int Ed Engl*, *55*(30), 8502-8527.

[2] **Zhang, M., Wang, L. and Zhong, D.** (2017). Photolyase: Dynamics and electron-transfer mechanisms of DNA repair. *Arch Biochem Biophys*, *632*, 158-174.

[3] **Smith, L. M., Motta, F. C., Chopra, G., Moch, J. K., Nerem, R. R., Cummins, B., Roche, K. E., Kelliher, C. M., Leman, A. R., Harer, J., Gedeon, T., Waters, N. C. and Haase, S. B.** (2020). An intrinsic oscillator drives the blood stage cycle of the malaria parasite Plasmodium falciparum. *Science*, *368*(6492), 754-+.

[4] **Subach, F. V., Patterson, G. H., Manley, S., Gillette, J. M., Lippincott-Schwartz, J. and Verkhusha, V. V.** (2009). Photoactivatable mCherry for high-resolution two-color fluorescence microscopy. *Nat Methods*, *6*(2), 153-159.

[5] **Hart, R. J., Abraham, A. and Aly, A. S. I.** (2017). Genetic Characterization of Coenzyme A Biosynthesis Reveals Essential Distinctive Functions during Malaria Parasite Development in Blood and Mosquito. *Front Cell Infect Microbiol*, *7*, 260.

[6] **Huestis, D. L., Dao, A., Diallo, M., Sanogo, Z. L., Samake, D., Yaro, A. S., Ousman, Y., Linton, Y. M., Krishna, A., Veru, L., Krajacich, B. J., Faiman, R., Florio, J., Chapman, J. W., Reynolds, D. R., Weetman, D., Mitchell, R., Donnelly, M. J., Talamas, E., Chamorro, L., Strobach, E. and Lehmann, T.** (2019). Windborne long-distance migration of malaria mosquitoes in the Sahel. *Nature*, *574*(7778), 404-408.

[7] **Sarı, N. D. and Yörük, G.** (2019). Retrospective Evaluation of 31 Malaria Cases Hospitalized in Our Clinic Between 2012-2018. *Turkiye Parazitol Derg*, *43*(4), 170-174.

[8] **Minakawa, N., Githure, J. I., Beier, J. C. and Yan, G.** (2001). Anopheline mosquito survival strategies during the dry period in western Kenya. *J Med Entomol*, *38*(3), 388-392.

[9] **Talipouo, A., Ngadjeu, C. S., Doumbe-Belisse, P., Djamouko-Djonkam, L., Sonhafouo-Chiana, N., Kopya, E., Bamou, R., Awono-Ambene, P., Woromogo, S., Kekeunou, S., Wondji, C. S. and Antonio-Nkondjio, C.** (2019). Malaria prevention in the city of Yaoundé: knowledge and practices of urban dwellers. *Malaria Journal*, *18*(1), 167.

[10] **Karuitha, M., Bargul, J., Lutomiah, J., Muriu, S., Nzovu, J., Sang, R., Mwangangi, J. and Mbogo, C.** (2019). Larval habitat diversity and mosquito species distribution along the coast of Kenya. *Wellcome Open Res*, *4*, 175.

[11] **Monge-Maillo, B. and López-Vélez, R.** (2012). Migration and malaria in europe. *Mediterr J Hematol Infect Dis*, *4*(1), e2012014.

[12] **Le Menach, A., Tatem, A. J., Cohen, J. M., Hay, S. I., Randell, H., Patil, A. P. and Smith, D. L.** (2011). Travel risk, malaria importation and malaria transmission in Zanzibar. *Sci Rep*, *1*, 93.

[13] **Roberts, D. and Matthews, G.** (2016). Risk factors of malaria in children under the age of five years old in Uganda. *Malar J*, *15*, 246.

[14] URL-1. from *<https://www.who.int/publications/i/item/world-malaria-report-2019>, date of access 2019, 4 December*

[15] **Rogerson, S. J.** (2017). Management of malaria in pregnancy. *Indian J Med Res*, *146*(3), 328-333.

[16] **White, N. J.** (2004). Antimalarial drug resistance. *J Clin Invest*, *113*(8), 1084-1092.

[17] URL-2. from *<https://www.mmv.org/malaria-medicines/malaria-treatment?gclid=EAIaIQobChMI0uekoOzP7QIVmOd3Ch0nXw6ZEAAYASAAEgI7IfD_BwE>, date of access 2020, November 2.*

[18] **Hart, R. J., Cornillot, E., Abraham, A., Molina, E., Nation, C. S., Ben Mamoun, C. and Aly, A. S.** (2016). Genetic Characterization of Plasmodium Putative Pantothenate Kinase Genes Reveals Their Essential Role in Malaria Parasite Transmission to the Mosquito. *Sci Rep*, *6*, 33518.

[19] **Reeder, S. M., Reuschel, E. L., Bah, M. A., Yun, K., Tursi, N. J., Kim, K. Y., Chu, J., Zaidi, F. I., Yilmaz, I., Hart, R. J., Perrin, B., Xu, Z., Humeau, L., Weiner, D. B. and Aly, A. S. I.** (2020). Synthetic DNA Vaccines Adjuvanted with pIL-33 Drive Liver-Localized T Cells and Provide Protection from Plasmodium Challenge in a Mouse Model. *Vaccines (Basel)*, *8*(1).

[20] **Mikolajczak, S. A., Aly, A. S. and Kappe, S. H.** (2007). Preerythrocytic malaria vaccine development. *Curr Opin Infect Dis*, *20*(5), 461-466.

[21] **Aly, A. S., Downie, M. J., Mamoun, C. B. and Kappe, S. H.** (2010). Subpatent infection with nucleoside transporter 1-deficient Plasmodium blood stage parasites confers sterile protection against lethal malaria in mice. *Cell Microbiol*, *12*(7), 930-938.

[22] **Ketema, T., Bacha, K., Alemayehu, E. and Ambelu, A.** (2015). Incidence of Severe Malaria Syndromes and Status of Immune Responses among Khat Chewer Malaria Patients in Ethiopia. *PLoS One*, *10*(7), e0131212.

[23] **İnkaya, A., Kaya, F., Yıldız, İ., Uzun, Ö. and Ergüven, S.** (2016). [Plasmodium falciparum malaria: evaluation of three imported cases]. *Mikrobiyol Bul*, *50*(2), 328-332.

[24] **Fleming, K. A., Naidoo, M., Wilson, M., Flanigan, J., Horton, S., Kuti, M., Looi, L. M., Price, C. P., Ru, K., Ghafur, A., Wang, J. and Lago, N.** (2017). High-Quality Diagnosis: An Essential Pathology Package. In D.T. Jamison, H. Gelband, S. Horton, P. Jha, R. Laxminarayan, C.N. Mock, R. Nugent, (Eds.), *Disease Control Priorities: Improving Health and Reducing Poverty*. Washington (DC): The International Bank for Reconstruction and Development / The World Bank © 2018 International Bank for Reconstruction and Development / The World Bank.

[25] **Bhat, S., Alva, J., Muralidhara, K. and Fahad, S.** (2012). Malaria and the heart. *BMJ Case Rep, 2012*.

[26] **Azikiwe, C. C., Ifezulike, C. C., Siminialayi, I. M., Amazu, L. U., Enye, J. C. and Nwakwunite, O. E.** (2012). A comparative laboratory diagnosis of malaria: microscopy versus rapid diagnostic test kits. *Asian Pac J Trop Biomed, 2*(4), 307-310.

[27] **Houzé, S.** (2017). [Rapid diagnostic test for malaria]. *Bull Soc Pathol Exot, 110*(1), 49-54.

[28] **Kassaza, K., Operario, D. J., Nyehangane, D., Coffey, K. C., Namugosa, M., Turkheimer, L., Ojuka, P., Orikiriza, P., Mwanga-Amumpaire, J., Byarugaba, F., Bazira, J., Guler, J. L., Moore, C. C. and Boum, Y., 2nd.** (2018). Detection of Plasmodium Species by High-Resolution Melt Analysis of DNA from Blood Smears Acquired in Southwestern Uganda. *J Clin Microbiol, 56*(1).

[29] **Kori, L. D., Valecha, N. and Anvikar, A. R.** (2018). Insights into the early liver stage biology of Plasmodium. *J Vector Borne Dis, 55*(1), 9-13.

[30] **Çulha, G., Zeyrek, F. Y., Önlen, Y. and Yentür Doni, N.** (2018). [Determination of imported malaria cases in Hatay by the use of molecular methods]. *Mikrobiyol Bul, 52*(2), 206-213.

[31] **Rai, P., Sharma, D., Soni, R., Khatoon, N., Sharma, B. and Bhatt, T. K.** (2017). Plasmodium falciparum apicoplast and its transcriptional regulation through calcium signaling. *J Microbiol, 55*(4), 231-236.

[32] **Milner, D. A., Jr.** (2018). Malaria Pathogenesis. *Cold Spring Harb Perspect Med, 8*(1).

[33] **Henry, N. B., Sermé, S. S., Siciliano, G., Sombié, S., Diarra, A., Sagnon, N., Traoré, A. S., Sirima, S. B., Soulama, I. and Alano, P.** (2019). Biology of Plasmodium falciparum gametocyte sex ratio and implications in malaria parasite transmission. *Malar J, 18*(1), 70.

[34] **Wahlgren, M., Goel, S. and Akhouri, R. R.** (2017). Variant surface antigens of Plasmodium falciparum and their roles in severe malaria. *Nat Rev Microbiol, 15*(8), 479-491.

[35] **Chiodini, P. and Bain, B. J.** (2017). Plasmodium knowlesi. *Am J Hematol, 92*(7), 716.

[36] **Adams, J. H. and Mueller, I.** (2017). The Biology of Plasmodium vivax. *Cold Spring Harb Perspect Med, 7*(9).

[37] **Kondrashin, A. V., Morozova, L. F., Stepanova, E. V., Turbabina, N. A., Maksimova, M. S. and Morozov, E. N.** (2018). On the epidemiology of Plasmodium vivax malaria: past and present with special reference to the former USSR. *Malar J, 17*(1), 346.

[38] **Kanjee, U., Rangel, G. W., Clark, M. A. and Duraisingh, M. T.** (2018). Molecular and cellular interactions defining the tropism of Plasmodium vivax for reticulocytes. *Curr Opin Microbiol, 46*, 109-115.

[39] **Grande, R., Antinori, S., Meroni, L., Menegon, M. and Severini, C.** (2019). A case of Plasmodium malariae recurrence: recrudescence or reinfection? *Malar J*, *18*(1), 169.

[40] **Li, P., Zhao, Z., Xing, H., Li, W., Zhu, X., Cao, Y., Yang, Z., Sattabongkot, J., Yan, G., Fan, Q. and Cui, L.** (2016). Plasmodium malariae and Plasmodium ovale infections in the China-Myanmar border area. *Malar J*, *15*(1), 557.

[41] **Okafor, C. N. and Finnigan, N. A.** (2020). Plasmodium Ovale Malaria. *StatPearls*. Treasure Island (FL): StatPearls Publishing Copyright © 2020, StatPearls Publishing LLC.

[42] URL-3. from *<https://en.wikipedia.org/wiki/Plasmodium_berghei#:~:text=It%20is%20a%20protozoan%20parasite,Plasmodium%20vinckei%2C%20and%20Plasmodium%20yoelii>, date of access 2020,11 December.*

[43] **Basir, R., Rahiman, S. F., Hasballah, K., Chong, W., Talib, H., Yam, M., Jabbarzare, M., Tie, T., Othman, F., Moklas, M., Abdullah, W. and Ahmad, Z.** (2012). Plasmodium berghei ANKA Infection in ICR Mice as a Model of Cerebral Malaria. *Iran J Parasitol*, *7*(4), 62-74.

[44] **Dehghan, H., Oshaghi, M. A., Mosa-Kazemi, S. H., Abai, M. R., Rafie, F., Nateghpour, M., Mohammadzadeh, H., Farivar, L. and Mohammadi Bavani, M.** (2018). Experimental Study on Plasmodium berghei, Anopheles Stephensi, and BALB/c Mouse System: Implications for Malaria Transmission Blocking Assays. *Iran J Parasitol*, *13*(4), 549-559.

[45] **Matz, J. M. and Kooij, T. W.** (2015). Towards genome-wide experimental genetics in the in vivo malaria model parasite Plasmodium berghei. *Pathog Glob Health*, *109*(2), 46-60.

[46] **Minkah, N. K., Schafer, C. and Kappe, S. H. I.** (2018). Humanized Mouse Models for the Study of Human Malaria Parasite Biology, Pathogenesis, and Immunity. *Front Immunol*, *9*, 807.

[47] **Qi, Y., Zhu, F., Eastman, R. T., Fu, Y., Zilversmit, M., Pattaradilokrat, S., Hong, L., Liu, S., McCutchan, T. F., Pan, W., Xu, W., Li, J., Huang, F. and Su, X. Z.** (2015). Regulation of Plasmodium yoelii oocyst development by strain- and stage-specific small-subunit rRNA. *mBio*, *6*(2), e00117.

[48] **Abel, S., Ueffing, K., Tatura, R., Hutzler, M., Hose, M., Matuschewski, K., Kehrmann, J., Westendorf, A. M., Buer, J. and Hansen, W.** (2016). Plasmodium yoelii infection of BALB/c mice results in expansion rather than induction of CD4(+) Foxp3(+) regulatory T cells. *Immunology*, *148*(2), 197-205.

[49] **Mota, M. M., Brown, K. N., Do Rosário, V. E., Holder, A. A. and Jarra, W.** (2001). Antibody recognition of rodent malaria parasite antigens exposed at the infected erythrocyte surface: specificity of immunity generated in hyperimmune mice. *Infect Immun*, *69*(4), 2535-2541.

[50] **Stephens, R., Culleton, R. L. and Lamb, T. J.** (2012). The contribution of Plasmodium chabaudi to our understanding of malaria. *Trends Parasitol*, *28*(2), 73-82.

[51] **Collins, W. E. and Jeffery, G. M.** (2002). A retrospective examination of sporozoite-induced and trophozoite-induced infections with Plasmodium ovale: development of parasitologic and clinical immunity during primary infection. *Am J Trop Med Hyg*, *66*(5), 492-502.

[52] **Birget, P. L. G., Prior, K. F., Savill, N. J., Steer, L. and Reece, S. E.** (2019). Plasticity and genetic variation in traits underpinning asexual replication of the rodent malaria parasite, Plasmodium chabaudi. *Malaria Journal*, *18*(1), 222.

[53] URL-4. from *<https://www.cdc.gov/malaria/about/biology/index.html>, date of access 2020,16 July.*

[54] **Frischknecht, F. and Matuschewski, K.** (2017). Plasmodium Sporozoite Biology. *Cold Spring Harb Perspect Med*, *7*(5).

[55] **Vaughan, A. M. and Kappe, S. H. I.** (2017). Malaria Parasite Liver Infection and Exoerythrocytic Biology. *Cold Spring Harb Perspect Med*, *7*(6).

[56] **Aly, A. S., Vaughan, A. M. and Kappe, S. H.** (2009). Malaria parasite development in the mosquito and infection of the mammalian host. *Annu Rev Microbiol*, *63*, 195-221.

[57] URL-5. from *<https://www.malariavaccine.org/malaria-and-vaccines/vaccine-development/life-cycle-malaria-parasite>, date of access 2020, october 23.*

[58] **Birget, P. L. and Koella, J. C.** (2015). An Epidemiological Model of the Effects of Insecticide-Treated Bed Nets on Malaria Transmission. *PLoS One*, *10*(12), e0144173.

[59] **Malede, A., Aemero, M., Gari, S. R., Kloos, H. and Alemu, K.** (2019). Barriers of persistent long-lasting insecticidal nets utilization in villages around Lake Tana, Northwest Ethiopia: a qualitative study. *BMC Public Health*, *19*(1), 1303.

[60] **Okumu, F. O. and Moore, S. J.** (2011). Combining indoor residual spraying and insecticide-treated nets for malaria control in Africa: a review of possible outcomes and an outline of suggestions for the future. *Malar J*, *10*, 208.

[61] **Cates, J. E., Westreich, D., Unger, H. W., Bauserman, M., Adair, L., Cole, S. R., Meshnick, S. and Rogerson, S. J.** (2018). Intermittent Preventive Therapy in Pregnancy and Incidence of Low Birth Weight in Malaria-Endemic Countries. *Am J Public Health*, *108*(3), 399-406.

[62] **Coertzen, D., Reader, J., van der Watt, M., Nondaba, S. H., Gibhard, L., Wiesner, L., Smith, P., D'Alessandro, S., Taramelli, D., Wong, H. N., du Preez, J. L., Wu, R. W. K., Birkholtz, L. M. and Haynes, R. K.** (2018). Artemisone and Artemiside Are Potent Panreactive Antimalarial Agents That Also Synergize Redox Imbalance in Plasmodium falciparum Transmissible Gametocyte Stages. *Antimicrob Agents Chemother*, *62*(8).

[63] **Hyde, J. E.** (2007). Drug-resistant malaria - an insight. *Febs j*, *274*(18), 4688-4698.

[64] **Fairhurst, R. M. and Dondorp, A. M.** (2016). Artemisinin-Resistant Plasmodium falciparum Malaria. *Microbiol Spectr*, *4*(3).

[65] **Sancar, A.** (2003). Structure and Function of DNA Photolyase and Cryptochrome Blue-Light Photoreceptors. *Chemical Reviews*, *103*(6), 2203-2238.

[66] **Mao, P., Wyrick, J. J., Roberts, S. A. and Smerdon, M. J.** (2017). UV-Induced DNA Damage and Mutagenesis in Chromatin. *Photochem Photobiol*, *93*(1), 216-228.

[67] **Lawrence, K. P., Douki, T., Sarkany, R. P. E., Acker, S., Herzog, B. and Young, A. R.** (2018). The UV/Visible Radiation Boundary Region (385-405 nm) Damages Skin Cells and Induces "dark" Cyclobutane Pyrimidine Dimers in Human Skin in vivo. *Sci Rep*, *8*(1), 12722.

[68] (1987). Structure and function of DNA photolyases. *Trends in Biochemical Sciences*, *12*, 259 - 261.

[69] **Leccia, M. T., Lebbe, C., Claudel, J. P., Narda, M. and Basset-Seguin, N.** (2019). New Vision in Photoprotection and Photorepair. *Dermatol Ther (Heidelb)*, *9*(1), 103-115.

[70] **Rastogi, R. P., Richa, Kumar, A., Tyagi, M. B. and Sinha, R. P.** (2010). Molecular mechanisms of ultraviolet radiation-induced DNA damage and repair. *J Nucleic Acids*, *2010*, 592980.

[71] **Mahaputra Wijaya, I. M., Iwata, T., Yamamoto, J., Hitomi, K., Iwai, S., Getzoff, E. D. and Kandori, H.** (2015). FTIR study of CPD photolyase with substrate in single strand DNA. *Biophysics (Nagoya-shi)*, *11*, 39-45.

[72] **Hashiya, F., Ito, S. and Sugiyama, H.** (2019). Electron injection from mitochondrial transcription factor A to DNA associated with thymine dimer photo repair. *Bioorg Med Chem*, *27*(2), 278-284.

[73] **Kavakli, I. H., Ozturk, N. and Gul, S.** (2019). DNA repair by photolyases. *Adv Protein Chem Struct Biol*, *115*, 1-19.

[74] **Zhang, M., Wang, L. and Zhong, D.** (2017). Photolyase: Dynamics and Mechanisms of Repair of Sun-Induced DNA Damage. *Photochem Photobiol*, *93*(1), 78-92.

[75] **Tan, C., Guo, L., Ai, Y., Li, J., Wang, L., Sancar, A., Luo, Y. and Zhong, D.** (2014). Direct determination of resonance energy transfer in photolyase: structural alignment for the functional state. *J Phys Chem A*, *118*(45), 10522-10530.

[76] **Cavga, A. D., Tardu, M., Korkmaz, T., Keskin, O., Ozturk, N., Gursoy, A. and Kavakli, I. H.** (2019). Cryptochrome deletion in p53 mutant mice enhances apoptotic and anti-tumorigenic responses to UV damage at the transcriptome level. *Funct Integr Genomics*, *19*(5), 729-742.

[77] **Chang, H., Guo, J. L., Fu, X. W., Wang, M. L., Hou, Y. M. and Wu, K. M.** (2019). Molecular Characterization and Expression Profiles of Cryptochrome Genes in a Long-Distance Migrant, Agrotis segetum (Lepidoptera: Noctuidae). *J Insect Sci*, *19*(1).

[78] **Cohrs, K. C. and Schumacher, J.** (2017). The Two Cryptochrome/Photolyase Family Proteins Fulfill Distinct Roles in DNA Photorepair and Regulation of Conidiation in the Gray Mold Fungus Botrytis cinerea. *Appl Environ Microbiol*, *83*(17).

[79] **Cook, G. M., Gruen, A. E., Morris, J., Pankey, M. S., Senatore, A., Katz, P. S., Watson, W. H., 3rd and Newcomb, J. M.** (2018). Sequences of Circadian Clock Proteins in the Nudibranch Molluscs Hermissenda crassicornis, Melibe leonina, and Tritonia diomedea. *Biol Bull*, *234*(3), 207-218.

[80] **Bennett, C. J., Webb, M., Willer, D. O. and Evans, D. H.** (2003). Genetic and phylogenetic characterization of the type II cyclobutane pyrimidine dimer photolyases encoded by Leporipoxviruses. *Virology*, *315*(1), 10-19.

[81] **Lucas-Lledó, J. I. and Lynch, M.** (2009). Evolution of mutation rates: phylogenomic analysis of the photolyase/cryptochrome family. *Mol Biol Evol*, *26*(5), 1143-1153.

[82] **Friedberg, E. C.** (2015). A history of the DNA repair and mutagenesis field: I. The discovery of enzymatic photoreactivation. *DNA Repair (Amst)*, *33*, 35-42.

[83] (1984). Escherichia coli DNA photolyase is a flavoprotein. *Journal of Molecular Biology*, *172*(2), 223 - 227.

[84] **Selby, C. P. and Sancar, A.** (2012). The second chromophore in Drosophila photolyase/cryptochrome family photoreceptors. *Biochemistry*, *51*(1), 167-171.

[85] **Jiang, Y., Rabbi, M., Kim, M., Ke, C., Lee, W., Clark, R. L., Mieczkowski, P. A. and Marszalek, P. E.** (2009). UVA generates pyrimidine dimers in DNA directly. *Biophys J*, *96*(3), 1151-1158.

[86] **Kemp, M. G. and Sancar, A.** (2012). DNA excision repair: where do all the dimers go? *Cell Cycle*, *11*(16), 2997-3002.

[87] **Kavakli, I. H., Baris, I., Tardu, M., Gül, Ş., Öner, H., Çal, S., Bulut, S., Yarparvar, D., Berkel, Ç., Ustaoğlu, P. and Aydın, C.** (2017). The Photolyase/Cryptochrome Family of Proteins as DNA Repair Enzymes and Transcriptional Repressors. *Photochem Photobiol*, *93*(1), 93-103.

[88] **Banaś, A. K., Zgłobicki, P., Kowalska, E., Bażant, A., Dziga, D. and Strzałka, W.** (2020). All You Need Is Light. Photorepair of UV-Induced Pyrimidine Dimers. *Genes (Basel)*, *11*(11).

[89] **Sancar, G. B., Smith, F. W., Reid, R., Payne, G., Levy, M. and Sancar, A.** (1987). Action mechanism of Escherichia coli DNA photolyase. I. Formation of the enzyme-substrate complex. *J Biol Chem*, *262*(1), 478-485.

[90] (2005). Light-driven enzymatic catalysis of DNA repair: a review of recent biophysical studies on photolyase. *Biochimica et Biophysica Acta (BBA) - Bioenergetics*, *1707*(1), 1 - 23.

[91] **Maestre-Reyna, M., Yamamoto, J., Huang, W. C., Tsai, M. D., Essen, L. O. and Bessho, Y.** (2018). Twist and turn: a revised structural view on the unpaired bubble of class II CPD photolyase in complex with damaged DNA. *IUCrJ*, *5*(Pt 5), 608-618.

[92] **Brettel, K. and Byrdin, M.** (2010). Reaction mechanisms of DNA photolyase. *Curr Opin Struct Biol*, *20*(6), 693-701.

[93] **Heelis, P. F., Kim, S. T., Okamura, T. and Sancar, A.** (1993). The photo repair of pyrimidine dimers by DNA photolyase and model systems. *J Photochem Photobiol B*, *17*(3), 219-228.

[94] **Munshi, S., Rajamoorthi, A. and Stanley, R. J.** (2017). Characterization of a cold-adapted DNA photolyase from C. psychrerythraea 34H. *Extremophiles*, *21*(5), 919-932.

[95] **Rijo-Ferreira, F., Acosta-Rodriguez, V. A., Abel, J. H., Kornblum, I., Bento, I., Kilaru, G., Klerman, E. B., Mota, M. M. and Takahashi, J. S.** (2020). The malaria parasite has an intrinsic clock. *Science*, *368*(6492), 746-753.

[96] **Nihongaki, Y., Kawano, F., Nakajima, T. and Sato, M.** (2015). Photoactivatable CRISPR-Cas9 for optogenetic genome editing. *Nat Biotechnol*, *33*(7), 755-760.

[97] **Adli, M.** (2018). The CRISPR tool kit for genome editing and beyond. *Nature Communications*, *9*(1), 1911.

[98] **Barrangou, R. and Marraffini, L. A.** (2014). CRISPR-Cas systems: Prokaryotes upgrade to adaptive immunity. *Mol Cell*, *54*(2), 234-244.

[99] **Wilkinson, R. and Wiedenheft, B.** (2014). A CRISPR method for genome engineering. *F1000Prime Rep*, *6*, 3.

[100] **Hsu, P. D., Lander, E. S. and Zhang, F.** (2014). Development and applications of CRISPR-Cas9 for genome engineering. *Cell*, *157*(6), 1262-1278.

[101] **Karvelis, T., Gasiunas, G., Miksys, A., Barrangou, R., Horvath, P. and Siksnys, V.** (2013). crRNA and tracrRNA guide Cas9-mediated DNA interference in Streptococcus thermophilus. *RNA Biol*, *10*(5), 841-851.

[102] **Lone, B. A., Karna, S. K. L., Ahmad, F., Shahi, N. and Pokharel, Y. R.** (2018). CRISPR/Cas9 System: A Bacterial Tailor for Genomic Engineering. *Genet Res Int*, *2018*, 3797214.

[103] **Chylinski, K., Makarova, K. S., Charpentier, E. and Koonin, E. V.** (2014). Classification and evolution of type II CRISPR-Cas systems. *Nucleic Acids Res*, *42*(10), 6091-6105.

[104] **Sapranauskas, R., Gasiunas, G., Fremaux, C., Barrangou, R., Horvath, P. and Siksnys, V.** (2011). The Streptococcus thermophilus CRISPR/Cas system provides immunity in Escherichia coli. *Nucleic Acids Res*, *39*(21), 9275-9282.

[105] **Cong, L., Ran, F. A., Cox, D., Lin, S., Barretto, R., Habib, N., Hsu, P. D., Wu, X., Jiang, W., Marraffini, L. A. and Zhang, F.** (2013). Multiplex genome engineering using CRISPR/Cas systems. *Science*, *339*(6121), 819-823.

[106] **Karginov, F. V. and Hannon, G. J.** (2010). The CRISPR system: small RNA-guided defense in bacteria and archaea. *Mol Cell*, *37*(1), 7-19.

[107] **Gleditzsch, D., Pausch, P., Müller-Esparza, H., Özcan, A., Guo, X., Bange, G. and Randau, L.** (2019). PAM identification by CRISPR-Cas effector complexes: diversified mechanisms and structures. *RNA Biol*, *16*(4), 504-517.

[108] **Liu, C., Zhang, L., Liu, H. and Cheng, K.** (2017). Delivery strategies of the CRISPR-Cas9 gene-editing system for therapeutic applications. *J Control Release, 266*, 17-26.

[109] (2015). The CRISPR-Cas immune system: Biology, mechanisms and applications. *Biochimie, 117*, 119 - 128.

[110] **Makarova, K. S. and Koonin, E. V.** (2015). Annotation and Classification of CRISPR-Cas Systems. *Methods Mol Biol, 1311*, 47-75.

[111] **Savić, N. and Schwank, G.** (2016). Advances in therapeutic CRISPR/Cas9 genome editing. *Transl Res, 168*, 15-21.

[112] **Wu, X., Kriz, A. J. and Sharp, P. A.** (2014). Target specificity of the CRISPR-Cas9 system. *Quant Biol*, *2*(2), 59-70.

[113] **Jiang, F. and Doudna, J. A.** (2017). CRISPR–Cas9 Structures and Mechanisms. *Annual Review of Biophysics*, *46*(1), 505-529.

[114] **Rodríguez-Rodríguez, D. R., Ramírez-Solís, R., Garza-Elizondo, M. A., Garza-Rodríguez, M. L. and Barrera-Saldaña, H. A.** (2019). Genome editing: A perspective on the application of CRISPR/Cas9 to study human diseases (Review). *Int J Mol Med*, *43*(4), 1559-1574.

[115] **Nemet, I., Ropelewski, P. and Imanishi, Y.** (2015). Applications of phototransformable fluorescent proteins for tracking the dynamics of cellular components. *Photochem Photobiol Sci*, *14*(10), 1787-1806.

[116] **Adam, V., Berardozzi, R., Byrdin, M. and Bourgeois, D.** (2014). Phototransformable fluorescent proteins: Future challenges. *Curr Opin Chem Biol*, *20*, 92-102.

[117] **Patterson, G. H. and Lippincott-Schwartz, J.** (2002). A photoactivatable GFP for selective photolabeling of proteins and cells. *Science, 297*(5588), 1873-1877.

[118] **Verkhusha, V. V. and Sorkin, A.** (2005). Conversion of the monomeric red fluorescent protein into a photoactivatable probe. *Chem Biol*, *12*(3), 279-285.

[119] **Wiedenmann, J., Ivanchenko, S., Oswald, F., Schmitt, F., Röcker, C., Salih, A., Spindler, K. D. and Nienhaus, G. U.** (2004). EosFP, a fluorescent marker protein with UV-inducible green-to-red fluorescence conversion. *Proc Natl Acad Sci U S A*, *101*(45), 15905-15910.

[120] **Kim, H., Grunkemeyer, T. J., Modi, C., Chen, L., Fromme, R., Matz, M. V. and Wachter, R. M.** (2013). Acid-base catalysis and crystal structures of a least evolved ancestral GFP-like protein undergoing green-to-red photoconversion. *Biochemistry*, *52*(45), 8048-8059.

[121] **Kim, H., Zou, T., Modi, C., Dörner, K., Grunkemeyer, T. J., Chen, L., Fromme, R., Matz, M. V., Ozkan, S. B. and Wachter, R. M.** (2015). A hinge migration mechanism unlocks the evolution of green-to-red photoconversion in GFP-like proteins. *Structure*, *23*(1), 34-43.

[122] **Mutoh, T., Miyata, T., Kashiwagi, S., Miyawaki, A. and Ogawa, M.** (2006). Dynamic behavior of individual cells in developing organotypic brain slices revealed by the photoconvertable protein Kaede. *Exp Neurol*, *200*(2), 430-437.

[123] **Karbowski, M., Arnoult, D., Chen, H., Chan, D. C., Smith, C. L. and Youle, R. J.** (2004). Quantitation of mitochondrial dynamics by photolabeling of individual organelles shows that mitochondrial fusion is blocked during the Bax activation phase of apoptosis. *J Cell Biol*, *164*(4), 493-499.

[124] **Baltrusch, S. and Lenzen, S.** (2008). Monitoring of glucose-regulated single insulin secretory granule movement by selective photoactivation. *Diabetologia*, *51*(6), 989-996.

[125] **Dempsey, W. P., Fraser, S. E. and Pantazis, P.** (2012). PhOTO zebrafish: a transgenic resource for in vivo lineage tracing during development and regeneration. *PLoS One*, *7*(3), e32888.

[126] **Pham, A. H., McCaffery, J. M. and Chan, D. C.** (2012). Mouse lines with photo-activatable mitochondria to study mitochondrial dynamics. *Genesis*, *50*(11), 833-843.

[127] **Kao, Y. T., Zhu, X. and Min, W.** (2012). Protein-flexibility mediated coupling between photoswitching kinetics and surrounding viscosity of a photochromic fluorescent protein. *Proc Natl Acad Sci U S A*, *109*(9), 3220-3225.

[128] **Salehi Sangani, G., Jajarmi, V., Khamesipour, A., Mahmoudi, M., Fata, A. and Mohebali, M.** (2019). Generation of a CRISPR/Cas9-Based Vector Specific for Gene Manipulation in Leishmania major. *Iran J Parasitol*, *14*(1), 78-88.

AUTOBIOGRAPHY

Name-Surname **:** İlknur YILMAZ

Birth Date and Place **:**

E-Mail **:**

EDUCATION STATUS:

- **Bachelor** **:** 2015, Istanbul University, Science Faculty, Molecular Biology and Genetic Department

EXPERIENCE:

- Laboratory Technician, Bezmialem Vakif University, Life Sciences and Biotechnology Institute (March 2018-May 2019).
- Molecular Biologist, Biruni University, Genome Center (June 2016-December 2017).
- Volunteer Doctor's Assistant, Istanbul University Cerrahpaşa, Medical Faculty, Genetic Research Center (October 2015-February 2016).

PUBLICATIONS, PRESENTATIONS AND PATENTS PRODUCED FROM THE MASTER THESIS:

- Aly A.S.I., Deveci G., **Yilmaz I**, Golshan A., Abraham A., Hart R.J**. 2019**. Phenotypic Analysis of Rodent Malaria Parasite Asexual and Sexual Blood Stages and Mosquito Stages, *Journal of Visual Experiments*, (147).
- Reeder, S.M., Reuschel, E. L., Bah, M. A., Yun K., Tursi N.J., Kim K.Y., Chu J., Zaidi F.I., **Yilmaz I.,** Hart R.J., Perrin B., Xu Z., Humeau L., Weiner D.B., Aly A.S.I**. 2020**. Synthetic DNA Vaccines Adjuvanted with Pıl-33 Drive Liver-Localized T Cells and Provide Protection from Plasmodium Challenge in a Mouse Model, *Vaccines*, 8(1), 21.

OTHER PUBLICATIONS, PRESENTATIONS AND PATENTS:

- **Yilmaz I.,** Palabiyik B.G., Temel B.A., Aly A.S.I., Gene Targeting Studies of the Malaria Parasite DNA Photolyase Gene Using CRISPR-Cas9 Genome Editing Technology, International Eurasian Conference on Biotechnology and Biochemistry, 16-18 December 2020, Ankara, Turkey, Poster Presentation.